

POLITECNICO DI TORINO

Corso di Laurea Magistrale in
Ingegneria Energetica e Nucleare

Tesi di Laurea Magistrale

Applications of innovative materials and thermal process for atmospheric water generation



Supervisor

Prof. Marco Simonetti

Co-supervisor

Vincenzo Maria Gentile

Candidate

Alessia Castellana

Anno accademico 2020-2021

Contents

Abstract	XI
1 Introduction	1
2 State of the art of techniques for water production	4
2.1 Access to water and sanitation	4
2.2 Water desalination worldwide.....	6
2.2.1 Solar thermal desalination.....	7
2.2.2 Membrane Desalination	9
2.3 Groundwater resource	12
2.4 Atmospheric Water Harvesting.....	13
2.4.1 Condensation technologies.....	14
2.4.2 Sorption technologies.....	17
2.4.3 Membrane atmospheric water harvesting	19
3 Materials for Atmospheric Water Harvesting	21
3.1 Isotherm standard models	21
3.1.1 Henry’s isotherm model.....	22
3.1.2 Dubinin-Radushkevich isotherm model.....	22
3.1.3 Langmuir isotherm model	23
3.2 Materials for solid cycles	25
4 Sodium Alginate	32

4.1	Current application.....	32
4.1.1	Water harvesting application.....	32
4.1.2	Removal of lead from water.....	33
4.1.3	Drug delivery application.....	34
4.1.4	Alginate and immobilization of cells	35
4.2	Production process	36
5	Experimental testing.....	40
5.1	Equipment and materials used	40
5.2	Testing protocol	42
5.3	Trial test	42
5.3.1	Silica gel tests – sample 1	43
5.3.2	Silica gel test-sample 2.....	46
5.4	Real tests	48
5.5	Silica gel.....	58
5.5.1	Testing silica gel at 80% of relative humidity.....	58
5.5.2	Testing silica gel at 60% of relative humidity.....	61
5.5.3	Testing silica gel at 40% of relative humidity.....	64
5.6	Alginate at 5% of concentration.....	67
5.6.1	Testing Alginate at 80% of relative humidity	67
5.6.2	Testing Alginate at 60% of relative humidity	69
5.6.3	Testing Alginate at 40% of relative humidity	71
6	Results and discussion	74
6.1	Silica gel comparisons.....	74

6.2	Alginate comparisons.....	80
6.3	Silica gel and Alginate comparisons	84
	Conclusions	88

List of figures

<i>List of figures</i>	V
Figure 1.1-Essential properties of moisture harvesters for AWH.....	3
Figure 2.1- Total renewable water resources per capita	4
Figure 2.2- Global water demand in 2000 and 2050 [1]	5
Figure 2.3-MSF distillation configuration [5]	8
Figure 2.4-Forward feed MED desalination plant[6].....	8
Figure 2.5-Mechanical Vapor compression[7]	9
Figure 2.6-Reverse osmosis.....	10
Figure 2.7-Stack for the electro-dialysis process[7]	10
Figure 2.8-Scheme of Membrane Distillation process.....	11
Figure 2.9-Groundwater resource[12]	13
Figure 2.10-Vapor compression cycle for water harvesting[14]	15
Figure 2.11-Scheme of a thermoelectric cooler[15].....	16
Figure 2.12-Scheme of a testing system[16].....	16
Figure 2.13-Absorption chiller.....	18
Figure 2.14- Elementary and complete membrane separation schemes for AWH[18].....	20
Figure 3.1- Six types of adsorption isotherm[20]	24
Figure 3.2-Water sorption isotherm for silica-gel[23].....	26
Figure 3.3-Water uptake with zeolite as adsorbent [23]	27
Figure 3.4-AHW with MOFs[25].....	28
Figure 3.5-Water uptake with MOFs[25].....	29
Figure 3.6-Water mass uptake from ACF/LiCl/MgSO ₄ composite[26]	30
Figure 3.7-Absorption isotherm for SWS materials[27]	30
Figure 4.1-Water sorption isotherms of the composite Alg-CaCl ₂ [28]	33
Figure 4.2-Incapsulation of live cell in alginate	35
Figure 4.3-Egg-box model of alginate.....	36
Figure 4.5-Adsorption and regeneration phase of the water harvesting system	39
Figure 5.1- Scheme of the thermobalance	41
Figure 5.2- The graph on the left-hand side shows the behavior of the total mass variation during the regeneration process(blue line) and the water uptake for the test performed at 120°C; on the right-hand side it is shown the behavior of the water content extracted from the sample with respect the initial wet mass, and the total mass variation for the test at 120°C. The dashed line represents the amount of water extracted from the sample.....	44

Figure 5.3- The graph on the left-hand side shows the behavior of the total mass variation during the regeneration process and the water uptake for the test performed at 200°C; on the right-hand side it is shown the behavior of the water content extracted from the sample with respect the initial wet mass, and the total mass variation for the test at 200°C. The dashed line represents the amount of water extracted from the sample..... 44

Figure 5.4- The graph on the left-hand side shows the behavior of the total mass variation during the regeneration process and the water uptake for the test performed at 50°C; on the right-hand side it is shown the behavior of the water content extracted from the sample with respect the initial wet mass, and the total mass variation for the test at 50°C. The dashed line represents the amount of water extracted from the sample..... 45

Figure 5.5 - The graph on the left-hand side shows the behavior of the total mass variation during the regeneration process and the water uptake for the test performed at 120°C; on the right-hand side it is shown the behavior of the water content extracted from the sample and the total mass variation for the test at 120°C, the dashed line represents the amount of water extracted from the sample..... 47

Figure 5.6- The graph on the left-hand side shows the behavior of the total mass variation during the regeneration process and the water uptake for the test performed at 200°C; on the right-hand side it is shown the behavior of the water content extracted from the sample and the total mass variation for the test at 200°C, the dashed line represents the amount of water extracted from the sample..... 47

Figure 5.7- The graph on the left-hand side shows the behavior of the total mass variation during the regeneration process and the water uptake for the test performed at 50°C; on the right-hand side it is shown the behavior of the water content extracted from the sample and the total mass variation for the test at 50°C, the dashed line represents the amount of water extracted from the sample..... 48

Figure 5.8- Configuration of the structure 49

Figure 5.9- Experimental and theoretical behaviors of the ratio mtm^∞ for the silica gel samples at 80% of relative humidity for the three different operating temperature conditions, in particular from left to right: 100°, 70°C, 50°C 55

Figure 5.10- Experimental and theoretical behaviors of the ratio mtm^∞ for the silica gel samples at 60% of relative humidity for the three different operating temperature conditions: from left to right: 100°, 70°C, 50°C 56

Figure 5.11- Experimental and theoretical behaviors of the ratio mtm^∞ for the silica gel samples at 40% of relative humidity for the three different operating temperature conditions: from left to right: 100°, 70°C, 50°C 56

Figure 5.12- Experimental and theoretical behaviors of the ratio mtm^∞ for the alginate (5%) samples at 80% of relative humidity for the three different operating temperature conditions: from left to right: 100°, 70°C, 50°C 57

Figure 5.13 -Experimental and theoretical behaviors of the ratio mtm_{∞} for the alginate (5%) samples at 60% of relative humidity for the three different operating temperature conditions: from left to right: 100°, 70°C, 50°C 57

Figure 5.14- Experimental and theoretical behaviors of the ratio mtm_{∞} for the alginate (5%) samples at 40% of relative humidity for the three different operating temperature conditions: from left to right: 100°, 70°C, 50°C 57

Figure 5.15-The graph on the left-hand side shows the behavior of the total mass variation during the regeneration process and the water uptake for the test performed at 100°C; on the right-hand side the behavior of the water content extracted from the sample and the total mass variation for the test at 100°C..... 60

Figure 5.16-The graph on the left-hand side shows the behavior of the total mass variation during the regeneration process and the water uptake for the test performed at 70°C; on the right-hand side it is shown the behavior of the water content extracted from the sample and the total mass variation for the test at 70°C. 61

Figure 5.17- The graph on the left-hand side shows the behavior of the total mass variation during the regeneration process and the water uptake for the test performed at 50°C; on the right-hand side the behavior of the water content extracted from the sample and the total mass variation for the test at 50°C..... 61

Figure 5.18 – The graph on the left-hand side shows the behavior of the total mass variation during the regeneration process and the water uptake for the test performed at 100°C; on the right-hand side it is shown the behavior of the water content extracted from the sample with respect the initial wet mass, and the total mass variation for the test at 100°. The dashed line represents the amount of water extracted from the sample..... 63

Figure 5.19- The graph on the left-hand side shows the behavior of the total mass variation during the regeneration process and the water uptake for the test performed at 70°C; on the right-hand side it is shown the behavior of the water content extracted from the sample referred to the initial wet mass and the total mass variation for the test at 70°C. The dashed line represents the amount of water extracted from the sample..... 63

Figure 5.20 The graph on the left-hand side shows the behavior of the total mass variation during the regeneration process and the water uptake for the test performed at 50°C; on the right-hand side it is shown the behavior of the water content extracted from the sample and the total mass variation for the test at 50°C. The dashed line represents the amount of water extracted from the sample 64

Figure 5.21 – The graph on the left-hand side shows the behavior of the total mass variation during the regeneration process and the water uptake for the test performed at 100°C; on the right-hand side it is shown the behavior of the water content extracted from the sample with respect the initial wet mass, and the total mass variation for the test at 100°C. The dashed line represents the amount of water extracted from the sample 65

Figure 5.22 – The graph on the left-hand side shows the behavior of the total mass variation during the regeneration process and the water uptake for the test performed at 70°C; on the right-hand side it is shown the behavior of the water content extracted from the sample with respect the initial wet mass, and the total mass variation for the test at 70°C, the dashed line represents the amount of water extracted from the sample..... 66

Figure 5.23-The graph on the left-hand side shows the behavior of the total mass variation during the regeneration process and the water uptake for the test performed at 50°C; on the right-hand side it is shown the behavior of the water content extracted from the sample with respect to the initial wet mass, and the total mass variation for the test at 50°C The dashed line represents the amount of water extracted from the sample..... 66

Figure 5.24 -The graph on the left-hand side shows the behavior of the total mass variation during the regeneration process and the water uptake for the test performed at 50°C; on the right-hand side it is shown the behavior of the water content extracted from the sample with respect the initial wet mass, and the total mass variation for the test at 50°C The dashed line represents the amount of water extracted from the sample..... 68

Figure 5.25- The graph on the left-hand side shows the behavior of the total mass variation during the regeneration process and the water uptake for the test performed at 70°C; on the right-hand side it is shown the behavior of the water content extracted from the sample with respect the initial wet mass, and the total mass variation for the test at 70°C The dashed line represents the amount of water extracted from the sample..... 69

Figure 5.26-The graph on the left-hand side shows the behavior of the total mass variation during the regeneration process and the water uptake for the test performed at 100°C; on the right-hand side it is shown the behavior of the water content extracted from the sample with respect to the initial wet mass, and the total mass variation for the test at 100°C The dashed line represents the amount of water extracted from the sample 69

Figure 5.27- The graph on the right-hand side displays the ratio between the water extracted and the initial we mass in comparison to the total mass variation during the transient at 50°C, on the left-hand side it is shown the behavior of the water uptake during the adsorption process and the variation of the mass of the sample when the regeneration process was performed at 50°C..... 70

Figure 5.28- The graph on the right-hand side displays the ratio between the water extracted and the initial we mass in comparison to the total mass variation during the transient at 70°C, on the left-hand side it is shown the behavior of the water uptake during the adsorption process and the variation of the mass of the sample when the regeneration process was performed at 70°C..... 71

Figure 5.29--The graph on the right-hand side displays the ratio between the water extracted and the initial we mass in comparison to the total mass variation during the transient at 100°C, on the left-hand side it is shown the behavior of the water uptake during the adsorption process and the variation of the mass of the sample when the regeneration process was performed at 100°C 71

Figure 5.30-The graph on the right-hand side displays the ratio between the water extracted and the initial wet mass in comparison to the total mass variation during the transient at 50°C, on the left-hand side it is shown the behavior of the water uptake during the adsorption process and the variation of the mass of the sample when the regeneration process was performed at 50°C..... 72

Figure 5.31- The graph on the right-hand side displays the ratio between the water extracted and the initial wet mass in comparison to the total mass variation during the transient at 70°C, on the left-hand side it is shown the behavior of the water uptake during the adsorption process and the variation of the mass of the sample when the regeneration process was performed at 70°C..... 73

Figure 5.32-The graph on the right-hand side displays the ratio between the water extracted and the initial wet mass in comparison to the total mass variation during the transient at 100°C, on the left-hand side it is shown the behavior of the water uptake during the adsorption process and the variation of the mass of the sample when the regeneration process was performed at 100°C 73

Figure 6.1- The graph on the left-hand side shows the comparison of water extracted from the silica gel sample concerning the initial wet mass for the three levels of RH when the regeneration process was performed at 100°C. On the right-hand side the behavior of the water uptake for the three levels of relative humidity..... 76

Figure 6.2- The graph on the left-hand side shows the comparison of water extracted from the silica gel sample concerning the initial wet mass for the three levels of RH when the regeneration process was performed at 70°C. On the right-hand side the behavior of the water uptake for the three levels of relative humidity..... 77

Figure 6.3- The graph on the left-hand side shows the comparison of water extracted from the silica gel sample concerning the initial wet mass for the three levels of RH when the regeneration process was performed at 50°C. On the right-hand side the behavior of the water uptake for the three levels of relative humidity..... 77

Figure 6.4- Comparison of the total mass variation and water uptake of the silica gel sample at constant relative humidity equal to 80% and varying the operating temperature conditions..... 79

Figure 6.5 - Comparison of the total mass variation and water uptake of the silica gel sample at constant relative humidity equal to 60% and varying the operating temperature conditions..... 79

Figure 6.6- Comparison of the total mass variation and water uptake at constant relative humidity equal to 40% and varying the operating temperature conditions..... 80

Figure 6.7- Graph on the left-hand side shows the comparison of water extracted from the alginate sample concerning the initial wet mass for the three levels of RH when the regeneration process was performed at 100°C. On the right-hand side the behavior of the water uptake for the three levels of relative humidity..... 80

Figure 6.8- Graph on the left-hand side shows the comparison of water extracted from the alginate sample concerning the initial wet mass for the three levels of RH when the regeneration process was

performed at 70°C. On the right-hand side the behavior of the water uptake for the three levels of relative humidity81

Figure 6.9- Graph on the left-hand side shows the comparison of water extracted from the alginate sample concerning the initial wet mass for the three levels of RH when the regeneration process was performed at 50°C. On the right-hand side the behavior of the water uptake for the three levels of relative humidity81

Figure 6.10- Comparison of the total mass variation and the water uptake of the alginate sample at 37% of relative humidity for three different levels of operating temperature conditions82

Figure 6.11- Comparison of the total mass variation and the water uptake of the sample at 60% of relative humidity for three different levels of operating temperature conditions83

Figure 6.12- Comparison of the total mass variation and the water uptake of the sample at 80% of relative humidity for three different levels of operating temperature conditions83

Figure 6.13- Comparison of the total mass variation and water uptake between silica gel and alginate at 40% of relative humidity and different temperatures: from left to right equal to 100°C, 70°C,50°C84

Figure 6.14- Comparison of total mass variation and water uptake between silica gel and alginate at 60% of relative humidity and different temperatures: from left to right equal to 100°C, 70°C,50°C ...86

Figure 6.15- Comparison of water content and water uptake between silica gel and alginate at 80% of relative humidity and different temperatures: from left to right equal to 100°C, 70°C,50°C87

Abstract

Water shortage is considered as one of the most important issues of the last years, and this problem may be due to physical shortage or scarcity in access due to the lack of appropriate infrastructure. In this context, Agenda 2030 was signed in 2015 to develop an action program for people, the planet, and prosperity. Goal number six of the agenda focuses on ensuring the availability and sustainable management of water and sanitation for all.

Different solutions can be implemented to provide fresh and drinkable water from natural resources, such as desalination of seawater, exploitation of groundwater, and water harvesting from the air.

The last solution may result in the most hopeful since the process can be also driven by using a low-grade renewable energy source.

The development of this thesis aims to highlight the adsorption and desorption properties of an innovative material, which is sodium alginate, to be used as sorption material within an atmospheric water harvesting system for the production of freshwater.

Tests have been done with the use of a moisture analyser which can measure the water content within a sample of testing material, at different temperature conditions. The regeneration process can be performed for different periods, according to the relative humidity of the material at the beginning of the test.

In the end, the properties obtained from the tests have been put in comparison with the well-known silica gel sorption material, to highlight differences or similarities.

Thanks to the results obtained it was clear that the alginate is suitable for water harvesting applications due to its high adsorption capacity.

1 Introduction

Water is considered the core of sustainable development. This resource, and all the other services they provide, support the economic development of the overall world and contribute to poverty reduction.

Water demand is foreseen to increase in all sectors of production, in particular, by 2030 the world will face a 40% water deficit under the Business As Usual (BAU) scenario. It means that no policies are put in place by the countries to achieve a pre-determined target.

Another factor that contributes to water scarcity is population growth, but the relationship is not linear: over the last decades, the rate of water demand has doubled the rate of population growth.

The OECD Environmental Outlook estimates that by 2050 water demand will increase dramatically both from manufacturing industries and thermal power generation, especially in developing countries and in the five major emerging national economies of Brazil, Russia, India, China, and South Africa (BRICS). [1]

According to the European Commission, all member countries are applying a human-rights based approach to act initiatives which facilitate access to water and sanitation. This approach can be summarized with the so-called 4A-criteria: Availability, Accessibility, Affordability, Acceptability, and Quality of water.[2]

To address the problem of lack of drinking water, different solutions can be implemented which can be fully renewables:

- Desalination of seawater
- Exploitation of groundwater
- Water harvesting from air

The following sheets will analyze and explain how to withdraw water from groundwater natural resources, which represents the only source of water supply from some countries of the world like Denmark, Malta, Saudi Arabia, etc.

Desalination of seawater technique is based on reverse osmosis: a porous material allows water to pass through it, but at the same time avoiding the passage of undesirable molecules such as viruses, bacteria, metals, and salts.

Since the two different technologies operate with fossil fuels and require complex systems, they are becoming expensive to operate, and the greenhouse gas emissions they produced, are recognized as harmful to the environment and climate.

The last solutions seem to be the most promising in terms of energy expenditure and pollution produced since they can be driven by renewable energy systems. The development of this thesis focuses on the analysis of the properties of an innovative material that is sodium alginate, in terms of the capability to harvest a certain amount of water from humid air, putting it in comparison with the well-known silica gel sorption material to highlight differences or similarities.

The sorption material under investigation has been constructed through inotropic gelation of the sodium alginate in an ionic solution of water and divalent cations at two different concentrations, producing alginate balls of different dimensions.

Tests have been done with the use of a thermal balance which can measure the water content within a sample of testing material, at different temperature conditions.

Before the tests, the alginate and silica gel has been prepared to reach specific conditions in terms of temperature and relative humidity.

In particular, three samples of silica gel and three of alginate have been tested to explore different conditions.

Before these, many trial tests were performed by using two silica gel samples arranged in two different ways.

The first sample of silica gel was prepared within a closed glass box filled with water, where many silica gel balls were inserted into a baker providing a multilayer structure. The second one was arranged in an aluminum dish, so providing a monolayer structure, deposited over 2 wet paper towels, and then covered by a plastic box.

These processes should bring the material to the saturation point, but here no sensors were inserted to monitoring the thermohygrometric conditions.

All the samples were tested under three different temperatures of 50°C, 120°C, and 200°C.

For the real tests, alginate and silica gel samples were prepared in two concentric plastic boxes, the bigger one was filled with water or with a solution of water and calcium chloride, while in the smaller ones, the material was deposited over an aluminum dish providing a monolayer texture. The overall closed structures were

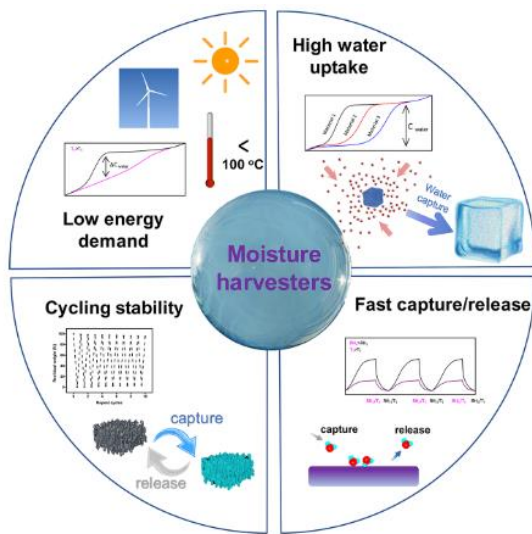
equipped with temperature and relative humidity sensors to check the initial ambient condition before the tests. Three alginate and three silica gel samples were tested, according to different thermohygrometric conditions. To reach 80% of relative humidity, only one liter of water was inserted within the box, while 60% and 40% of relative humidity were obtained by using a solution of water and calcium chloride at different concentrations.

All the samples of silica and alginate were tested under three temperatures of 50°C, 70°C, and 100°C respectively.

Results provided by the thermal balance were analyzed and manipulated by the Excel program, and comparisons between the two materials will be shown afterward.

The main goals of testing this innovative material are to understand its properties and to use it within an adsorption heat exchanger to produce fresh water.

Four main properties will be analyzed, which represent the requirements that an innovative sorption material should fulfill to be recognized as an efficient material for water harvesting application, and they are shown in **Errore. L'origine riferimento**



non è stata trovata.:

Low energy demand refers to the amount of heat needed to perform the regeneration process. By using low-grade energy sources, like renewables, will reduce the amount of electrical energy requested providing a more efficient process.

The material under investigation should also have high water uptake, so it should be able to adsorb a high amount of water

molecule. The cycling stability refers to the capability of the material to recover all its

Figure 1.1-Essential properties of moisture harvesters for AWH

properties after performing many adsorption/desorption cycles. The last

property refers to the velocity at which the material can adsorb or release all the water molecules.

2 State of the art of techniques for water production

2.1 Access to water and sanitation

Since 2010 access to water and sanitation has been recognized as human rights. In 2015 17 Sustainable Development Goals were adopted by all UN Member States, as part of the 2030 Agenda which elaborates a 15 years plan to reach the Goals. In particular, the 6th refers to ensure access to safe water and sanitation for all. [3]

The distribution and availability of water over the world is not equal, it means that different countries of the world receive different quantities of water. Figure 2.1 shows the total renewable water per capita of the entire world clearing the differences.[1]

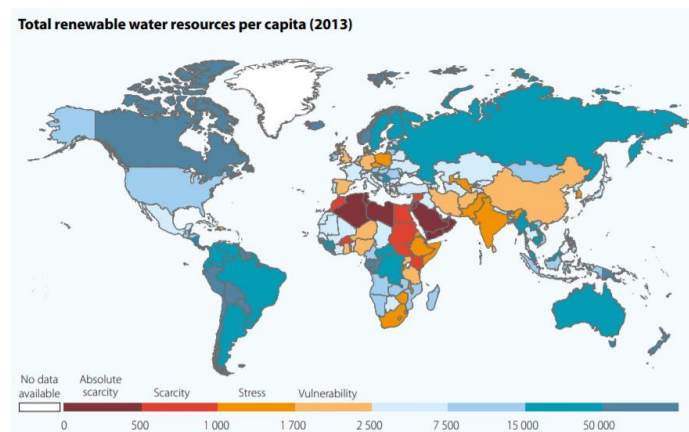


Figure 2.1- Total renewable water resources per capita

Rapid urbanization in developing countries, together with increased industrialization and improvement in living standards, are directly connected with an increase in the water demand in cities.

As illustrated in the graph below, global water demand is projected to increase by 55% in 2050.

The factors which require a higher amount of drinking water are irrigation, electricity, and the manufacturing sector.

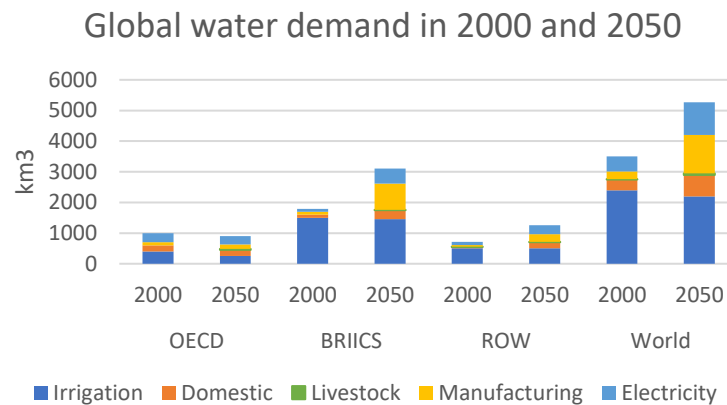


Figure 2.2- Global water demand in 2000 and 2050 [1]

For this reason, cities should find a solution and dig deeper to find or improve innovative and renewables technologies to meet water demand worldwide.

However, access to safe drinking water is a major problem in cities in developing countries, where the urbanization process is happening most rapidly like in sub-Saharan Africa.

Similar to this trend, people without access to improved sanitation increased by 40%, between 1990 and 2012. [1]

In most of the cases, the increase in the number of people without access to drinking water and sanitation is centered in areas or countries where the concentration of slum populations is very high. They are also more vulnerable to the impact of extreme wheater conditions.

To reach the proposed target on universal access to safe water, sanitation, and hygiene, actions should be implemented to address this critical issue and governments should learn from previous experiences of successful and innovative initiatives that focus on the essential requirement of the urban poor.

Until this decade, different solutions have been exploited for the satisfaction of the water demand, which are the withdrawal of groundwater resources and the process of desalination of seawater.

In this framework, another developing innovative technique is atmospheric water harvesting, which exploits the water vapor included in the airflow and condenses it to produce water.

2.2 Water desalination worldwide

Water desalination is becoming an innovative and competitive solution for the satisfaction of the drinking water demand for many communities and industries.

With the current amount of desalination plants in the world, several billion of water per day have been produced.

Desalination is a process where saline water is separated into two parts, the first one which has a low concentration of salts representing the freshwater, and the other which has a higher concentration of dissolved salts and minerals called brine concentrate. Saline water is classified as either brackish water or seawater relying on the salinity and water source.

The oldest desalination plants worked with fossil fuel as a medium for the energy needed within the process. The production of 1000 m³ per day of freshwater requires 10.000 tonnes of oil per year, which is high energy consumption.

This is a serious problem especially for regions such as Africa, Pacific Asia, and region of the Middle East. Here, the continuous increase in population together with agricultural and industrial development has contributed to the deterioration of natural freshwater resources.

Furthermore, these areas have not the financial possibility to support the construction of these types of plants. For this reason, solutions that utilize renewable energy sources to drive desalination plants have emerged. [4]

Water desalination processes can be divided into two types: thermal and membrane processes. There are other two types of desalination plants basing on freezing and ion exchanging but they are not very used today.

Another classification of this technology powered by solar energy source relates to the direct or indirect solar desalination.

Direct solar desalination units are called solar still which represent a natural hydrologic cycle. It is made up of a basin containing saltwater and two glass plastic panels creating a triangular structure. Solar radiation hits the two panels and the greenhouse effect is generated so inside the structure the temperature of the saltwater rises.

The water vapor increases reaching the sloping panels where it condenses to liquid water that is collected at the bottom of the structure.

The indirect solar desalination unit is divided into two sub-systems, the solar collector coupled with any thermal desalination processes. Systems that use photovoltaic devices are employed to generate electricity to support the reverse osmosis processes or the electro dialysis.

2.2.1 Solar thermal desalination

Indirect solar desalination is based on the two concepts of evaporation and condensation.

In this process, the saline water is increased in temperature until it reaches the saturation temperature and evaporates thanks to the thermal energy provided by the solar collector, then the humid air is condensed producing freshwater.

There are three main thermal desalination plants:

1. Multi-stage flash distillation (MSF)
2. Multi-effect distillation (MED)
3. Vapour compression evaporation (VC)

The **Multi-stage flash desalination** system consists of four or more tanks: water is pumped in each tank, vaporized into steam, and later condensed. Seawater is heated between 90-110°C and the tanks decrease in pressure at each stage and this phenomenon allows water to flash and vaporize.

MSF desalination plants normally reach 20 stages, before the first stage a saltwater heater powered by hot steam by a steam generator is responsible to bring the brine until the inlet temperature value. Of course, the higher is this temperature, the more will be the distillation rate because in this way a larger amount of vapor can be extracted from the brine.

Furthermore, a brine preheater can be installed on the top of each evaporator to slightly increase the temperature of the brine.

When the brine enters each stage, the temperature falls until its saturation temperature at a specific pressure. This temperature gap is linked to the amount of fresh water produced.[5]

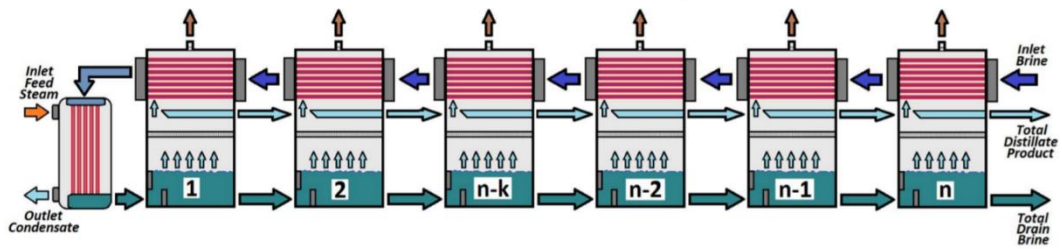


Figure 2.3-MSF distillation configuration [5]

In the **Multi-effect distillation**, the feed water is heated by steam in tubes. At each phase, some water evaporates and the remaining steam goes inside the other tube to heat and evaporate more water. In the last cell, the steam condenses on a traditional shell and tube heat exchanger.

MED desalination plant is composed of different variable stages, generally from five to ten. In this case, the brine is inserted from the top of the evaporator and falls on the tube surface.

The brine film absorbs the condensation enthalpy of the vapor flowing inside the tube. The vapor produced by the evaporation is filtered through a demister, the remaining part of the brine together with the droplets caught fall in the brine pool, ready to go in the next stage. Sometimes, if the pressure of the effect is smaller than the brine pressure, it happens that the brine evaporates into vapor and is added to the one previously produced. From the second effect forward, a condensation chamber is installed and part of the condensate turns into vapor.[6] Figure 2.4 shows one example of the possible configuration of this technology.

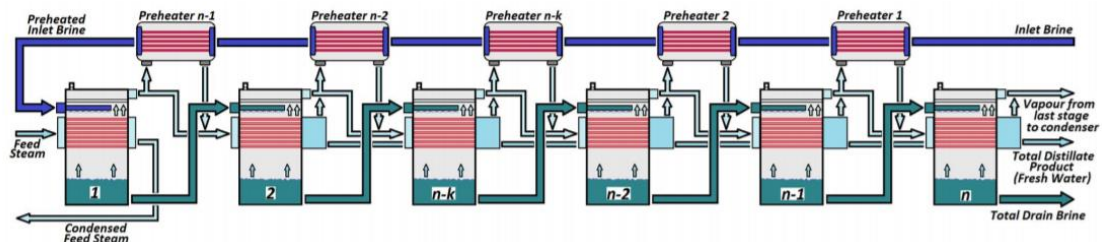


Figure 2.4-Forward feed MED desalination plant[6]

With **vapor compression**, the entering water is converted to vapor after passing through a heat exchanger, then it is compressed by mechanical or thermal means. A mechanical compressor is driven by electricity while a thermal compressor uses a

steam ejector to create a vacuum. The compressed vapor, at high temperature and pressure, flows into the pre-heater producing freshwater by exchanging heat with the initial saline feed.[7]

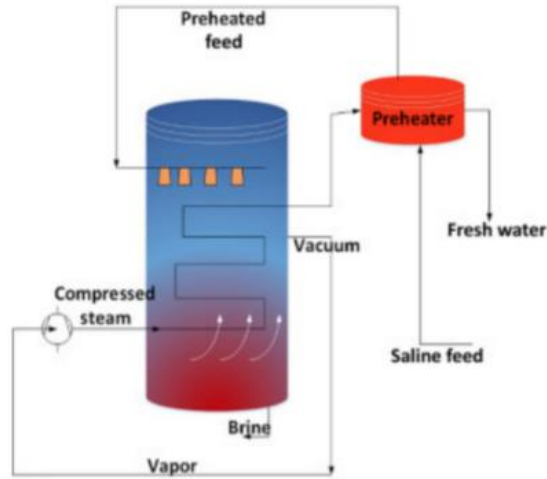


Figure 2.5-Mechanical Vapor compression[7]

2.2.2 Membrane Desalination

Membrane desalination is a technology that uses a permeable membrane to separate and move the saline water into two zones of different concentrations to produce fresh water.

One of the most reliable separation processes is **reverse osmosis** which removes ions, molecules, and large and undesirable particles such as viruses, bacteria, and salt, under the influence of externally applied pressure through the membrane. The membrane has a static charge on its surface which inhibits the absorption of ions within the membrane while water molecules are soluble in the membrane and pass from an area at high pressure to the low-pressure pure waterside.

The amount of water that passes through the membrane is a function of the applied differential pressure and the osmotic pressure across the membrane. Reverse osmosis occurs when a force is applied to the concentrated side with the salt, causing the movement of the solvent to the less concentrated side.

A complete reverse osmosis system should include a pre-treatment process, the membrane, pressure pumps, and a post-treatment process.

The efficiency of this technology depends on the characteristics of the feed water, the membrane performances, and other operational parameters.

Two of the most interesting membrane in terms of fulfillment are the spiral wound membrane and the hollow fine fibre.

The first one is manufactured as a flat sheet while the second one is a U-shaped fibre bundle housed in a pressure vessel.[8]

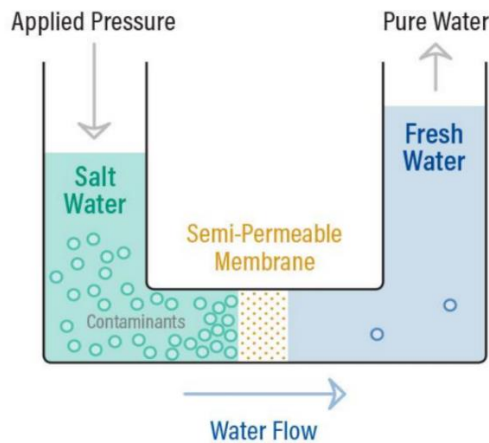


Figure 2.6-Reverse osmosis

Another important technology used for membrane desalination is the **electro-dialysis**. The structure of the cell is made up of a series of ionic and anionic membranes that are aligned between two electrodes. A low DC voltage applied between anode and cathode electrodes and passing through the membranes is used to separate charged species like ions from uncharged matters and the aqueous solution.

The membranes (Cation Exchanging Membrane and Anion Exchanging Membrane) work as a barrier to the nutrients migration that allows or prevents ions to pass through, following their electric charge.

When the feeding water enters within the stack, the applied voltage leads to a reduction reaction at the cathode producing hydroxide ions and an oxidation reaction at the anode which generates protons in the anion compartment. Consequently, salts are removed from the feeding solution to the concentrate side of the stack, producing dilute and concentrated wastewater.[9]

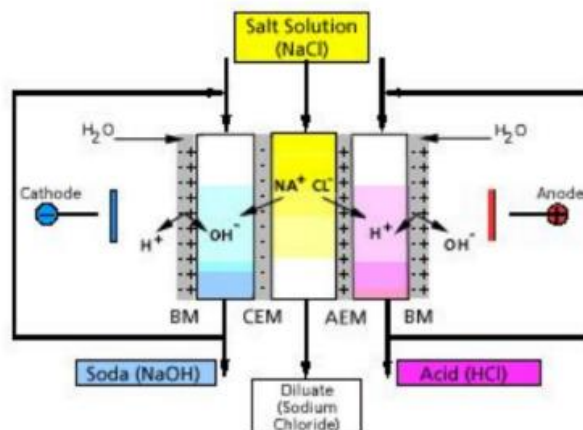


Figure 2.7-Stack for the electro-dialysis process[7]

The last membrane desalination technology is **membrane distillation** which is a thermally driven separation process of the aqueous solution through the use of a hydrophobic membrane.

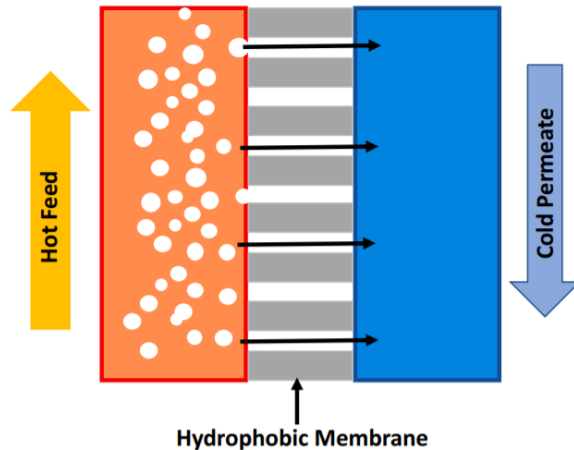


Figure 2.8-Scheme of Membrane Distillation process

In conventional membrane

distillation, vapor pressure is generated across the two sides of the hydrophobic porous membrane through the circulation of the hot feed and the coolant, so it is due to a temperature difference across the membrane.

The vapor molecules pass through the pore of the membrane from the side with high vapor pressure to the low vapor pressure side.

The transportation of vapor inside the membrane occurs in three main steps:

1. Evaporation of the feeding solution on the high-temperature side
2. Transportation of the water molecules within the pore of the porous membrane
3. Condensation on the vapor molecules on the low-temperature side

In this case, the membrane is not directly involved in the separation process, the only function is to act as a barrier between the two phases. The typical temperature of the feeding solution ranges from 60°C to 90°C, which means that a low exergy heat source like solar energy can be employed to support the process.

There are many configurations of the membrane distillation, according to the different methods used to generate the water vapor on the feed side, to transport, and collect it on the permeate side:

1. Direct Contact Membrane Distillation: this is the simplest configuration in which the membrane is in direct contact with the cold water.
2. Air Gap Membrane Distillation: in this case, an air gap is created between the membrane and the condensing surface
3. Sweep Gas Membrane Distillation: an inert gas is used as a means for the transportation of the vapor produced to the outside condenser.

4. Vacuum Membrane Distillation: vapor on the permeant side is removed by applying the vacuum and condensed outside the module.[10]

2.3 Groundwater resource

Groundwater can be considered the water found under mineral deposits, in the cracks, sand, and rocks.

This big source is used to satisfy the drinking water demand of more than 50% of the people in the United States, even if the highest exploitation of groundwater is to irrigate crops.

Groundwater, as a natural resource, is dual: on one hand, is a moving resource in the earth's depth, on the other, it is part of the total water resource of the earth. This dual character of groundwater is caused by different features which make this particular resource different from the other, that are:

1. Complete and partial renewability of groundwater
2. Possibility of a new groundwater storage formation
3. Possibility of changing the quality of the resource by human actions

Groundwater is used as a domestic and potable water supply in Australia and many countries of Asia and Africa. Furthermore, it can be used for the industrial process which needs a water supply in many countries.

The main advantages of the exploitation of groundwater resources are surely the availability and high-quality together with better protection from pollution. Besides, they are not exposed to seasonal variation or fluctuation.

The main negative aspects of groundwater withdrawal are the reduction of the reservoirs and possible changes in the landscape. [11]

One of the most used techniques to extract water from the ground is the wellpoint system. It is mostly applied in areas where the soil is permeable by porosity such as gravel, sand, and clay.

The wellpoint system is constituted by a series of wellpoints, installed in the area of the ground where the aquifer must be lowered, and connected between each other and with a high level of vacuum pump through a series of collectors, connections, and connecting joints.

The working principle of this technology is based on the deviation of the water flow in the direction of filtering elements (wellpoints) depressed by the pump. The pressure

gradient created between the atmospheric pressure and the filtering elements directs the groundwater flow towards the latter with a speed that depends on the permeability of the different soils.

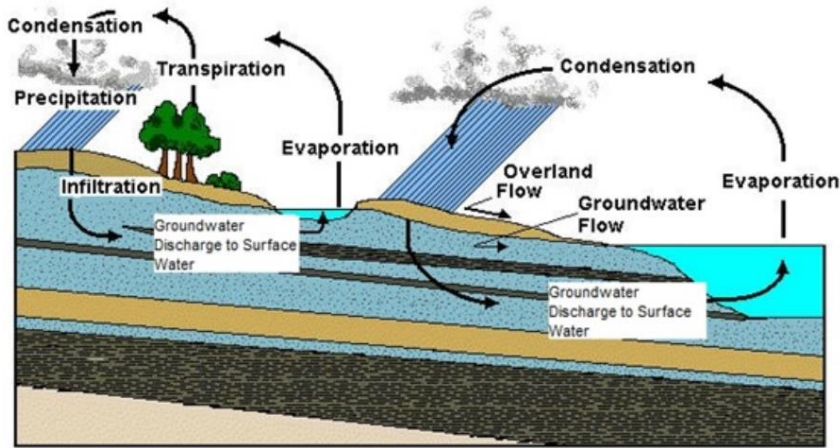


Figure 2.9-Groundwater resource[12]

2.4 Atmospheric Water Harvesting

Atmospheric Water Harvesting (AWH) technologies can be classified according to the working principle, which are the condensation technology, sorption technologies, and other minors.

Condensation technologies utilize different refrigeration methods like vapor compression cycle and thermoelectric cooling for condensing water vapor.

Most of the water harvesting processes are operated only in the case of electrical supply and for this reason, it is looking for innovative solutions such as renewable energy-powered Vapor Compression Cycle, solar chimney, or geothermal cooling system.

The performances of the condensing technologies can be measured in terms of harvested water mass per hour (WHR) and the power consumption per unit mass of water harvested (UPC). High WHR and low UPC are required to have a good performance because more water can be produced in a given time with a lower amount of power required.

2.4.1 Condensation technologies

Condensation technologies use a refrigeration cycle based on vapor compression heat pumps or absorption chillers to cool the air under the dew point and condense the moisture.

The vapor compression refrigeration cycle involves mainly four components: compressor, condenser, expansion valve, and evaporator.

The first step is compression, here the refrigerant enters at low temperature and pressure. The compression takes place to increase the temperature and refrigerant pressure but this process requires a certain amount of work, so an electric motor may be used. After this stage, the refrigerant leaves the compressor and goes into the condenser.

In the second step, the hot compressed vapor can be condensed with either cooling water or cooling airflow across the coil of the tube of the heat exchanger, and the heat released is carried away.

The condensed liquid refrigerant in the thermodynamic state of saturated liquid passes through an expansion valve to reduce its pressure. This process results in adiabatic flash evaporation which causes a temperature reduction of the liquid and vapor refrigerant mixture.

The cold mixture is later sent to the evaporator. A fan circulates the warm and humid air in the confined space around the tubes which transport the cold refrigerant liquid and vapor mixture.

The warm air can evaporate the liquid part of the cold refrigerant and at the same time, the circulating air is cooled below the dew point temperature producing water. Different studies showed that the water harvested rate (WHR) for these technologies was around 1.50 kg h^{-1} when the ambient dry bulb and wet bulb temperatures were 26.7°C and 19.4°C , respectively.

It was also found that the WHR is largely influenced by the inlet relative humidity of the dehumidification air. At 35°C of inlet air temperature, when the relative humidity is increased from 20 to 40%, WHR is increased up to 2 kg h^{-1} . It means that a higher

humidity ratio is beneficial for water harvesting when using a vapor compression cycle.[13]

Figure 2.10 shows an example of water harvesting employing a vapor compression cycle.

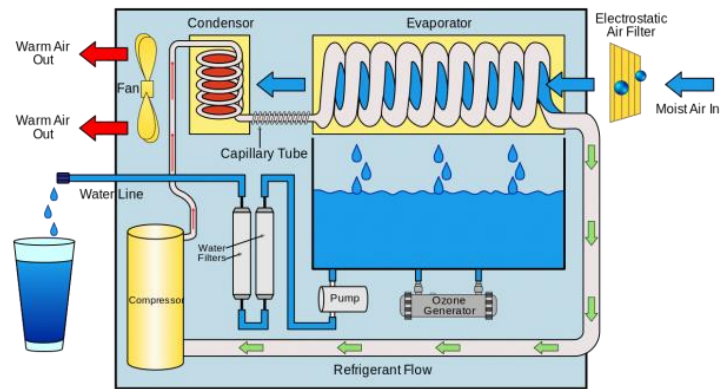


Figure 2.10-Vapor compression cycle for water harvesting[14]

Thermoelectric coolers are devices based on the Peltier effect. A Peltier thermoelectric heat pump is a solid-state active heat pump that transfers heat from one side of the device to the other through electric energy.

When an electric current passes through the two sides, it produces a temperature difference, so that one side gets cooler and the other side gets hotter.

The most important advantages that make thermoelectric coolers applied to refrigeration for the classic vapor compression cycle is the lack of moving parts or circulating liquid, long life, small size, and flexible shape.

A typical TEC system is constituted by several thermoelectric coolers connected in series: air flows through two channels on the cold and hot sides of the device.

The entering air stream first passes through the cold side of the thermoelectric cooler where it is cooled and dehumidified, and after that, the air goes through the warm channel to the hot side of the thermoelectric cooler. Here the dehumidified air condenses producing a certain amount of water.

The coefficient of performance of this technology depends on the thermoelectric length: a typical reasonable value of this parameter is about 1.5 for cooling mode and 2 for heating mode.

Another significant aspect that significantly affects the performance of TECs is the electrical current: the amount of current needed must be determined to achieve the optimal cold side temperature.[15]

Figure 2.11 illustrates the scheme of a thermoelectric cooling system.

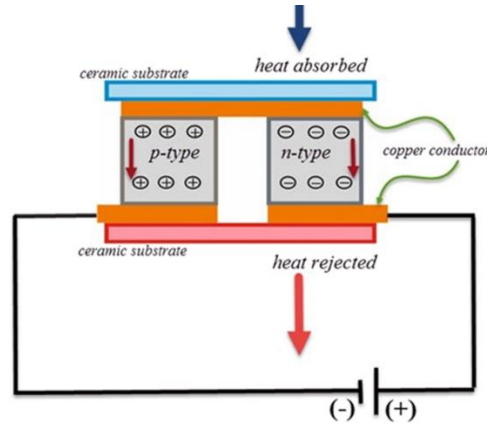


Figure 2.11-Scheme of a thermoelectric cooler[15]

An important study carried out by Farshid Bagheri [16] shows the performance and limitation of three types of atmospheric water harvesting systems driven by electrical power, manufactured in the United States, Canada, and China.

The tests are made under different climatic conditions and results have been analyzed to determine the realistic functionality, performance, and limitation of the tested AWH systems.

The test-bed was equipped with a large environmental chamber to provide the inlet air stream with a wide range of temperature and relative humidity to mimic different climatic conditions.

Figure 2.12 shows a schematic of the set-up of the test-bed:

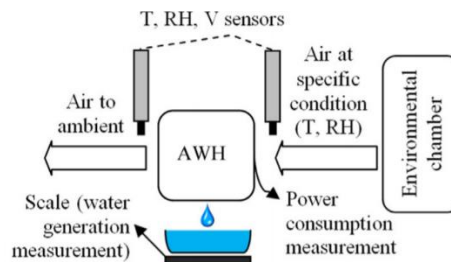


Figure 2.12-Scheme of a testing system[16]

The temperature and relative humidity have been varied from 0-45°C and 10-100% respectively.

Investigating the variation of water harvesting and energy consumption rates for each

test, it has been noted that the temperature and relative humidity are not the most important parameter but also the water content and the dew point temperature play an important role.

As expected, the results show that the water harvesting rate increases at higher water content and the energy consumption per liter of harvested water decreases when the water content or the dew point temperature increases. At higher temperatures, the rate of water harvesting will decrease and the energy consumption per liter of water will increase.

In conclusion, it is possible to say that the higher water harvesting rates, or the lowest rate of energy consumption per liter, appear in areas with simultaneous low air temperature and high-water content or dew-point temperature.

The average water harvesting rate varied from 0.05 L/h for cold and humid conditions up to 0.65 L/h for warm and humid climates, while the energy consumption changed from 1.02 kWh/L for warm and humid to 6.23 kWh/L for cold and humid climates.[16]

2.4.2 Sorption technologies

In an **absorption chiller**, a thermal compression of the refrigerant is achieved by using a liquid refrigerant/sorbent solution and a heat source, replacing the electrical power with mechanical compression. For chilled water above 0°C, typically a liquid H₂O/LiBr solution is used as the refrigerant. An absorption refrigerator changes the gas back into a liquid by using a method that needs only heat without any moving parts.

The general scheme is composed of a generator, a condenser, an absorber, and an evaporator with a working fluid heat exchanger. In between, there should be two valves called the refrigeration control valve and the working fluid control valve.

The absorption cooling cycle can be described in four main steps.

The refrigerant leaving the generator condenses through a condenser and circulates until the evaporator with the help of an expansion valve. The evaporator works at low pressure and the refrigerant boils and evaporates at a temperature of about 0-5°C. Here is a useful effect on where the water is produced.

The cold refrigerant vapor leaves the evaporator and goes into the absorber where the solution is regenerated at an absorber temperature of 30 to 40°C, using the concentrated solution that comes from the generator through a working fluid heat exchanger.

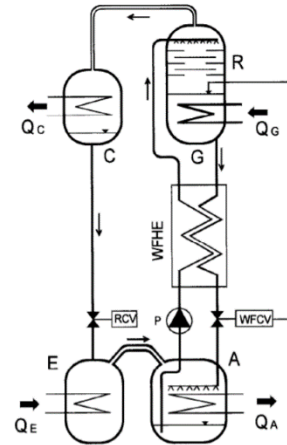


Figure 2.13 on the right-hand side shows a schematic of the process.[17]

Figure 2.13-Absorption chiller

Adsorption and desorption methods are based on the adsorption of water vapor from atmospheric air through the use of solid or liquid adsorbent during the night, and recovery of the extracted water by heating the adsorbent and condensing the water desorbed.

Usually, sorption commercial systems use water as refrigerant and silica gel or zeolite as adsorbent. Since solid sorbent cannot be circulated, the adsorption chillers consist of two separate chambers, both containing the adsorbent. All system is composed of these two chambers, an evaporator, and a condenser, packed in a vacuum-sealed enclosure.

The adsorption process is mainly divided into three steps: the adsorbent containing water is heated and the water is desorbed, pressure increases, and water vapor is exhausted to the condenser where it condensed. As the second step, the condensed water is transported through the throttling valve until the evaporator where it evaporates at low pressure taking up the heat from the chilled water circuit. After that, the water vapor is absorbed in the adsorbent: this process is exothermic so the heat has to be removed by the cooling tower.

The component which presents the desiccant to the air stream is the most critical element of the system.

Theoretically, the desiccant contactor should have an infinitely large surface area for optimal desiccant-air interaction, furthermore, the contact media should be very durable as it is periodically wetted and dried whenever the desiccant moves through the sorption-desorption cycle.

There are many different technologies suited for the construction of the adsorber and regenerator such as a packed bed, spray chamber, or heated coil.

As said before, desiccant materials can be either solid or liquid. Systems that use solid desiccant can produce a high amount of potable water but require a large volume of desiccant. Moreover, high electrical energy is required to feed the blowers to circulate both the fresh air for adsorption and the hot air for desorption. This problem could be solved by adding an air filter, but this solution can cause additional pressure drops. For these reasons, solid adsorbent materials are not so attractive. Innovative materials such as nano porous inorganic material, metal-organic frameworks (MOFs), and composite materials seem to be greater innovative solutions to drive the atmospheric water harvesting system through the adsorption process.

2.4.3 Membrane atmospheric water harvesting

Due to the high amount of latent heat of the water, the energy required to condense water with the classic vapor cycle is usually orders of magnitude larger than the energy required for the water purification method. For this reason, atmospheric water harvesting can be remunerative only in the case of a natural heat sink or in areas where the humidity harvesting unit can be driven by renewables sources like solar or wind energy.

The energy is also needed for cooling the body of air in which the water vapor is embedded: a way to circumvent this sensible heat requirement is to use a water vapor selective membrane to separate the water vapor from the other gases before the cooling process.

The driving force for the separation is the partial pressure difference across the membrane: thanks to the dense polymer membrane which is extremely selective for water vapor, all the other non-desirable gasses and pollutants are not allowed to pass the membrane, in this way the condensed water will be very pure.

The core of the system is a selective membrane subjected to the air stream, where water vapor permeates through the membrane and the remaining dried air is discharged. The driving force of this process is the difference of pressure which is maintained by two components, a vacuum pump that regulate the total pressure on the permeate side and a heat pump which has the role to cool down and condense the water vapor in the condenser. The condensed water is collected in a water collection tank form which can be distributed. The scheme of all system can be sketched as follows :[18]



Figure 2.14- Elementary and complete membrane separation schemes for AWH[18]

3 Materials for Atmospheric Water Harvesting

3.1 Isotherm standard models

The process of atmospheric water harvesting is based on the adsorption capacity of the sorbent material, which uptakes the water vapor contained within the air stream.

Adsorption, as a surface phenomenon, is considered one of the most used separation techniques, in which sorption occurs by the formation of chemical or physical bonds between a porous solid medium and a mixture of liquid or gas component fluid. The solid porous medium provides high micropore volume, leading to high adsorption capacity.

By taking into consideration the equilibrium data and the adsorption properties of the adsorbent and the adsorbate, the adsorption isotherm models are useful to describe the interaction mechanism of the two materials at a constant temperature.

Since the adsorption process depends mostly on the adsorbent, it should have good adsorption capacity and kinetics. Adsorbent material with small pore size but high porosity and high micropore volume, as well as material with large pores, are considered suitable for the success of the adsorption process.

Adsorption is usually described as a chemisorption or physisorption process based on the interaction between the adsorbate and the substrate. Physisorption occurs due to the weak interaction between the two materials, such as London forces, Dipole-dipole forces, and Van der Waals interactions, where the bands can be broken easily.

Isothermic heat is considered one of the basic quantities of the adsorption studies, it represents the ratio of the infinitesimal change in the enthalpy of the adsorbate to the infinitesimal change in the adsorbent amount, and it can be calculated with the Van't Hoff equation.

According to IUPAC (International Union of Pure and Applied Chemistry), adsorption isotherms can be classified into six types based on the isotherm shape.

In the past year, a wide variety of isotherm models have been formulated based on three fundamental approaches, such as Langmuir, Freundlich, Dubinin-Radushkevich, and others.[19]

3.1.1 Henry's isotherm model

Henry isotherm of adsorption is considered one of the simplest formulations, as the partial pressure of the adsorptive gas is proportional to the amount of surface adsorbate.

In this model, all the adsorbate molecules are considered isolated from their closest neighbors. It means that the equilibrium concentrations of the adsorbate in the adsorbent phases are described by a linear relationship:

$$q_e = K_{HE}C_e \quad \text{Eq. 3.1}$$

Where K_{HE} represent Henry's isotherm model adsorption constant and C_e is the equilibrium concentration of adsorbate on the adsorbent (mg/L). [19]

3.1.2 Dubinin-Radushkevich isotherm model

This model is used to describe the adsorption mechanism with the distribution of the Gaussian energy onto the heterogeneous surfaces.

This is a semiempirical model in which the adsorption process follows the mechanism of pore filling.

This model assumes that it is a multilayer character, which involves Van der Waals forces.

The equation that expresses the concentration of the adsorbate in the liquid phase can be expressed with both linear and non-linear form:

$$\text{Linear form:} \quad q_e = q_s e^{-K\varepsilon^2} \quad \text{Eq. 3.2}$$

$$\text{Non-linear form:} \quad \ln q_e = \ln q_s - K\varepsilon^2 \quad \text{Eq. 3.3}$$

Here, q_s represents the theoretical isotherm saturation capacity, K is a parameter that depends on another variable which predicts the adsorption type, while ε can be calculated as:

$$\varepsilon = RT \ln \left(\frac{P_s}{P} \right) \quad \text{Eq. 3.4}$$

Where P_s is the saturation vapor pressure and P is the adsorbate equilibrium pressure. This parameter will reflect the Gibbs free energy change of the adsorbent after the adsorption of a unit of the molar mass of the adsorbate.[19]

3.1.3 Langmuir isotherm model

Langmuir's theory is based on the concept according to which the adsorption process in a solid surface is based on a kinetic principle where there is a continuous shelling of the molecules towards the surface together with molecules' evaporation from the surface with a zero-accumulation rate at the surface. It means that the adsorption or desorption rates are equal.

Langmuir classified six different types of adsorption mechanisms according to different surface chemistry and structural geometry of solid material.

- I. Single-site adsorption: is the simplest case of gas-solid adsorption, where the surface has an equal adsorption site which can host only a single adsorbate molecule
- II. Multisite adsorption: more than one type of adsorbent sites are available on the surface but each site can host only one adsorbate molecule
- III. Generalized adsorption: the adsorbent material is treated as an ungovernable number of adsorption sites where the adsorption isotherm follows the binding energy distribution.
- IV. Cooperative adsorption: in this case the adsorption sites are identical but they can host more than one molecule of the adsorbate.
- V. Dissociative adsorption: here the adsorption is assumed to be performed in a two-fold process: chemical bonds cause the residence on the surface adsorption site and the molecular dissociation, then it will be submitted to the desorption process where two atoms have to reassociate into a molecule and leave the surface.
- VI. Multilayer adsorption: each adsorption site is independent and identical, and there is no limit on the number of adsorbed molecules.

Figure 3.1 depicts the six different type of adsorption isotherm described above:

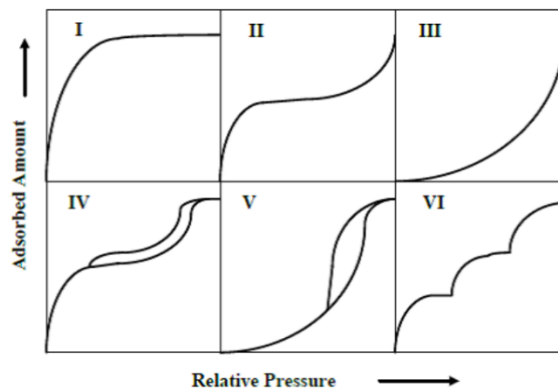


Figure 3.1- Six types of adsorption isotherm[20]

Differently from the Dubinin model, the Langmuir isotherm adsorption model is an empirical model, and it is based on the following assumptions:

- Mono-dimensional covering
- All sites are energetically equivalent
- The adsorption mechanism is a reversible process
- Only interactions between adsorbate and adsorbent are considered, all the others like those between two molecules of adsorbate are neglected

The adsorption isotherm which expresses the equilibrium concentration of the adsorbate can be expressed in the linear or non-linear form:

Linear form:
$$q_e = Q_0 - \frac{q_e}{bC_e} \quad \text{Eq. 3.5}$$

Non-linear form:
$$q_e = \frac{Q_0 b C_e}{1 + b C_e} \quad \text{Eq. 3.6}$$

Where Q_0 represents the maximum monolayer coverage capacity, b is the Langmuir isotherm constant, and C_e is the equilibrium concentration of the adsorbate on the adsorbent.[19]

3.2 Materials for solid cycles

Silica Gel Silica gel is an incompletely dehydrated polymeric structure of colloidal silicic acid with the formula $\text{SiO}_2 \cdot n\text{H}_2\text{O}$. This material is constituted by microspherical particles with a diameter of 2-20 nm, bonding together to construct the adsorbent silica gel.

This material exhibits an adsorption capacity of water vapor up to 30-40% of its dry mass, and a regeneration capability at low heat source temperature from 50 to 90°C.[21]

The surface properties of silica gel depend on the presence of silanol groups, which can make such a surface hydrophilic. The OH groups within the surface act as the center of the molecular adsorption during their interaction with the adsorbate which can form hydrogen bonds with the OH groups.

It means that the properties of silica gel are determined by the chemical activity of the surface, which rely on the distribution and concentration of the OH groups and the presence of the siloxane bridge, and by the porous structure of the material.[22]

Silica-gel/water is one of the most preferred working pairs because it is not toxic, stable over a wide range of operating temperatures, moreover, it also requires low regeneration/desorption temperature.

The adsorption capacity of silica gel can be tested both using a volumetric or gravimetric method. The volumetric one is developed by monitoring the pressure change during the adsorption, while the gravimetric method measures directly the adsorbent capacity by using mass balance at specific operating conditions.

Experimental tests carried out on two different types of silica gel at different pressure and temperature, have demonstrated that the maximum water uptake from silica-gel is around 0.38-0.48 kg/kg.

From the graphs displayed in Figure 3.2, it is possible to point out an inflection point at a relative pressure of 0.4: this can be attributed to the fact that the region of adsorption isotherm where the relative pressure is higher than 0.4, is typically dominated by capillary condensation. [23]

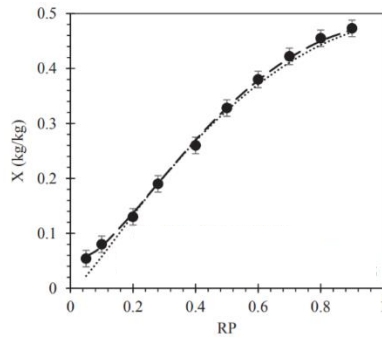


Figure 3.2-Water sorption isotherm for silica-gel[23]

Zeolite Natural zeolites are hydrated aluminosilicate minerals with porous structure and useful physicochemical properties such as cation exchange, catalysis, and sorption.

In the past decades, the use of natural zeolites was focused only on ammonium or heavy metal removal, but in recent years applications of natural zeolites for water or wastewater treatment have been realized. Zeolite can be also used to thermodynamically store solar heat harvested from solar thermal collectors or for adsorption refrigeration. In these applications, the ability of this material of high heat adsorption and to hydrate and dehydrate while maintaining their structural stability is exploited.

The adsorption cycle which uses zeolite-water or silica gel/water as adsorbent-refrigerant pairs has evident advantages as they can be driven by heat at low temperatures. Moreover, the systems are not corrosive and require no moving part which leads to less need for maintenance.

The properties of zeolite FAM Z01 (Functional Adsorbent Material) have been studied by Aung Myat et al. [24]. The advantage of zeolite FAM Z01 over silica gel is that the regeneration can be performed at temperatures between 50 and 80°C.

The adsorption property investigated is the equilibrium uptake of water vapor at different temperatures.

The water uptake has been set in comparison with the relative pressure, defined as the ratio between the vapor pressure of the reactor bed and the saturation pressure at a given temperature.

With an adsorption temperature of 25°C (298 K), which corresponds to a saturation pressure of 3.17 kPa whilst an adsorption pressure of 0.8 kPa, the relative pressure will be equal to 0.25.

As shown in Figure 3.3, the corresponding amount of adsorbate water is about 0.19 kg of H₂O/kg of dry mass of zeolite FAM Z01.

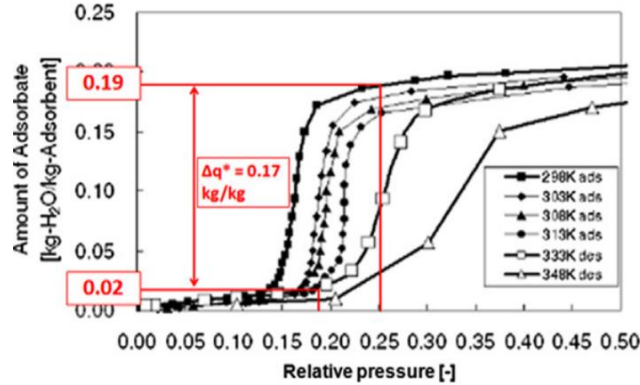


Figure 3.3-Water uptake with zeolite as adsorbent [23]

During the desorption phase, the relative pressure is around 0.18, so the corresponding equilibrium uptake is approximately equal to 0.02 kg of H₂O/kg of dry mass of FAM Z01.

The average adsorption capacity would be equal to 0.17 kg H₂O/kg of dry mass of FAM Z01 at an adsorption and desorption temperature of 298 K and 333 K respectively.

MOFs Metal-organic Framework is porous and crystalline materials constituted from organic and inorganic building blocks with a high surface that can host a larger amount of water vapor.

Zr₆O₄(OH)₄(-COO)₁₂ secondary building units are linked together with fumarates to form MOF-801. The structure of MOF-801 contains three symmetrically cavities where the water molecules can be captured.

The advantages of this material are firstly its very good performance due to the high aggregation of the water molecules into clusters within the pores of the MOF, then it is very stable and widely available at low-cost.

Figure 3.4 shows the process of water harvesting by using metal-organic framework material:



Figure 3.4-AHW with MOFs[25]

The MOF water harvesting system is composed of a MOF layer and a condenser, undergoing solar-assisted water harvesting and adsorption process.

As indicated on the left-hand side of the previous figure, during the water harvesting process the desorbed water vapor is condensed at ambient temperature through the use of a passive heat sink so avoiding the need for additional energy sources.

During the adsorption process shown on the right-hand side of the picture, the water vapor is adsorbed by the MOF layer, and the adsorption heat is released to the surrounding environment.

To use MOF to harvest water for atmospheric air with high revenue and minimum energy consumption, an isotherm with a steep increase in the water uptake within a restricted range if the relative humidity is required.

Recent studies have demonstrated that the metal-organic framework (MOFs) is particularly suitable for application in areas as North Africa where the relative humidity is around 20%.

For MOF-801, in a temperature range of the inlet air between 25°C and 65°C, it is possible to harvest more than 0.25 l/kg of air. Figure 3.5 displays the behavior of the water adsorption isotherm of different MOFs materials at 25°C, which show a rapid increase in the water uptake with a small change in the relative humidity.[25]

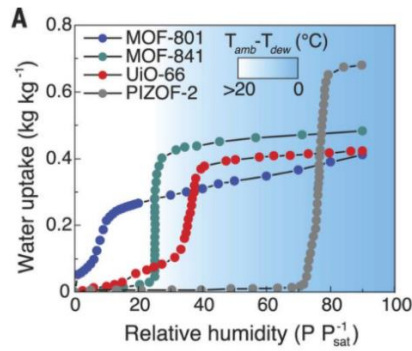


Figure 3.5-Water uptake with MOFs[25]

ACF Active Carbon Fiber is a well know physical adsorbent in many adsorption applications, due to its uniform distribution and small diffusion distance.

Even if ACF seems to have not high water adsorption capability, it can be adopted as a host matrix for hygroscopic salt composite which increases the amount of water sorption. Salt ions adsorb the water vapor molecules by a hydration reaction, which occurs only on the surface of the particles exposed to the air stream, so it means that the inner part of the salt's crystal is not getting involved in the adsorption process.

Many studies have demonstrated that a composite of ACF and LiCl can be able to uptake around 2.9 g of water per kg of adsorbent with a relative humidity of 70%. This solution seems to be not adequate for a water harvesting system because it should be improved in terms of adsorption capacity and prevention of leakage.

For this reason, another application where LiCl salt is incorporated into the magnesium sulfate has been investigated.

LiCl salt absorbs the water vapor and converts it into hydrated salt: this process continues until the salt is fully hydrated. After that, the hydrated LiCl adsorb more water vapor to form liquid droplets. The function of MgSO₄ is only to increase the ability of the matrix to keep more water by absorbing the excess water produced from LiCl salt.

Performing some experiments at different levels of relative humidity, it has been demonstrated that the sorbent water and consequently the collected water per each gram of adsorbent, reach the values of 2.3 and 1.5 g/g respectively, at 70% of relative humidity.[26]

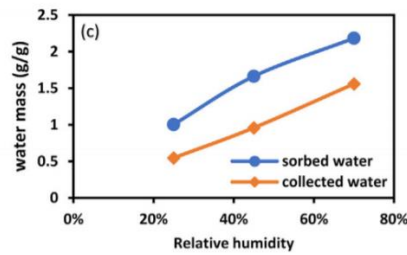


Figure 3.6-Water mass uptake from ACF/LiCl/MgSO₄ composite[26]

SWS (Selective Water Sorbent) Typically, an SWS is a two-phase system that consists of two porous host matrices and a hygroscopic substance that could be also an inorganic salt, impregnated into pores.

Silica-gel or γ -alumina can be used as a host material, while Lithium bromide or calcium chloride can be used as hygroscopic salt.

Aristov et al. [27] developed an interesting study about the sorption properties of an SWS material made up of mesoporous silica-gel as a host matrix and calcium chloride as hygroscopic salt. The isotherm sorption curve is represented as N as a function of the relative pressure, where N represents the number of water molecules sorbed concerning one molecule of calcium chloride.

Looking at Figure 3.7, it is possible to recognize a one-to-one correspondence between the amount of water sorbed and the relative pressure defined as the ratio P_{H_2O} / P_0 of water vapor.

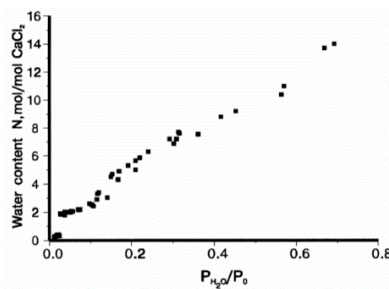


Figure 3.7-Absorption isotherm for SWS materials[27]

It is found that the equilibrium water content depends strongly on the relative pressure and at the value of the relative pressure equal to 0.7, the corresponding equilibrium water content may reach 0.7-0.8 of water adsorbed by 1 g of SWS. So, these types of materials have a high sorption capacity.

The efficiency of water production from an atmospheric water harvesting system that uses SWS as sorbent material depends on the climatic conditions and it is expected to increase with the rise in the difference of temperature between day and night, and consequently between their relative humidity.

4 Sodium Alginate

The purpose of this thesis is to make an in-depth study of an innovative material that can be used as a sorption material in a water harvesting system to be installed in areas with an arid climate where water scarcity is one of the most important problems.

The innovative material is sodium alginate which, as mentioned in previous studies, can lead to many advantages, such as:

- **Large water uptake capacity** in the arid climate
- The **manufacturing process** for the construction of this innovative sorbent material does not involve any toxic compound.
- The **production process** of the material and the other composites don't require particular efforts

4.1 Current application

The following section will describe the most important applications of the alginate material in different fields.

Nowadays only a few articles focus on water harvesting applications, the preferred field is the biomedical one for drug delivery applications or procedures for the immobilization of cells.

4.1.1 Water harvesting application

Some studies have been performed to test this material for different applications, and by analyzing these papers, many differences with this new technology proposed were just come out.

In the past two decades, alginate has emerged as one of the most popular and the most effective encapsulation material for the controlled delivery application.

An interesting recent article focused on the investigation of the performances of a composite material made up of calcium chloride incorporated into an alginate-derived matrix.

Here, CaCl_2 is used as a source for the ionotropic gelation of a sodium alginic acid solution. Droplets of alginate solution are dropped into the CaCl_2 solution, to form spherical hydrogel beads. After the initial hydrogel formation, ions of Ca^{2+} and Cl^- diffuse into the hydrogel sphere until an equilibrium of the salt concentration is reached.

The experiments conducted to investigate the isotherm of adsorption of this material were performed under three different temperatures of 28°C , 65°C , 85°C , while the water vapor pressure was stepwise increased.

The results show that at 65°C and 30mbar of water vapor pressure, a water uptake of 17%wt was observed. At 85°C , no mentionable water uptake can be noted, while at 28°C it is possible to recognize the highest value of water uptake from composite.[28]

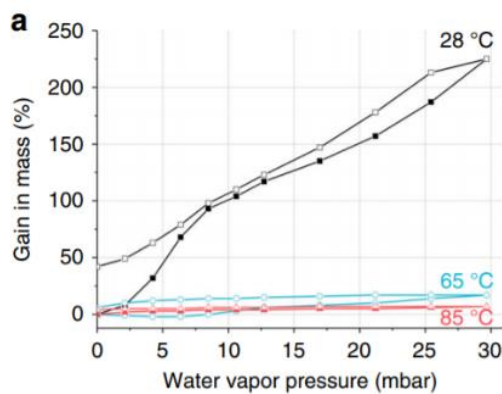


Figure 4.1-Water sorption isotherms of the composite Alg- CaCl_2 [28]

4.1.2 Removal of lead from water

Calcium alginate beads doped with hydrazine sulfate-treated red mud can be also used as adsorbers to remove lead ions from water.

It has been tested that this material has 138.6 mg/g adsorption capacity towards Pb^{2+} ions. The behavior of the adsorbent towards lead ions mainly depends on the solution pH: by varying the pH from 2 to 12, the optimal pH for the successful removal of the lead is around 6.

The % of removal still depends also on the concentration of lead ions, in particular when the concentration increases from 25 mg/L to 200 mg/L, the % of removal decreases from 100 to 57%.[29]

4.1.3 Drug delivery application

Drug delivery systems such as microsphere and nanoparticles have been utilized to overcome the weakness of traditional drug administration in terms of therapeutic efficiency and patient compliance.

Drug delivery is a system that transports therapeutic substances into the body to achieve a desired therapeutic effect.

In this context, the alginate microsphere is one of the materials most studied because it offers both control of drug release rate and delivery of the drug to a specific treatment target: they act as a cover to protect the encapsulated drug such as enzymes, proteins, or peptides.

Microspheres are characterized as powders consisting of a natural or synthetic polymer, which are biodegradable. The selection of polymers used to prepare the microsphere plays a crucial role in the drug delivery process; there are two types of polymers, natural or synthetic. Natural polymers are gelatine or polysaccharide (e.g. alginate), while synthetic include non-biodegradable polymers such as silicone and biodegradable ones like polylactic acid.

Natural polymers offer many advantages such as natural abundance, low cost, and renewable sources in nature. Alginate is utilized in many applications because of its properties of inexpensiveness, nontoxicity, and biodegradability. Three different methods can be used to produce the alginate microsphere which are the spray drying techniques, extrusion process, and emulsification /gelation techniques.

The parameters that influence the properties of drugs loaded with the alginate microspheres (AMs) are of course the particle size and their distribution, and these features will influence their drug release kinetic and therapeutic efficiency. The particle size strictly depends on the AMs characteristics, including alginate concentration, an oil phase, surfactant, cross-linker concentrations, or cross-linking

time. High alginate concentration is also effective in improving the drug, which was 100% at 3% w/v of alginate concentration.

Alginate concentration is one of the most important factors that affect the behavior of the alginate microspheres: from different studies, it can be summarized that the mean particle size increases with the increase of the alginate concentration. This phenomenon occurs because increasing the alginate concentration, will lead to an increase in viscosity of the alginate solution, which raises the interfacial tension between alginate droplets and the oil phase. Hence, larger micropores are formed. It means that increasing alginate concentration leads to a rising number of entrapped drugs.

Furthermore, some studies have demonstrated that the size and the size distribution of the microspheres are also dependent on the viscosity of the oil phase, and on the cross-linking time: the particle size of the alginate microsphere increase by increasing the cross-linking time.

The procedure of the drug delivery can be obtained by following two different pathways: drug release through the degradation of the alginate network or the diffusion of the drug through the alginate network. The degradation of the alginate could lead to a dramatic release of the drug, and for this reason, this way is not optimal for controlling the release of the drug.

Hence, alginate microspheres have been applied in the drug delivery based on the diffusion pathway, so the drug diffuses out through the swell polymer network.[30]

4.1.4 Alginate and immobilization of cells

Calcium alginate balls are becoming the most common vehicle for the delivery of live cells.

The cell suspension is mixed with an alginate sodium solution and subsequently, this mixture is dripped inside a gelling bath containing multivalent cations (usually calcium ions) so that every single drop instantly freezes trapping cells in a three-dimensional lattice as illustrated in

Errore. L'origine riferimento non è stata trovata..

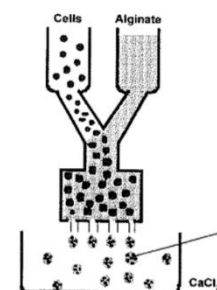


Figure 4.2-Incapsulation of live cell in alginate matrix [31]

The immobilization of live cells can be applied in different contexts:

- In the industrial sector, where it can be utilized for the immobilization of yeast or the ethanol production
- In the agriculture sector, it can be adopted in the production of artificial seed
- In medicine, where the immobilized cells can be used for transportation purposes, for treatment of human pathology

In the latter application, the main role of the alginate gel is to act as a barrier between cells transplanted and the host immune system.

One of the most important problems of the encapsulation of cell technique in the alginate matrix is that not always it is successful.[31]

4.2 Production process

Alginates are a family of linear copolymers with homopolymeric blocks linked β -D-mannuronate and its C-5 epimer α -L-guluronate residues.[32]

These are linked together in different sequences to form an egg-box model shown in Figure 4.3.

There are two conventional ways to gel alginate: by lowering the pH below a certain set point, or by introducing cations.

Two different types of alginate have been produced in the laboratory of the DENERG department within the Politecnico of Turin.

The two materials are solutions of water and alginate at 2% concentration, which were jellified by using a water and calcium chloride solution at 40% and 5% of concentration. In this analysis, only the material at 5% of concentration has been tested.

The production of alginate is divided into two main steps. The first step relates to the formation of the salt solution at 40% and 5% of concentration and this can be done by putting a certain amount of water within a beaker and adding gradually the calcium chloride mixing continuously the solution to avoid the formation of particles in the bottom part of the beaker. The mixing procedure can be done both manually with a plastic rod or with a magnetic mixer.

The second step relates to the formation of the alginate solution with water at 2% concentration. This process can be done by putting the alginate powders into a glass

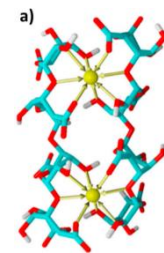


Figure 4.3-Egg-box model of alginate

backer and adding step by step the water trying to do not bring the dust into the surface. To mix the two components, a hand blender may be used by paying attention to the formation of clumps.

After that, the dripper is activated to construct the alginate balls: a circulation pump is activated which has the role to take the alginate and water solution from the backer until the emptying of the container, at the same time the solution pass through the dripper and is percolated within the salt solution where there will be an exchange of Ca^{2+} ions. In the end, the mixture must be closed with a transparent foil and left to rest for 24 hours. As the last steps, the alginate balls were retrieved from the salt solution and left to stand for the other 24 hours, after that the alginate balls are bake into a desiccator at maximum temperature condition. Once cooked, they are stored in a box hermetically closed.

The sodium alginate, polymer constituted of repeating blocks of guluronate and mannuronate monomers, is the starter of a cross-linking process that, in the presence of an ionic solution with water and divalent cations (Ca^{+2} , Mg^{+2} , etc...), leads to the jellification of the viscous fluid into a solid hydrogel.

The crosslinking process, transforming the viscous gel in a solid hydrogel, is realized with an ionotropic gelation technique in which the Na^+ , contained as a functional group in the alginate, is exchanged with Ca^{+2} cation dissolved in a water solution. Having calcium a higher valence number, it can activate a cross-linking among the different polymeric chains of the alginate, realizing the so-called egg-box geometry.

In this thesis, a deep study on the properties of the alginate balls produced with calcium chloride and water solution was developed.

The application of this innovative material for the water harvesting system can lead to numerous advantages because it is a component characterized by high water uptakes in a larger spectrum of operative environments and low regeneration temperature.

Errore. L'origine riferimento non è stata trovata. shows the adsorption capacity of the polymer at different temperature and pressure of the water vapor in equilibrium. It is shown that during the adsorption phase, where the temperature is no more than 30 °C and the vapor pressure is between 0.8-1 kPa, the water uptake can reach values as

much as 80% of the dry basis. This number is very high in comparison to that of the silica-gel sorption material.

The regeneration can be carried out at a temperature as low as 60°C, through which it is possible to reduce the water content by up to 10%.

These properties are achieved thanks to the high internal porosity of the material.

The proposed study aims to analyze an innovative material for the realization of a high-performance adsorption heat exchanger.

The adsorption heat exchanger is a component that works in a batch process and performing co-located heat and mass transfer. The working principle is based on continuous cycles of adsorption/release of water vapor combined with the thermal exchange between the sorbent material and a source of cold/hot. The heat transfer together with the mass transfer phenomena leads to a high rate of water vapor exchanged between the humid air and the sorbent material.

During the adsorption phase, the stream of humid air is put in contact flows through the channel realized with the sorbent polymer. In the contact area between the air and sorbent, the water vapor is separated from the humid air and stored within the pores of the hygroscopic polymer. Being an exothermic process, a high amount of heat is released, increasing the equilibrium temperature of both air and the sorbent material. The heat exchanger medium can remove the heat of adsorption from the hygroscopic material performing an isothermal or subcooled process, by transferring the produces adsorption heat to a cooling fluid and rejecting it to an external heat sink.

An impermeable frame separates the cooling fluid from the sorbent material, preventing the bypass of water and allowing the transfer of energy. At the end of the process, the air exiting the sorbent material is drier and colder than the inlet, in this way it can be utilized for air conditioning applications or industrial processes. When the saturation of the sorbent material is reached, the adsorption heat exchanger has switched for the regeneration phase, by inverting the direction of the heat and mass transfer. So, the cooling fluid is substituted with a heating one that has the task to deliver heat to the sorbent material. This process provides energy to the water molecules trapped into the pores of the hygroscopic material, actuating a diffusive flux of water from the wet sorbent to the air that flows in the same channel. The outlet air stream is now hot and extremely wet, with a very high dew point. In this way the

condensation at ambient temperature is spontaneous and the water can be collected in a proper tank. The regeneration process continues until the sorbent material reaches its dry state.

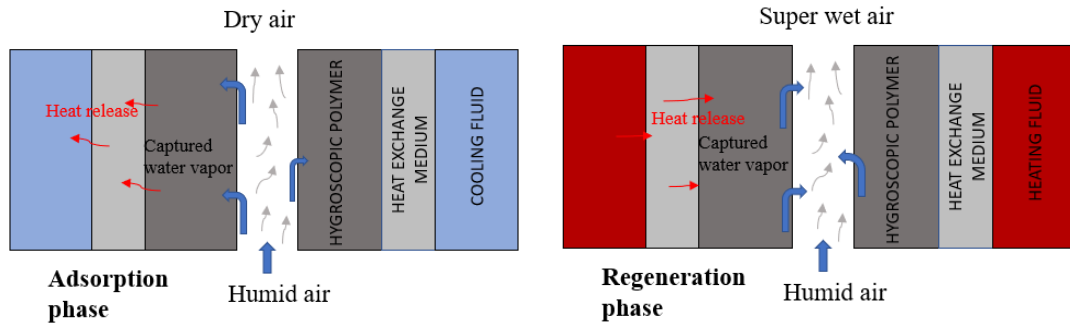


Figure 4.4-Adsorption and regeneration phase of the water harvesting system

5 Experimental testing

The following paragraph will be describing all the testing procedure and their results in terms of water content within the sorbent material or capacity of water uptake.

5.1 Equipment and materials used

The equipment used to obtain the adsorption properties of the testing material is a moisture analyser Kern DBS 60-3.

It is used to quickly and reliably determine the moisture content of liquid, porous and solid substances based on the thermogravimetric analysis. Through constant measurements of the weight changes during the drying process, the moisture analyser allows to "extract" all the humidity present in a sample. Results are presented in terms of initial wet weight, dry residual weight, and % of moisture present initially.

With the moisture analyser, the heating process goes from the inner side to the outside, and it occurs thanks to the radiation from the halogenic lamp which enters the sample, and here it is transformed into thermal energy.

The complete characteristics of the moisture analyser are listed in Table 5.1.

Radiator type	Halogen
Range of Temperature	50°C-200°C
Maximum load	60 g
Minimum weight	0,02 g
Reading accuracy	0,01%
Drying mode	1. Standard drying (AUTO) 2. Gradual (STEP) drying 3. Rapid drying (RAPID) 4. Protective adsorption (SLOW)
Dimensions	202 x 336 x 157 mm

Ambient conditions	1. Ambient temperature: 5°C-40°C 2. Maximum humidity: 45%-75%
Criterion of shutdown	<ul style="list-style-type: none"> · AUTO: the drying process stops when the weight loss is stable for 30 seconds · TIME: the drying process ends after a predetermined period.
Unit of measures	[M/W]: [%] of humidity [D/W]: % of dry weight.
Degree of pollution	2

Table 5.1-Properties of moisture analyser

The sketch of the design of the moisture analyser is shown in Figure 5.1

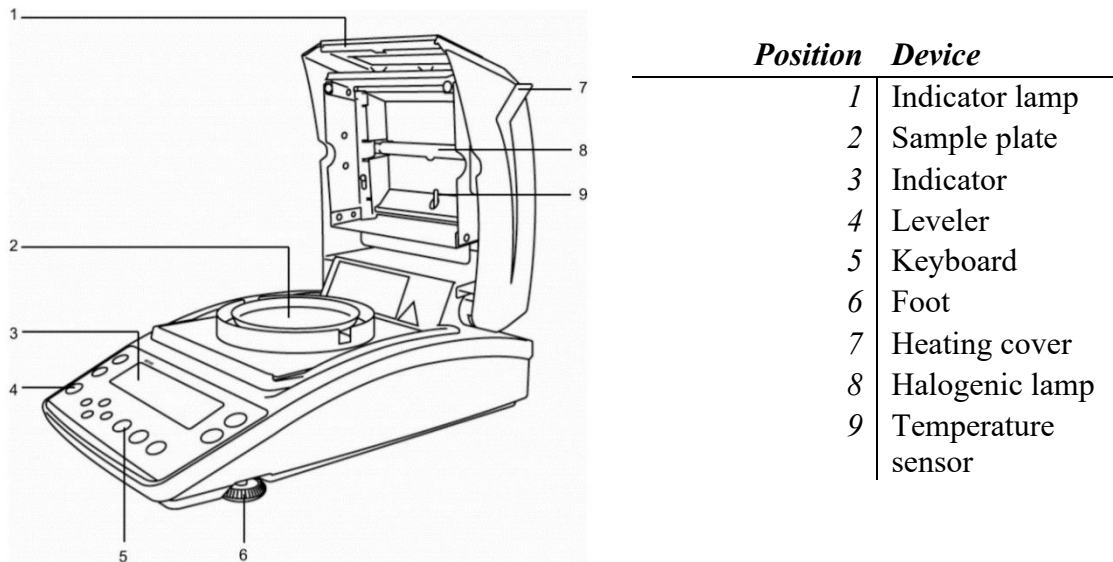


Figure 5.1- Scheme of the thermobalance

The materials under investigation are sodium alginate with spherical form and silica gel balls.

Before testing, they have been prepared to reach specific conditions in terms of temperature and relative humidity.

In particular, three samples of silica gel and three samples of alginate have been tested to explore different conditions. Before the real test, some measurements have been done employing two silica gel samples to test the properties of the moisture analyser.

The first sample of silica gel for the trial tests was prepared within a closed glass box filled with water, where many silica gel balls were inserted into a baker providing a multilayer structure.

The second sample of silica gel balls was arranged in an aluminum dish, so providing a monolayer structure, deposited over 2 wet paper towels, and then covered by a plastic box.

These processes should bring the material to the saturation point, but here no sensors were inserted to monitoring the thermohygrometric conditions.

For the real tests, alginate and silica gel samples were prepared in two concentric plastic boxes, the bigger one was filled with water or any other solution, while in the smaller ones, the material was inserted with the aluminum dish providing a monolayer texture. The overall closed structures were equipped with temperature and relative humidity sensors to check the initial ambient condition before the tests.

5.2 Testing protocol

The preparation of the samples has to be done one at a time because in this way should be avoided the relative exchange of humidity between the sample and the ambient.

Moreover, the uneven extension of the sample in the aluminum dish could produce the non-homogeneous heat distribution in the dried sample, resulting in an incomplete drying or prolonged drying time.

Before inserting the sample of any material, the balance should be tared and it can be done by close the cover of the moisture analyser and press an appropriate button.

At that time, after setting all the variables requested by the balance, the aluminum dish is filled with the material and the process begin.

The engine relates to a personal laptop, where the data are sent every five seconds, according to the selected output desired.

Subsequently, all these data were reorganized and analyzed using different plots.

5.3 Trial test

Two trial tests were performed to understand the behavior and the characteristic of the moisture analyser.

5.3.1 Silica gel tests – sample 1

The first set of tests was performed on the silica gel prepared in a glass box covered, trying to reach the saturation condition.

Because no temperature or relative humidity sensors have been installed to control these parameters, there is no valid information about the initial condition of the material inserted in the moisture analyser. It is only possible to deduce that the sample was at an ambient temperature equal to 21°C.

The moisture analyser properties set for these experiments are visible in the table below:

<i>Test Number</i>	<i>Temperature</i>	<i>Mode</i>	<i>Time</i>	<i>Output</i>
1	50°C	TIME	6 h	M/W [%]
2	120°C	TIME	1:10 h	M/W [%]
3	200°C	TIME	3:00 h	M/W [%]

Table 5.2-Properties of tests for sample 1

The difference in the number of hours at which the test was performed is that for the test performed at 120 and 200°C, monitoring the output data it was evident that the percentage of moisture extracted was constant in the last 10 minutes. So, it means that the regeneration process was completed.

The results obtained from the data collected are shown in the figures below:

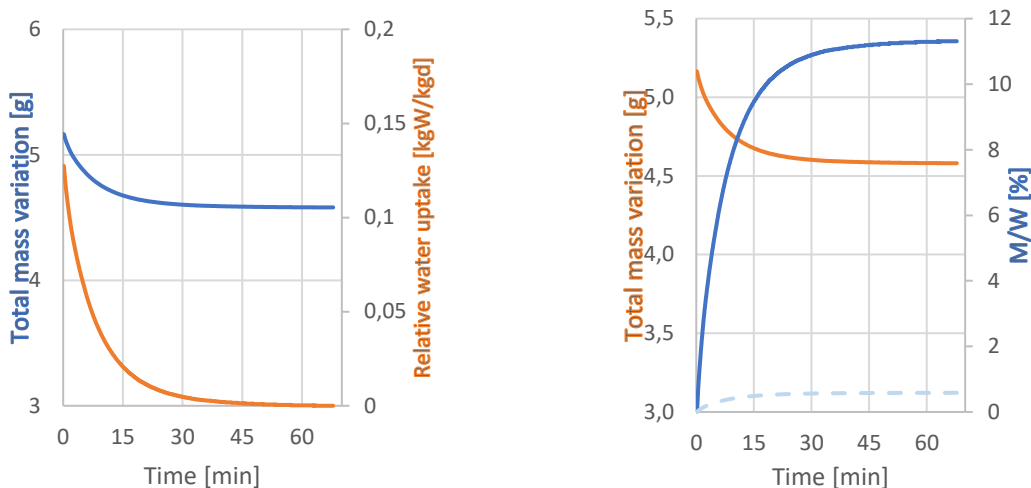


Figure 5.2- The graph on the left-hand side shows the behavior of the total mass variation during the regeneration process (blue line) and the water uptake for the test performed at 120°C; on the right-hand side it is shown the behavior of the water content extracted from the sample with respect the initial wet mass, and the total mass variation for the test at 120°C. The dashed line represents the amount of water extracted from the sample.

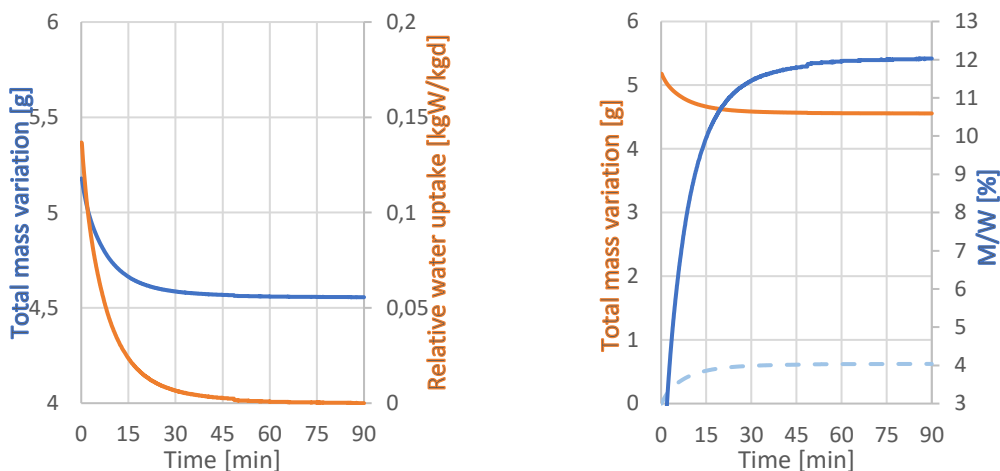


Figure 5.3- The graph on the left-hand side shows the behavior of the total mass variation during the regeneration process and the water uptake for the test performed at 200°C; on the right-hand side it is shown the behavior of the water content extracted from the sample with respect the initial wet mass, and the total mass variation for the test at 200°C. The dashed line represents the amount of water extracted from the sample

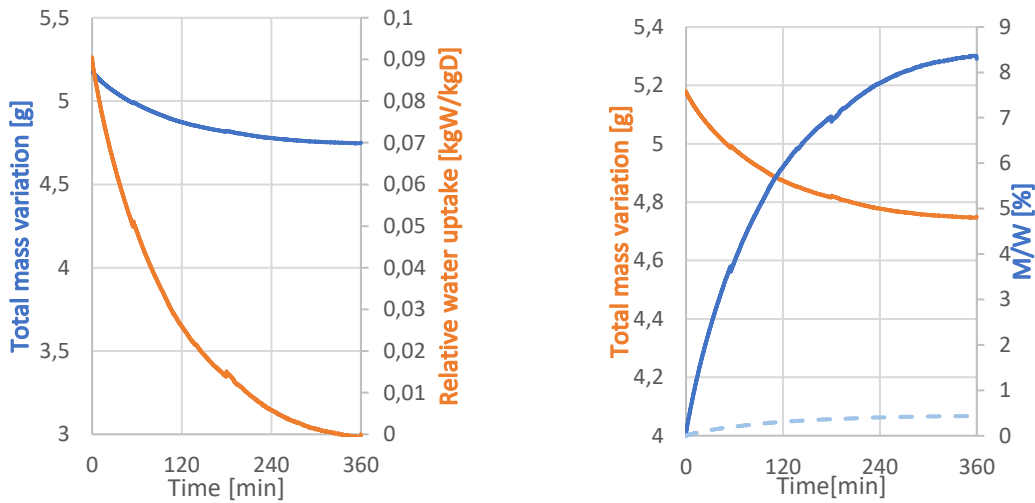


Figure 5.4- The graph on the left-hand side shows the behavior of the total mass variation during the regeneration process and the water uptake for the test performed at 50°C; on the right-hand side it is shown the behavior of the water content extracted from the sample with respect the initial wet mass, and the total mass variation for the test at 50°C. The dashed line represents the amount of water extracted from the sample

As was expected, the behavior of the water content concerning the wet mass of the material is increasing in all three scenarios. In the first two, where the temperature is high, the stability is reached in few hours and the percentage of water content was almost the same, while at a temperature of 50 °C the behavior is slower, and it takes a lot of time to perform the regeneration process. Moreover, to carry out the latter, two continuous tests have been done: the first one lasted three hours but in the end, the behavior of the water content in time was not constant so the regeneration process was not ended. The same sample has undergone the balance for the other three hours, and a more complete regeneration process occurs by reaching almost 8% of moisture content concerning the wet sample.

The unusual step visible in the graph displayed above is related to the reactivation of the moisture analyser, during which the sample may increase its weight.

The water uptake in all of the three test reaches almost the same value because this parameter does not depend on the temperature of the regeneration process but the adsorption phenomenon. It takes a really low value and this can be explained by the fact that the glass box container was not suitable to reach the saturation conditions.

5.3.2 Silica gel test-sample 2

The second sample tested was the silica gel prepared in a dish over two paper towels impregnated with water and covered by a plastic box.

In this case, silica gel balls are homogeneously placed in the aluminum dish covering all the diameter to form a thin layer. As a result of the non-homogeneous extension, non-homogeneous heat distribution occurs in the dried sample, resulting in an incomplete drying or prolonged drying time.

Even in this case, no temperature or relative humidity sensor was put in place to monitoring these data. It could be reasonable to suppose that the sample was at the initial conditions of 21°C and in a range between 80 and 100% as relative humidity.

The same sample was tested at three different temperature levels of 50°C, 120°C, and 200°C respectively. The moisture analyser properties set for the three different tests are listed in the table below:

<i>Test Number</i>	<i>Temperature</i>	<i>Mode</i>	<i>Time</i>	<i>Output</i>
1	50°C	TIME	9:00 h	M/W [%]
2	120°C	TIME	2:00 h	M/W [%]
3	200°C	TIME	1:30 h	M/W [%]

Table 5.3- Properties of test for sample 2

Different times for the regeneration process have been imposed according to their behavior. During test number one (at 50°C), monitoring the data collected throughout the experiments, it was evident that after few hours no evident change in mass of silica gel was recorded, so it means that the water content within the sample was not exhausted. To reach this point, the test has been extended up to nine hours.

When the temperature achieved is 120°C or 200°C the problem mentioned above doesn't exist. Indeed, results were obtained after a few hours.

The figures displayed below shows the water content extracted from the sample concerning the initial wet mass, defined as $\frac{M_{wet} - M_{dry}}{M_{wet}}$, and the relative water uptake

evaluated through the data collected, in comparison with the total mass variation during the regeneration process:

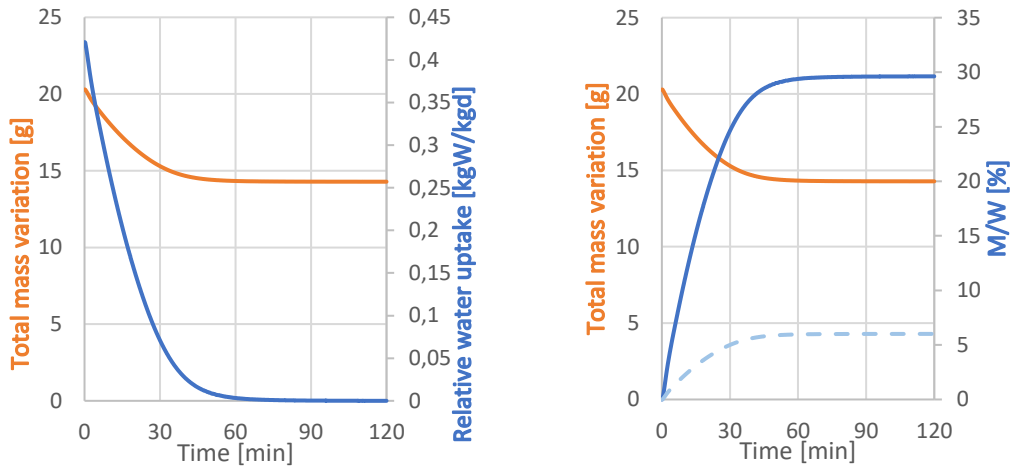


Figure 5.5 - The graph on the left-hand side shows the behavior of the total mass variation during the regeneration process and the water uptake for the test performed at 120°C; on the right-hand side it is shown the behavior of the water content extracted from the sample and the total mass variation for the test at 120°C, the dashed line represents the amount of water extracted from the sample.

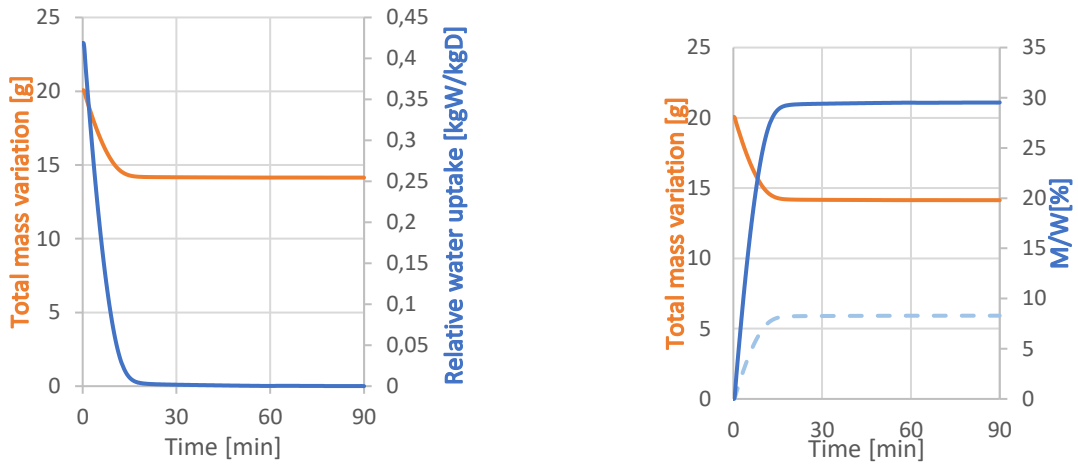


Figure 5.6-The graph on the left-hand side shows the behavior of the total mass variation during the regeneration process and the water uptake for the test performed at 200°C; on the right-hand side it is shown the behavior of the water content extracted from the sample and the total mass variation for the test at 200°C, the dashed line represents the amount of water extracted from the sample

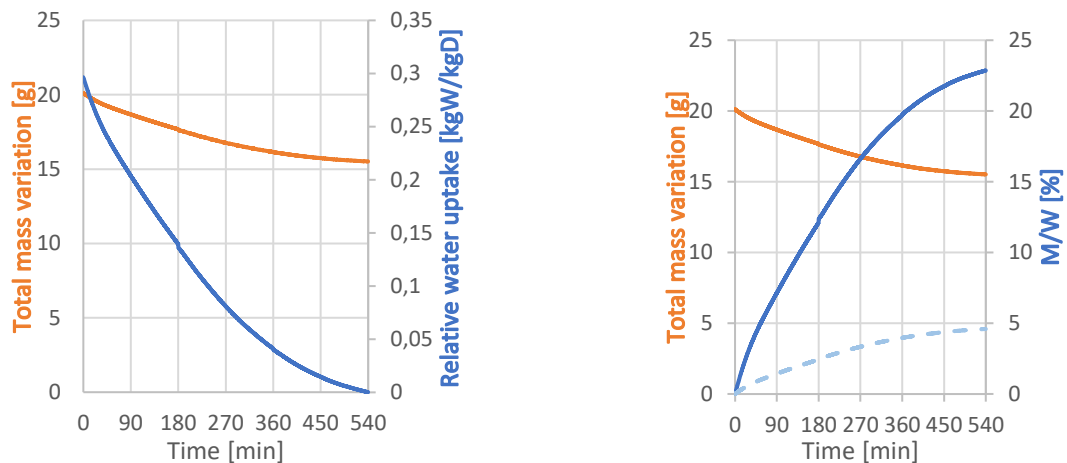


Figure 5.7- The graph on the left-hand side shows the behavior of the total mass variation during the regeneration process and the water uptake for the test performed at 50°C; on the right-hand side it is shown the behavior of the water content extracted from the sample and the total mass variation for the test at 50°C, the dashed line represents the amount of water extracted from the sample

5.4 Real tests

After the trials, an innovative solution was found to control the temperature and the relative humidity of the materials that must be submitted to the test.

A basic structure composed of two concentric plastic boxes were constructed in a way such that the bigger one can host a certain amount of water or any other solution, while the smaller one can host a thin aluminum dish with the material under investigation.

These constructions are closed with a plastic tap on which it has been mounted as a mini fan (5V) to move the air stream rate inside and increase the relative humidity.

Moreover, the engines were connected to temperature and humidity sensors with Arduino software.

Figure 5.8 shows a sketch of the above-mentioned configuration:

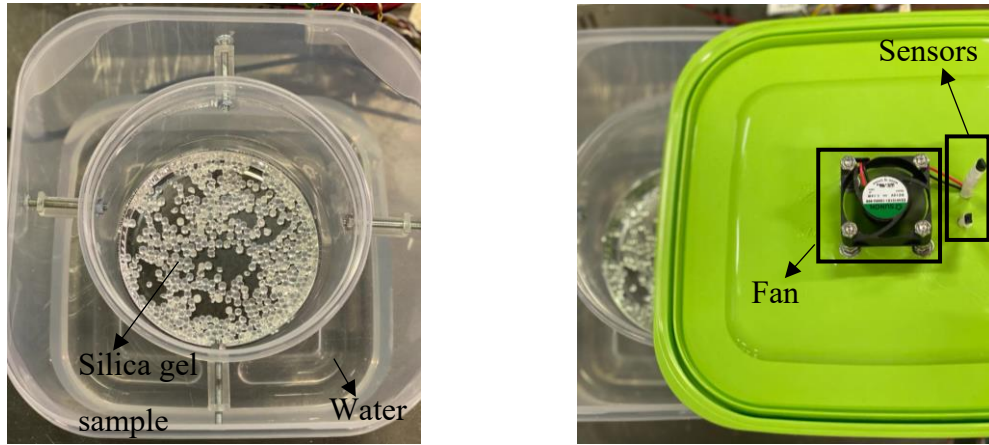


Figure 5.8-Configuration of the structure

The three boxes are filled with different solutions to reach a predetermined value of relative humidity. Box A was filled only with water to get a relative humidity of almost 80%.

Within the other two boxes, a solution made of water and calcium chloride (CaCl_2) was inserted to reach a relative humidity of 50 and 20%.

The amount of CaCl_2 needed to reproduce the desired conditions has been evaluated by using the equation derived by R. Conde [33] from experimental data.

This formula expresses the relative vapor pressure (π) as a function of the mass fraction of the solute, defined as the ratio between the mass of the substance and the total mass of the mixture. The related vapor pressure is defined as the pressure exerted by a vapor in thermodynamic equilibrium conditions in a closed system.

$$\pi = \frac{p_{sol}(\xi, T)}{p_{H_2O}(T)} = \pi_{25} * f(\xi, \theta) \quad \text{Eq. 5.1}$$

Where:

$$f(\xi, \theta) = A + B\theta \quad \text{Eq. 5.2}$$

$$A = 2 - \left[1 + \left(\frac{\xi}{\pi_0} \right)^{\pi_1} \right]^{\pi_2} \quad B = \left[1 + \left(\frac{\xi}{\pi_3} \right)^{\pi_4} \right]^{\pi_5} \quad \text{Eq. 5.3}$$

$$\pi_{25} = 1 - \left[1 + \left(\frac{\xi}{\pi_6} \right)^{\pi_7} \right]^{\pi_8} - \pi_9 * e^{-\frac{(\xi-0.1)^2}{0.005}} \quad \text{Eq. 5.4}$$

The parameters π_i are fixed values derived from experimental data, while θ represents the reduced temperature concerning the critical temperature of the water, defined as:

$$\theta = \frac{T}{T_{c,H_2O}} \quad \text{Eq. 5.5}$$

Since the desired relative humidity within the boxes was 50% and 20% respectively, an iterative procedure was implemented to find the correct values of the mass fraction of calcium chloride which fits best the requirement. In the table below are listed the results in terms of vapor pressure, obtained by substituting a single value of the mass fraction in the equation described before:

ξ	π
0.28	0.682946
0.29	0.661932
0.30	0.640234
0.31	0.617897
0.32	0.594984
0.33	0.571574
0.34	0.54776
0.35	0.523651
0.36	0.499363
0.37	0.475018
0.4	0.402901
0.45	0.292596
0.5	0.202913

Table 5.4 – Iterative process

Since the values of vapor pressure required are 0.5 and 0.2, an interpolation equation was used, which returns the following equation:

$$\xi = \frac{0.01 * \pi - 0.01373731}{-0.024288} \quad \text{Eq. 5.6}$$

This results in a mass fraction equal to 0.359 and 0.483 to obtain a relative humidity of 50% and 20% respectively. From the real background, it turns out that the relative humidity reached was around 60% and 40%.

The mass fraction is directly connected with the calcium chloride mass needed in the solution with the following correlation:

$$\xi = \frac{m_{solute}}{m_{solute} + m_{solvent}} \quad Eq. 5.7$$

Considering 1000ml of water as a solvent, the mass of CaCl₂ needed to produce a solution which in equilibrium condition can reach a relative humidity of 50% and 20% are 560g and 1000g respectively.

Once putting the sample of the material inside the structure, it will start to adsorb water molecules, increasing its weight.

The kinetics of adsorption was studied through a differential step method carried out by Artistov et al. [34].

This study focuses on the determination of the influence of the particle size, temperature, and pressure on the adsorption kinetic.

Experimental isobars of water adsorption on silica gel demonstrate the gradual decrease of water uptake with increasing of temperature and reduction of vapor pressure.

By analyzing the data collected, from the slope of a typical temporal variation at a constant temperature of the vapor pressure as well as of its weight, the diffusion constant, the apparent diffusivity and pore diffusivity of water can be extracted.

Many experimental methods have been developed to measure these diffusivities but the differential step isothermal method can be considered the most preferable one because it allows the reduction of the thermal effects caused by the water adsorption.

The dependence of water uptake on the square root of time was turned out to be linear according to the following equation:

$$\frac{m_t}{m_\infty} = A\sqrt{t} \quad Eq. 5.8$$

Through the inverse formula it was possible to determine the parameter A which represents the slope of the water sorption curves at constant temperature:

$$A = \frac{m_t}{m_\infty \sqrt{t}} \quad \text{Eq. 5.9}$$

This allows the calculation of the apparent water diffusivity and the diffusion constant based on the following equations:

$$D_{ap} = \frac{A^2 \pi R_p^2}{36} \quad \text{Eq. 5.10}$$

$$k_D = \frac{D_{ap}}{R_p^2} \quad \text{Eq. 5.11}$$

Where D_{ap} is the apparent water diffusivity and R_p is the radius of the molecular grains.

At high temperatures, mainly larger than 40°C, the slope and hence the diffusion constant is smaller than the one predicted by the isothermal theory. This may be due to the thermal effects caused by the heat released during water sorption.

To avoid or reduce this effect, it is necessary to intensify the dissipation of adsorption heat or to increase the heat capacity.

The diffusion constant and the apparent diffusion coefficient were evaluated for the two materials under investigation. Since the diffusion coefficient strictly depends on time, an average value has been taken. The silica gel and alginate diffusion coefficient were measured for the three temperatures of operation, to make a comparison with the reference value find in the literature [34]. The results are shown in the tables below:

Silica Gel Apparent diffusion coefficient D_{ap}

RH	Temperature			
	Average	Minimum	Maximum	
80%	100°C	3.65E-10	2.73E-11	7.62E-08
	70°C	1.37E-10	9.02E-12	7.42E-08
	50°C	6.96E-11	4.55E-12	6.75E-08
60%	100°C	4.60E-10	3.64E-11	7.33E-08
	70°C	1.85E-10	1.36E-11	5.32E-07
	50°C	6.48E-11	4.54E-12	6.25E-08
40%	100°C	3.47E-10	3.11E-11	4.37E-07
	70°C	1.62E-10	1.36E-11	5.88E-08
	50°C	5.66E-11	4.55E-12	5.39E-08

Table 5.5- Silica Gel apparent diffusion coefficient

All the values, or more exactly their order of magnitude founded seem to match the theoretical values.

Alginate Apparent diffusion coefficient D_{ap}				
RH	<i>Temperature</i>			
		<i>Average</i>	<i>Minimum</i>	<i>Maximum</i>
80%	100°C	1.9E-11	5.59E-13	6.81E-09
	70°C	6.88E-11	1.35E-12	4.08E-08
	50°C	4.5E-11	1.57E-12	2.4E-08
60%	100°C	4.60E-11	1.57E-12	1.98E-08
	70°C	3.08E-11	1.18E-12	2.42E-08
	50°C	3.32E-11	1.57E-12	1.08E-08
40%	100°C	2.72E-11	1.57E-12	1.17E-07
	70°C	2.09E-11	1.18E-12	1.59E-08
	50°C	2.38E-11	1.57E-12	1.26E-08

Table 5.6- Alginate apparent diffusion coefficient

At that point, it was possible to evaluate the diffusion constant as the ratio of the apparent diffusion coefficient and the radius to the power of two of the samples.

Silica Gel diffusion constant k_d				
RH	<i>Temperature</i>			
		<i>Average</i>	<i>Minimum</i>	<i>Maximum</i>
80%	100°C	1.62E-04	1.2E-05	0.034
	70°C	6.06E-05	4.04E-06	0.0329
	50°C	3.09E-05	2.02E-06	0.03
60%	100°C	2.04E-04	1.61E-05	0.0325
	70°C	8.2E-05	6.06E-06	0.03
	50°C	2.88E-05	2.02E-06	0.0277
40%	100°C	1.54E-04	1.38E-05	0.0278
	70°C	7.19E-05	6.06E-06	0.026
	50°C	2.5E-05	2.02E-06	0.0239

Table 5.7- Silica gel diffusion constant

Alginate diffusion constant k_d				
RH	<i>Temperature</i>			
		<i>Average</i>	<i>Minimum</i>	<i>Maximum</i>
80%	100°C	4.97E-05	1.46E-06	0.0174
	70°C	1.76E-04	3.46E-06	0.123
	50°C	1.16E-04	4.04E-06	0.063
60%	100°C	1.17E-04	4.04E-06	0.0806
	70°C	7.89E-05	3.03E-06	0.062
	50°C	8.52E-05	4.04E-06	0.046

40%	100°C	6.97E-05	4.04E-06	0.0483
	70°C	5.35E-05	3.03E-06	0.04
	50°C	6.01E-05	4.04E-06	0.032

Table 5.8- Alginate diffusion constant

From these data, it was also possible to evaluate the normalized dry mass ratio through the use of the isothermal differential step method [34]. The uptake rate is given by solving a differential mass balance equation, that for uniform adsorbent particles it can be written as follow:

$$(1 - \varepsilon) \frac{\partial w}{\partial t} + \varepsilon \frac{\partial c}{\partial t} = \varepsilon D_e \left(\frac{\partial^2 c}{\partial R^2} + \frac{2}{R} \frac{\partial c}{\partial R} \right) \quad \text{Eq. 5.12}$$

Here, ε represents the porosity of the material, D_e is the effective diffusivity, w is the adsorbate concentration in the adsorbed phase, and c represents the adsorbate concentration in the gas phase. By manipulating the equation written before, it could be demonstrated that the solution is:

$$\frac{m_t}{m_\infty} = \frac{\bar{w} - w_0}{w_\infty - w_0} = 1 - \frac{6}{\pi^2} \sum_{n=1}^{\infty} \frac{1}{n^2} \exp\left(-\frac{n^2 \pi^2 D_{apt}}{R_p^2}\right) \quad \text{Eq. 5.13}$$

Where \bar{w} is the average water uptake in the sample which depends on time, and n has been set equal to six.

This parameter has been evaluated with the use of a Matlab script for all the experimental tests performed, to check that the empirical data collected are in line with the theoretical ones. The value of the apparent diffusivity which best verifies this target has been chosen from a list of possible solutions selected based on the average value on the time of the experimental data. Many $\frac{m_t}{m_\infty}$ ratio and the corresponding relative errors were evaluated according to the equation mentioned above. The value of apparent diffusivity which shows the lowest relative error has been selected as a parameter that fits best the experimental behavior. The following table will show the values of the apparent diffusion coefficient selected to represent the theoretical behavior of the silica gel and alginate samples in terms of $\frac{m_t}{m_\infty}$ ratio.

<i>RH</i>	<i>Temperature [°C]</i>	<i>D_{ap} Silica Gel</i>	<i>D_{ap} Alginate-5%</i>
80%	100	1.2E-10	1E-10
	70	0.8E-10	3.5E-11
	50	1.5E-11	1.9E-11
60%	100	1E-10	1.8E-10
	70	0.4E-10	3.08E-11
	50	1.7E-11	2E-11
40%	100	1.5E-10	1E-10
	70	0.5E-10	1E-10
	50	2E-11	2.38E-11

Table 5.9- Apparent diffusion coefficient comparison

As regards the silica gel samples, the following graphs will show the theoretical and experimental behaviors of the ratio $\frac{m_t}{m_\infty}$ for three different levels of temperature at the same relative humidity condition equal to 80%.

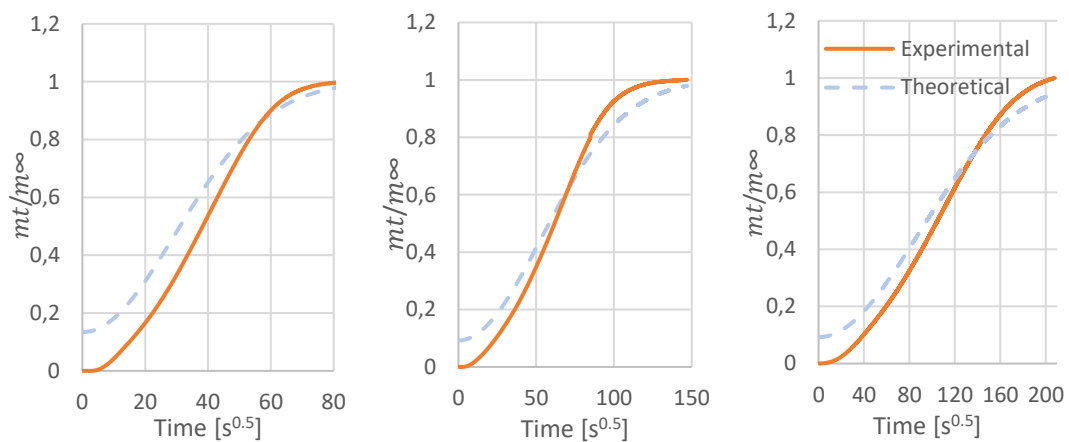


Figure 5.9- Experimental and theoretical behaviors of the ratio $\frac{m_t}{m_\infty}$ for the silica gel samples at 80% of relative humidity for the three different operating temperature conditions, in particular from left to right: 100°, 70°C, 50°C

The same procedure has been developed also for the samples at 60% and 40% of relative humidity, the results are shown below:

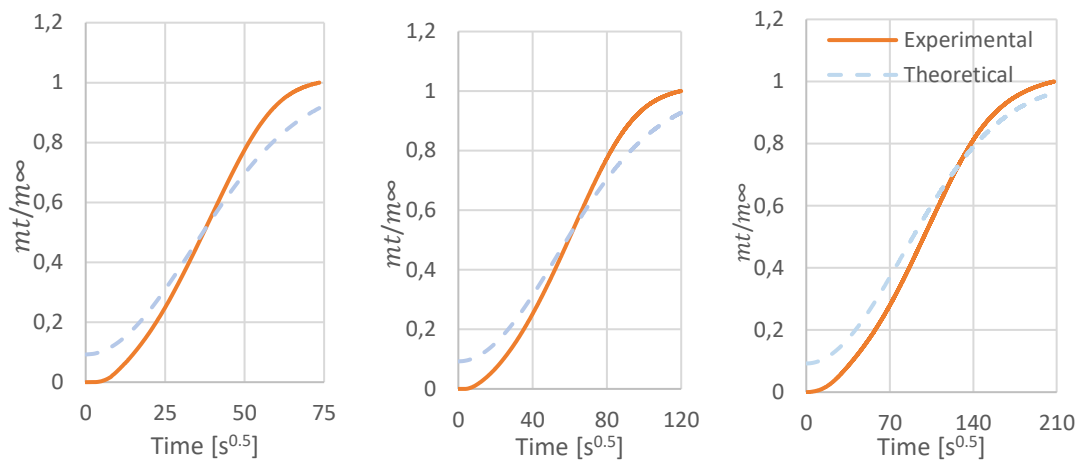


Figure 5.10- Experimental and theoretical behaviors of the ratio $\frac{m_t}{m_\infty}$ for the silica gel samples at 60% of relative humidity for the three different operating temperature conditions: from left to right: 100°, 70°C, 50°C

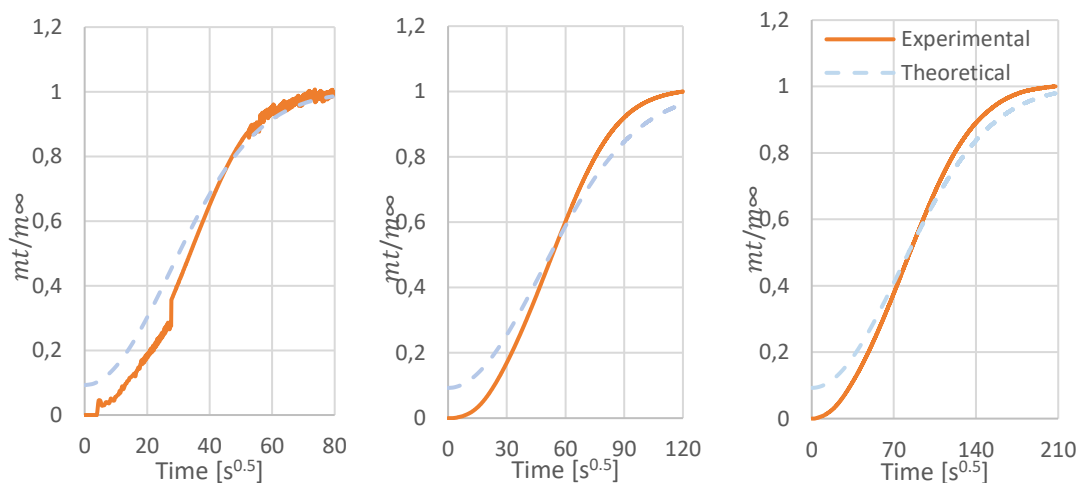


Figure 5.11- Experimental and theoretical behaviors of the ratio $\frac{m_t}{m_\infty}$ for the silica gel samples at 40% of relative humidity for the three different operating temperature conditions: from left to right: 100°, 70°C, 50°C

Since the parameters which described the adsorption kinetic of the silica gel, evaluated with the procedure described above, seem to reflect the theoretical values, the same method has been used for the sodium alginate. This allows us to make comparisons between the different apparent diffusion coefficients to understand who has the faster adsorption kinetic, and so who is more able to adsorb water molecules.

Figure 5.12, Figure 5.13, and Figure 5.14 show the behaviors of the ratio $\frac{m_t}{m_\infty}$ of the alginate at different relative humidity conditions of 80%, 60% and 40% respectively.

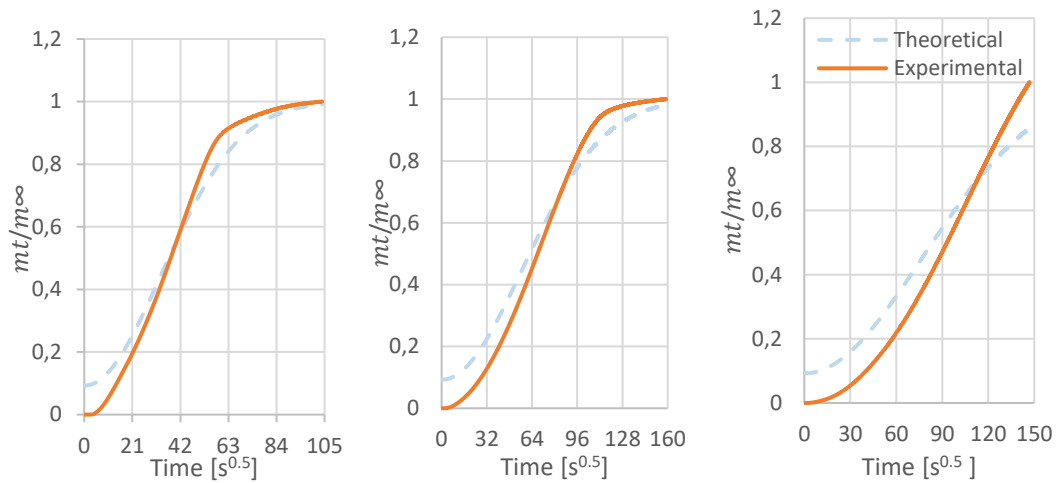


Figure 5.12- Experimental and theoretical behaviors of the ratio $\frac{m_t}{m_\infty}$ for the alginate (5%) samples at 80% of relative humidity for the three different operating temperature conditions: from left to right: 100°, 70°C, 50°C

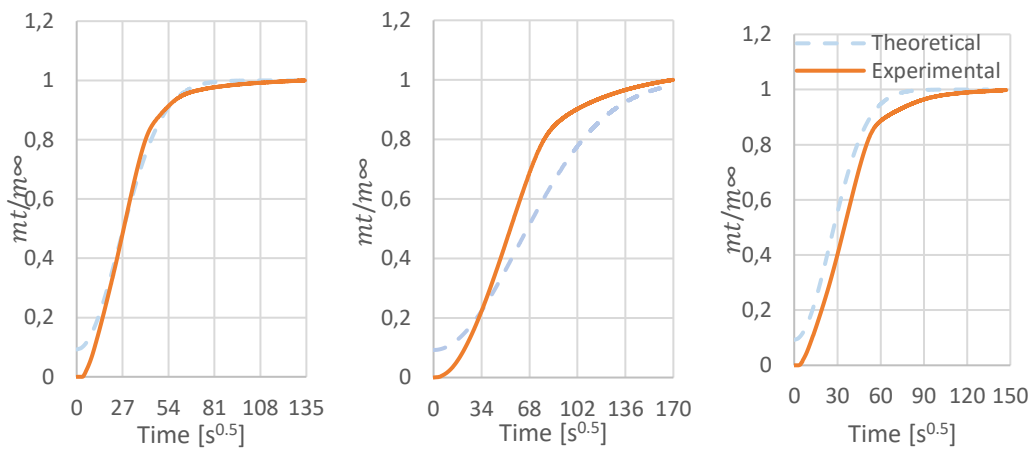


Figure 5.13 -Experimental and theoretical behaviors of the ratio $\frac{m_t}{m_\infty}$ for the alginate (5%) samples at 60% of relative humidity for the three different operating temperature conditions: from left to right: 100°, 70°C, 50°C

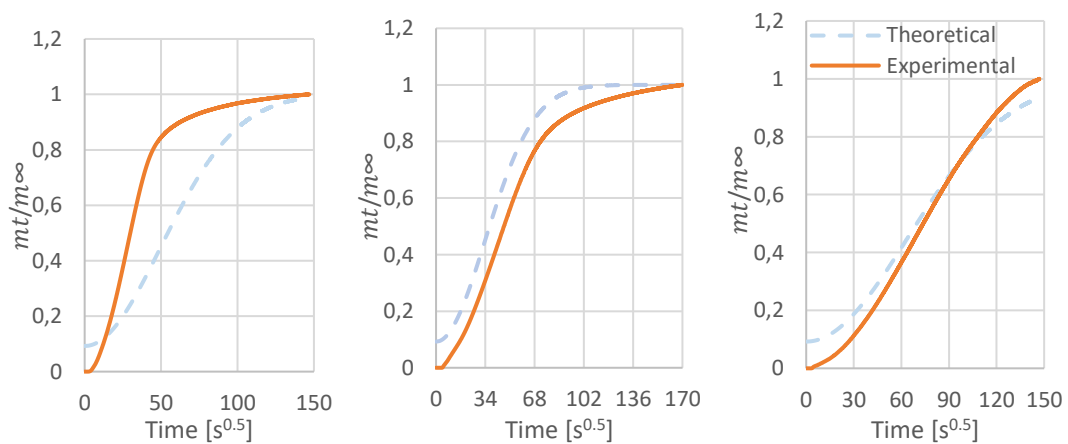


Figure 5.14- Experimental and theoretical behaviors of the ratio $\frac{m_t}{m_\infty}$ for the alginate (5%) samples at 40% of relative humidity for the three different operating temperature conditions: from left to right: 100°, 70°C, 50°C

The theoretical behaviors are subjected to uncertainty connected to the value of n, representing the number of times the summary of the formula is repeated. For n which tends to infinity, the theoretical curve will start from 0 value, but due to some limitation, in this analysis, the value of n equal to six has been chosen.

As highlighted in the table represented above, the apparent diffusion coefficients of the alginate and silica gel have in some cases are comparable, the rest of the cases have lower values, even if the amount of water adsorbed is higher with respect to the silica gel.

Since the diffusion coefficient represents a measure of the kinetic of the diffusion of the water molecule within the solid sorption material, it is possible to conclude that the silica gel material, in some conditions, could have a faster adsorption rate. Other factors contribute to the adsorption kinetic like the porosity of the material and the slope of the adsorption isotherm.

5.5 Silica gel

5.5.1 Testing silica gel at 80% of relative humidity

The condition of relative humidity equal to 80% is reached only by using a water solution. Starting from this point, three different tests were performed at temperatures equal to 50°C, 70°C, and 100°C. By putting a temperature sensor within the moisture analyser it has been discovered that the real equilibrium temperatures reached within the device are a little bit lower as shown in the following table:

T. SET	T. EQ	TIME EQ.
100°C	96.4°C	8 min
70°C	65°C	10 min
50°C	43.5°C	10 min

Table 5.10- Equilibrium temperature of the moisture analyser

Higher temperatures could be reached by the moisture analyser for the regeneration process, but in real applications, one of the main standards is the low regeneration temperature that should not overcome 70°C-100°C.

In this way, a low-temperature heat source like a solar thermal collector can be used to perform the regeneration process within a water harvesting engine to the production of fresh water from humid air. This solution enables us to avoid the use of electric energy to produce heat to carry out the regeneration.

In the table below, all the variables and the initial condition of the three tests are displayed:

<i>Date</i>	<i>Hour</i>	<i>Operating Temperature</i>	<i>N. Hours</i>	<i>Starter Temperature</i>	<i>Relative humidity</i>	<i>Initial weight</i>	<i>Final weight</i>
27/10/2020	16:45	100°C	2	25.4°C	83%	20,826	14,946
28/10/2020	09:20	70°C	6	23.7°C	83%	20,886	15,183
28/10/2020	20:10	50°C	12	25.3°C	79%	20,670	15,761

Table 5.11- Silica gel (80%) and moisture analyser properties

The temperature and relative humidity of the initial sample was monitored with the use of Arduino software up to reaching the desired thermohygro-metric conditions. The values of these parameters are listed in the table above are an average of the data collected before the tests.

Thanks to the instruments inserted within the box a relative humidity of 80% has been achieved together with an ambient temperature equal to approximately 25 °C.

After the first test, the sample results dried so its water content should be the minimum acceptable.

By re-entering the material within the plastic structure, it will start again to adsorb water from the air surrounding until the equilibrium condition is reached.

Even if the three tests were performed at the same initial conditions in terms of temperature and relative humidity, the final water content detected within the samples is different, and this could be related to the different temperature conditions set within the moisture analyser.

At 100°C, the material requires only two hours to reach the highest rate, equal to 28.23%.

The second test performed at 70°C reaches only 1% less in terms of water content but it takes six hours to achieve that target. In particular, two continuous tests were carried

out, the first one lasted two hours, but in the end, no significant data were collected so another test of four hours was performed.

The last one at 50°C was programmed to last 12 hours to be sure of not turn into the same mistake as before. The water content pointed out from this test is only of 23.75%. The figures below display the results obtained in the three tests in terms of water content extracted from the sample concerning the initial wet mass and relative water uptake, defined as $\frac{M_{wet}-M_{dry}}{M_{dry}}$. These two parameters are put in comparison with the variation of wet mass during the regeneration process. The dashed line present in all three scenarios represents the amount of water extracted from the sample.

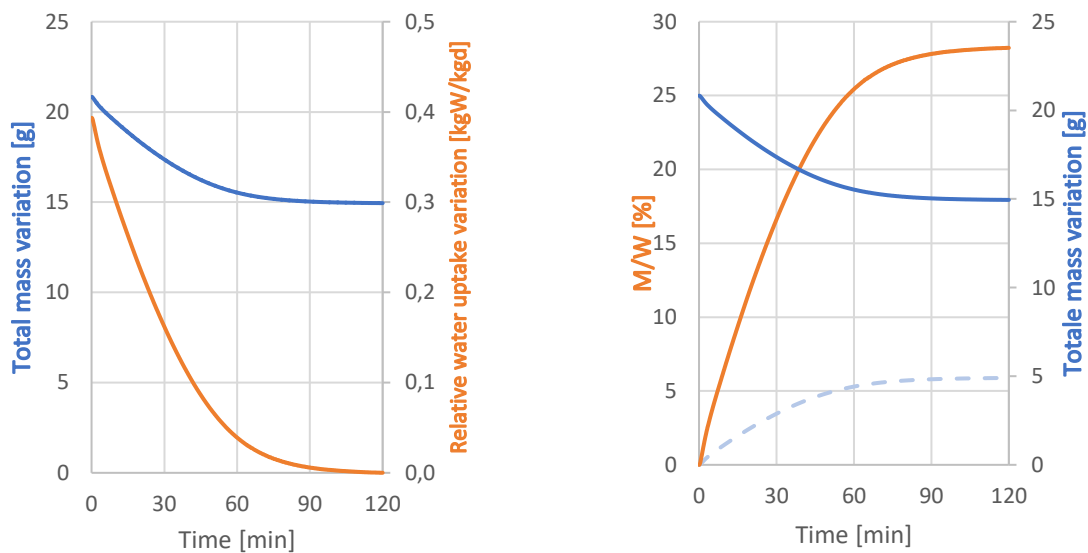


Figure 5.15-The graph on the left-hand side shows the behavior of the total mass variation during the regeneration process and the water uptake for the test performed at 100°C; on the right-hand side the behavior of the water content extracted from the sample and the total mass variation for the test at 100°C.

To evaluate the water uptake when tests have been performed at 70°C and 50°C, the reference dry mass used to perform the ratio is that evaluated at the end of the regeneration process at 100°C.

For this reason, the water uptake will not reach the value 0, because the regeneration process is ended, but the sample was not completely dried.

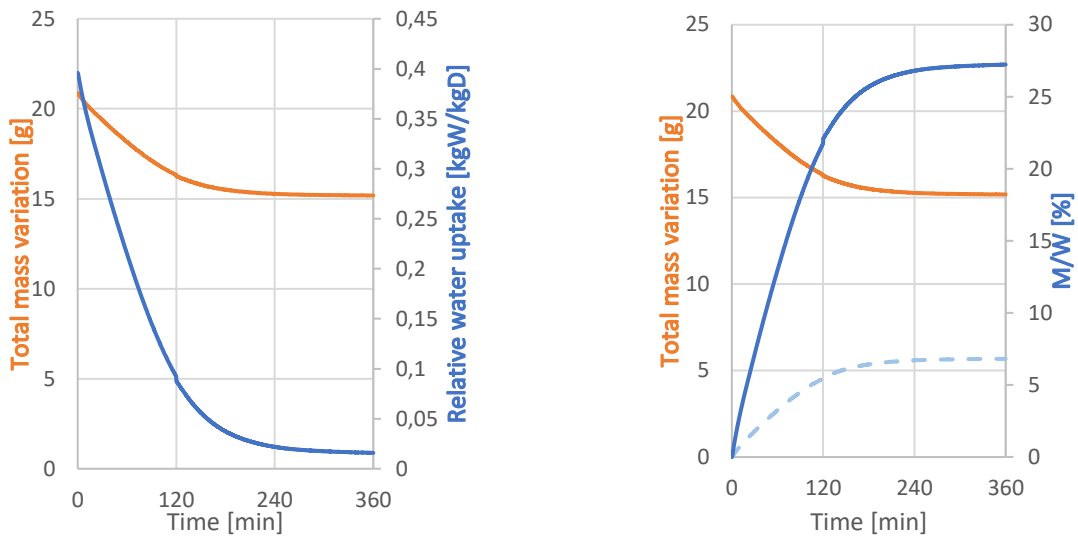


Figure 5.16-The graph on the left-hand side shows the behavior of the total mass variation during the regeneration process and the water uptake for the test performed at 70°C; on the right-hand side it is shown the behavior of the water content extracted from the sample and the total mass variation for the test at 70°C.

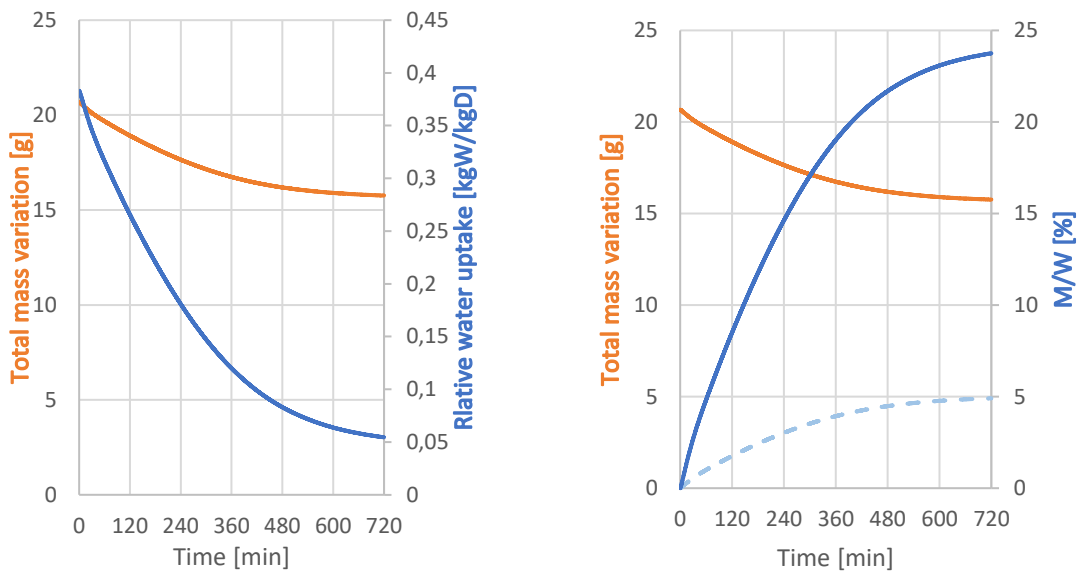


Figure 5.17- The graph on the left-hand side shows the behavior of the total mass variation during the regeneration process and the water uptake for the test performed at 50°C; on the right-hand side the behavior of the water content extracted from the sample and the total mass variation for the test at 50°C.

5.5.2 Testing silica gel at 60% of relative humidity

The second sample tested was that prepared into the box where the solution of water and calcium chloride provides a relative humidity equal to 60%.

The solution has been made by stirring 560 g of calcium chloride into 1 liter of water with a magnetic mixer.

Even in this case, three different tests were carried out at 100°C, 70°C, and 50°C respectively, and different results in terms of water content were obtained.

The following table displays all the characteristic properties of the sample and the corresponding operative conditions within the moisture analyser.

<i>Date</i>	<i>Hour</i>	<i>Operating Temperature</i>	<i>N. Hours</i>	<i>Starter Temperature</i>	<i>Relative humidity</i>	<i>Initial weight</i>	<i>Final weight</i>
28/10/2020	16:15	100°C	1:30	23.4°C	59%	20,070	14,685
29/10/2020	09:15	70°C	4	22.46°C	59.6%	19,731	14,959
29/10/2020	18:10	50°C	12	23.84°C	58%	19,521	15,466

Table 5.12- Silica gel (60%) and moisture analyser properties

The difference in the number of hours at which the tests were performed is to attribute to the diverse operating conditions.

At 100°C, the regeneration process is very fast; indeed, it takes only one hour and a half to obtain the highest rate of water content.

The results obtained from these other three tests are a little bit different from those reached with the previous set of tests, and this is because of the lower relative humidity of the initial sample.

The behavior of the thermohygrometric conditions in terms of temperature and relative humidity have been obtained from the data collected with Arduino software. For the first test performed at 100°C, data related to three hours before the test were available, and it is reasonable to assume that the conditions don't change until the beginning of the test because no perturbation of the internal and external environment occurs. A mean value of these quantities has been selected for the three tests as starting conditions.

Even if the relative humidity of the sample at the beginning of each test was the same, different results in terms of water content within the sample were obtained. This phenomenon can be explained with the different temperatures as operating conditions. The first test carried out at 100°C reaches a water content value equal to 26.83% and it takes only one hour and a half to reach that point.

The second and third tests at 70°C and 50°C lasted four and twelve hours respectively, and in this case, no additional test was needed because a constant behavior has been reached at the end of the test. The results collected are shown in the figures below:

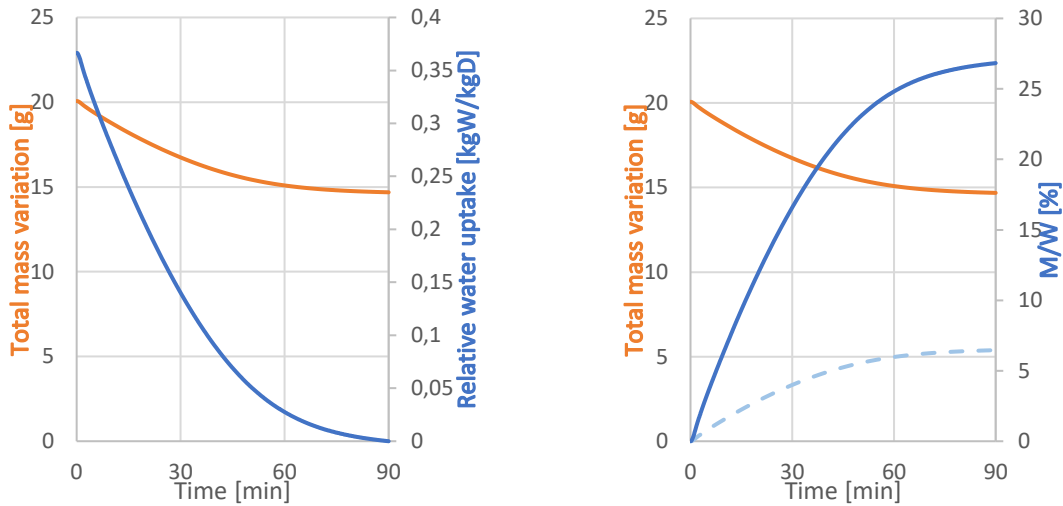


Figure 5.18 – The graph on the left-hand side shows the behavior of the total mass variation during the regeneration process and the water uptake for the test performed at 100°C; on the right-hand side it is shown the behavior of the water content extracted from the sample with respect the initial wet mass, and the total mass variation for the test at 100°. The dashed line represents the amount of water extracted from the sample

Even in this case, the reference dry mass used to evaluate the water uptake for the sample regenerated at 70°C and 50°C was that resulting at the end of the regeneration process at 100°C.

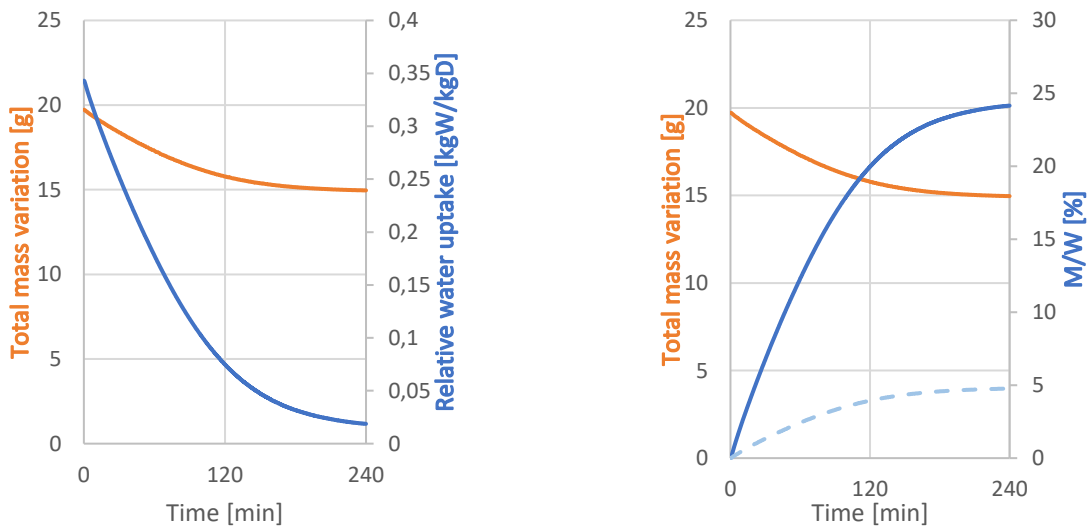


Figure 5.19- The graph on the left-hand side shows the behavior of the total mass variation during the regeneration process and the water uptake for the test performed at 70°C; on the right-hand side it is shown the behavior of the water content extracted from the sample referred to the initial wet mass and the total mass variation for the test at 70°C. The dashed line represents the amount of water extracted from the sample

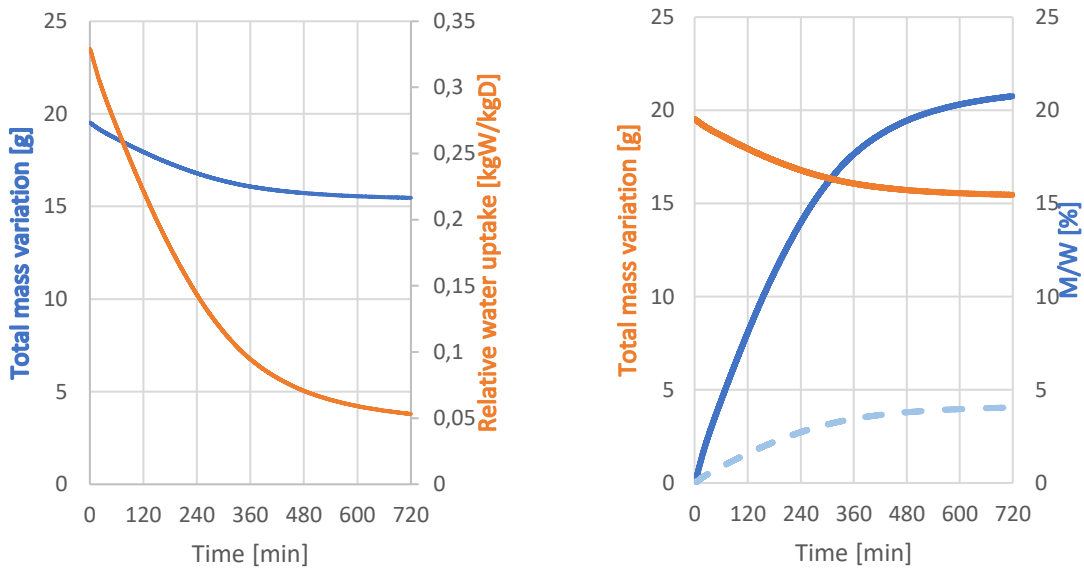


Figure 5.20 The graph on the left-hand side shows the behavior of the total mass variation during the regeneration process and the water uptake for the test performed at 50°C; on the right-hand side it is shown the behavior of the water content extracted from the sample and the total mass variation for the test at 50°C. The dashed line represents the amount of water extracted from the sample

5.5.3 Testing silica gel at 40% of relative humidity

The third test was prepared within the box where the relative humidity reaches the value of 40%.

To create the solution to be inserted in the plastic box, 1000g of calcium chloride was blended with 1 liter of water with the use of a magnetic mixer.

Even in this case, three tests at different temperature conditions of 50°C, 70°C, and 100°C were performed. Temperature and relative humidity conditions were monitored during the hours before the beginning of the tests, and at the end, an average value was picked up.

The following table shows the characteristic properties of the sample under investigation together with the operating condition set within the moisture analyser:

<i>Date</i>	<i>Hour</i>	<i>Operating Temperature</i>	<i>N. Hours</i>	<i>Starter Temperature</i>	<i>Relative humidity</i>	<i>Initial weight</i>	<i>Final weight</i>
28/10/2020	17:50	100°C	1:45	25.1°C	36%	17,82	14,117

29/10/2020	13:25	70°C	4	23.44°C	36.2%	17,702	14,959
30/10/2020	09:15	50°C	12	23°C	37.3%	17,57	15,00

Table 5.13- Silica gel (40%) and moisture analyser properties

As for the previous case, the difference in the number of hours at which the tests were performed is to attribute to the different temperature of operation within the moisture analyser. The test performed at 100°C is the faster one and it reaches the highest value of water content, as in the previous cases. The other two tests take more time to obtain a lower result in terms of water content.

The results obtained from the tests shown a different level of water content concerning the three operating temperature conditions. Moreover, these values are lower with respect to that obtained with the tests performed at a higher level of relative humidity. This aspect can be explained by the fact that 40% of the relative humidity of the ambient air, the material is not able to absorb a high amount of water vapor. This phenomenon is well evident by comparing the behaviors of the water uptake. Results of the three tests are shown below:

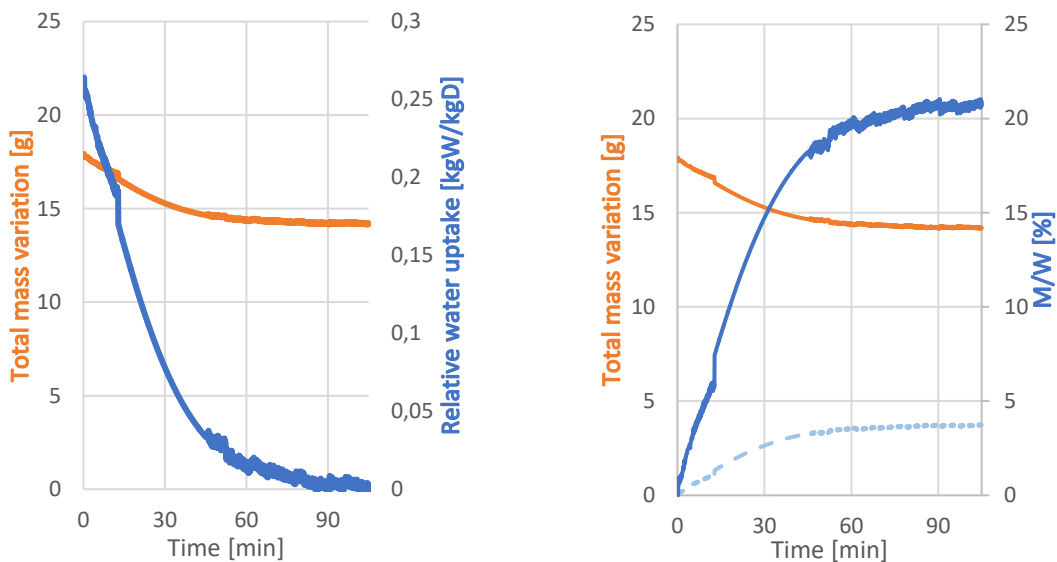


Figure 5.21 – The graph on the left-hand side shows the behavior of the total mass variation during the regeneration process and the water uptake for the test performed at 100°C; on the right-hand side it is shown the behavior of the water content extracted from the sample with respect the initial wet mass, and the total mass variation for the test at 100°C. The dashed line represents the amount of water extracted from the sample

The strange behavior experienced around the twelfth minute may be due to the accidental movement of the moisture analyser which messed up the condition of the sample inside.

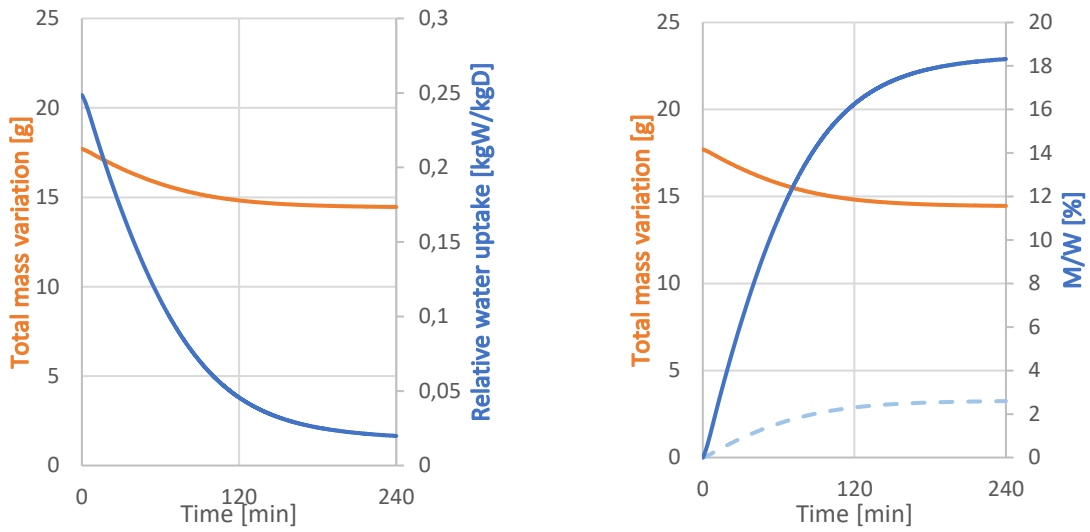


Figure 5.22 – The graph on the left-hand side shows the behavior of the total mass variation during the regeneration process and the water uptake for the test performed at 70°C; on the right-hand side it is shown the behavior of the water content extracted from the sample with respect the initial wet mass, and the total mass variation for the test at 70°C, the dashed line represents the amount of water extracted from the sample

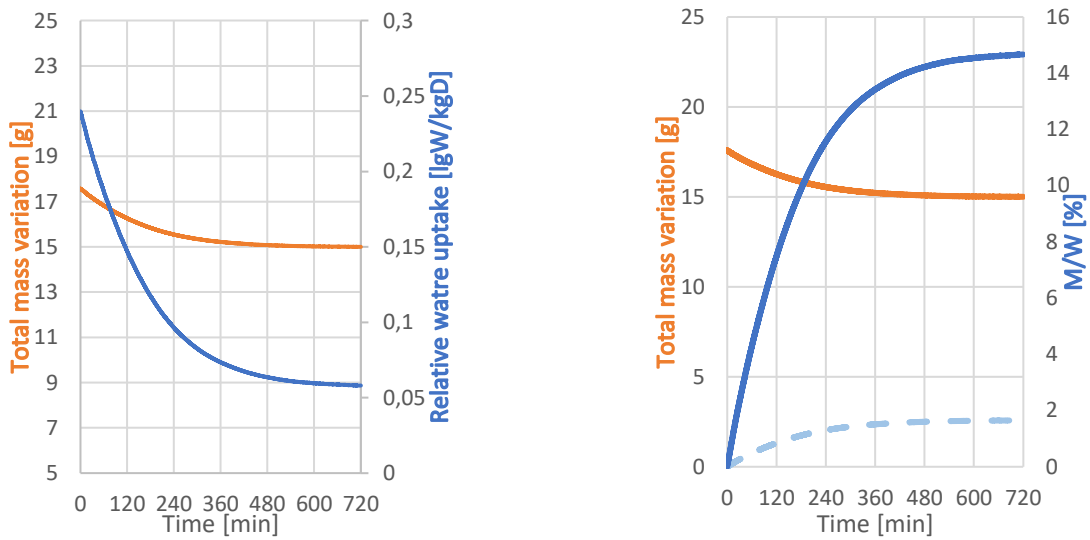


Figure 5.23-The graph on the left-hand side shows the behavior of the total mass variation during the regeneration process and the water uptake for the test performed at 50°C; on the right-hand side it is shown the behavior of the water content extracted from the sample with respect to the initial wet mass, and the total mass variation for the test at 50°C The dashed line represents the amount of water extracted from the sample

5.6 Alginate at 5% of concentration

The second material tested was alginate at 5% of concentration, so the alginate balls were created by leaching the alginate and water solution in a container where the water and calcium chloride solution was at 5% of concentration.

The testing procedure was the same illustrated for the previous tests, the temperature and relative humidity conditions were monitored through the use of Arduino software. The results provided by the moisture analyser, expressed in terms of the ratio between the water extracted from the sample and the initial wet mass, were manipulated to evaluate different parameters such as the amount of water uptake or the total mass variation during the regeneration process.

Even in this case, three samples were tested according to different original relative humidity conditions. Tests were performed at three different operating temperature set within the moisture analyser equal to 50°C, 70°C, and 100°C.

5.6.1 Testing Alginate at 80% of relative humidity

The sample tested, in this case, has the highest relative humidity starting condition, equal to 80% which has been reached by putting the alginate in the box with only the water.

As well as how it was produced, the alginate is a highly hygroscopic material, it means that it is well crafted to adsorb water molecule from the surrounding environment. Indeed, only in case of high relative humidity conditions, the structure is not able to hold all the water collected, by forming a layer of liquid water within the dish containing the sample.

For the above-mentioned reason, the water content and the water uptake will have very high values concerning that obtained with silica gel sorption material.

The following table shows the properties of the material and the moisture analyser operating conditions at which the three tests were performed:

Date	Hour	Operating Temperature	N. Hours	Starter Temperature	Relative humidity	Initial weight	Final weight
16/11/2020	08:59	50°C	6	22°C	80%	12.812	6.718
16/11/2020	20:31	100°C	3	22°C	80%	11.284	4.749
19/11/2020	11:17	70°C	7	22°C	80%	13.277	4.99

Table 5.14- Alginate (80%) and moisture analyser properties

The graphs displayed below will show the behaviors of the water uptake and the water extracted from the sample with respect to the total mass variation during the regeneration process at different operating temperature conditions.

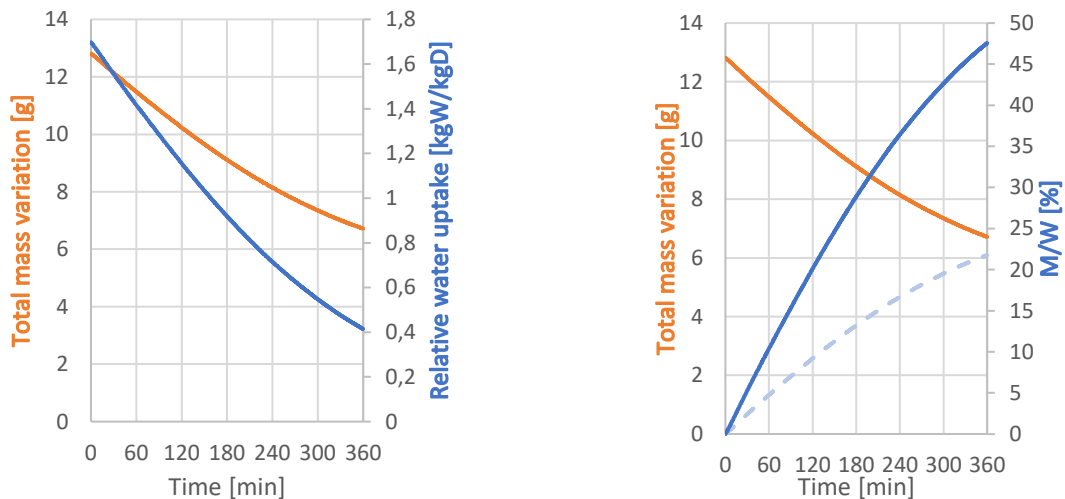


Figure 5.24 -The graph on the left-hand side shows the behavior of the total mass variation during the regeneration process and the water uptake for the test performed at 50°C; on the right-hand side it is shown the behavior of the water content extracted from the sample with respect the initial wet mass, and the total mass variation for the test at 50°C The dashed line represents the amount of water extracted from the sample

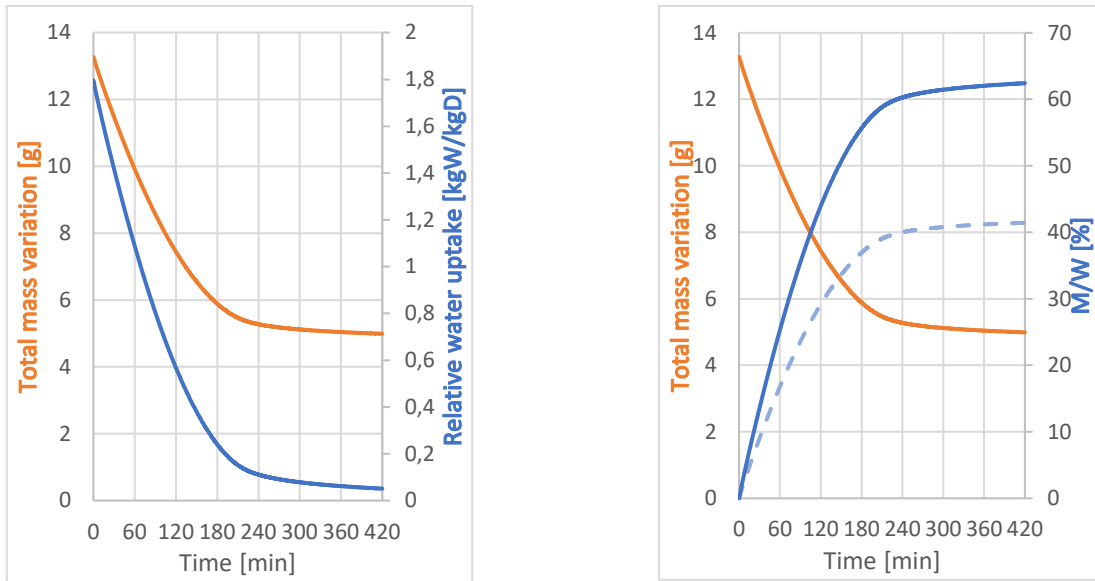


Figure 5.25- The graph on the left-hand side shows the behavior of the total mass variation during the regeneration process and the water uptake for the test performed at 70°C; on the right-hand side it is shown the behavior of the water content extracted from the sample with respect the initial wet mass, and the total mass variation for the test at 70°C The dashed line represents the amount of water extracted from the sample

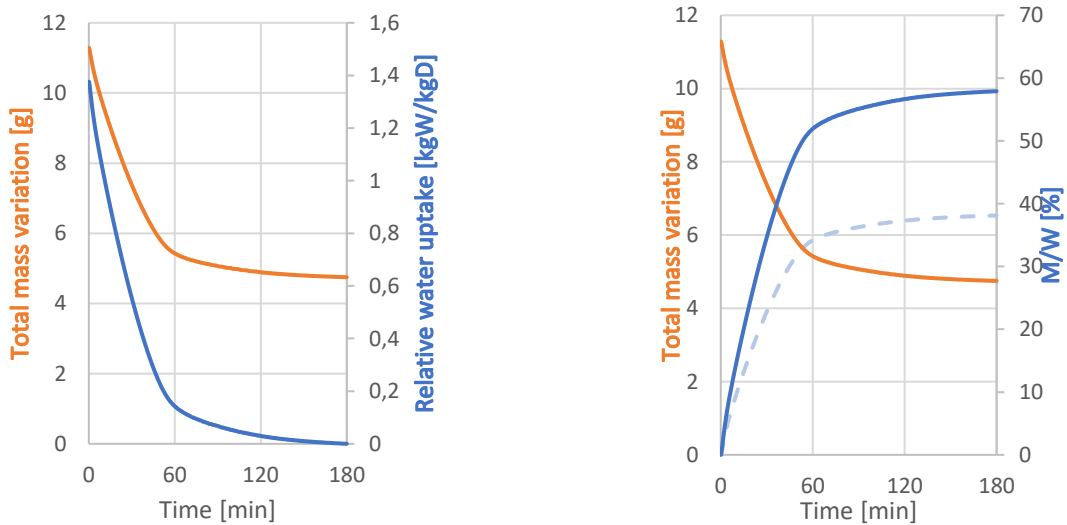


Figure 5.26-The graph on the left-hand side shows the behavior of the total mass variation during the regeneration process and the water uptake for the test performed at 100°C; on the right-hand side it is shown the behavior of the water content extracted from the sample with respect to the initial wet mass, and the total mass variation for the test at 100°C The dashed line represents the amount of water extracted from the sample

5.6.2 Testing Alginate at 60% of relative humidity

In this case, the sample tested was prepared within the box where the solution of water and calcium chloride can reach 60% of relative humidity. Having a lower relative

humidity condition, no liquid water was formed within the aluminum dish before the test. Even in this case, three operating temperature conditions have been investigated. The properties of the tests were summarized in the table below:

<i>Date</i>	<i>Hour</i>	<i>Operating Temperature</i>	<i>N. Hours</i>	<i>Starter Temperature</i>	<i>Relative humidity</i>	<i>Initial weight</i>	<i>Final weight</i>
08/11/2020	02:10	70°C	8	22°C	57%	7.805	4.138
09/11/2020	10:46	100°C	5	22°C	57%	8.133	3.698
11/11/2020	14:59	50°C	6	22°C	57%	7.685	4.722

Table 5.15- Alginate (60%) and moisture analyser properties

Results from the three tests are shown in the following figures:

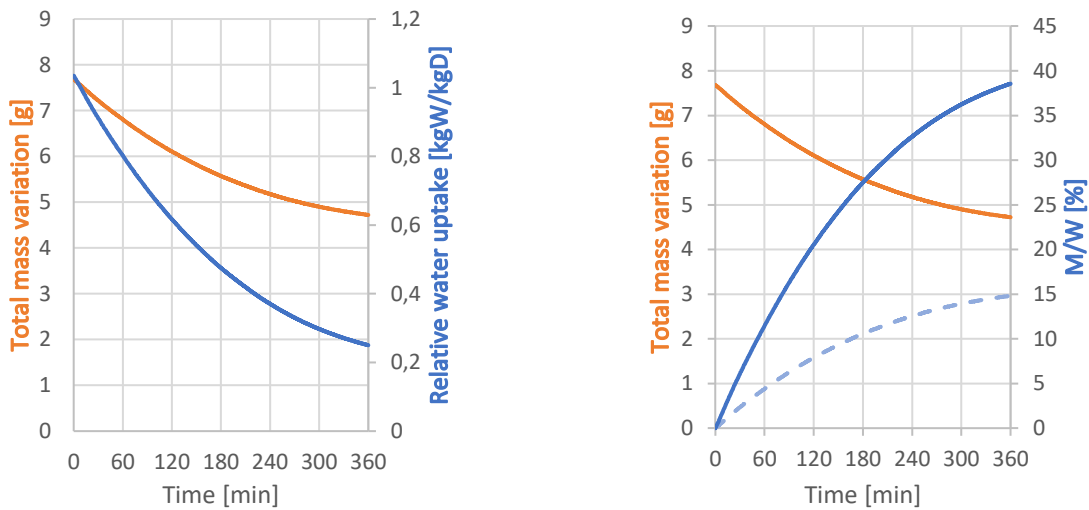


Figure 5.27- The graph on the right-hand side displays the ratio between the water extracted and the initial we mass in comparison to the total mass variation during the transient at 50°C, on the left-hand side it is shown the behavior of the water uptake during the adsorption process and the variation of the mass of the sample when the regeneration process was performed at 50°C

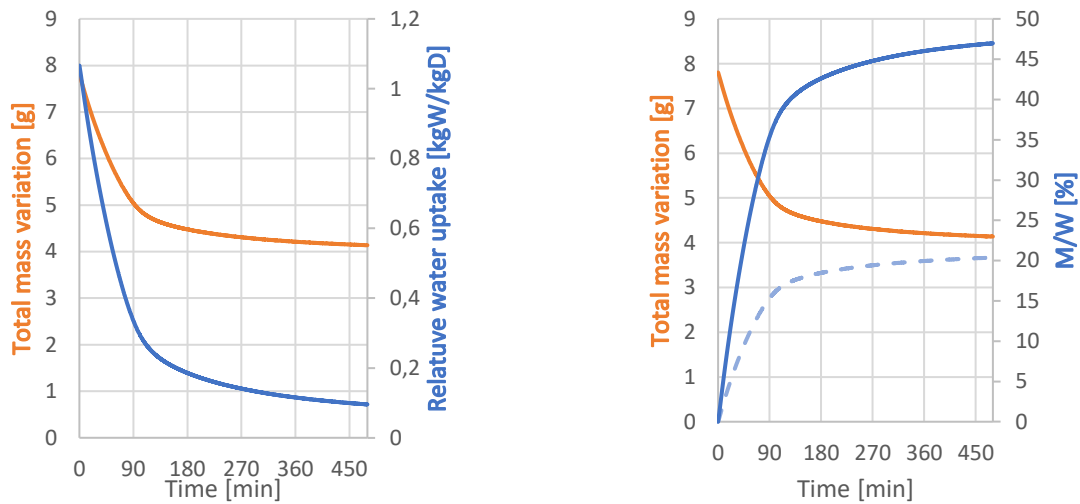


Figure 5.28- The graph on the right-hand side displays the ratio between the water extracted and the initial we mass in comparison to the total mass variation during the transient at 70°C, on the left-hand side it is shown the behavior of the water uptake during the adsorption process and the variation of the mass of the sample when the regeneration process was performed at 70°C

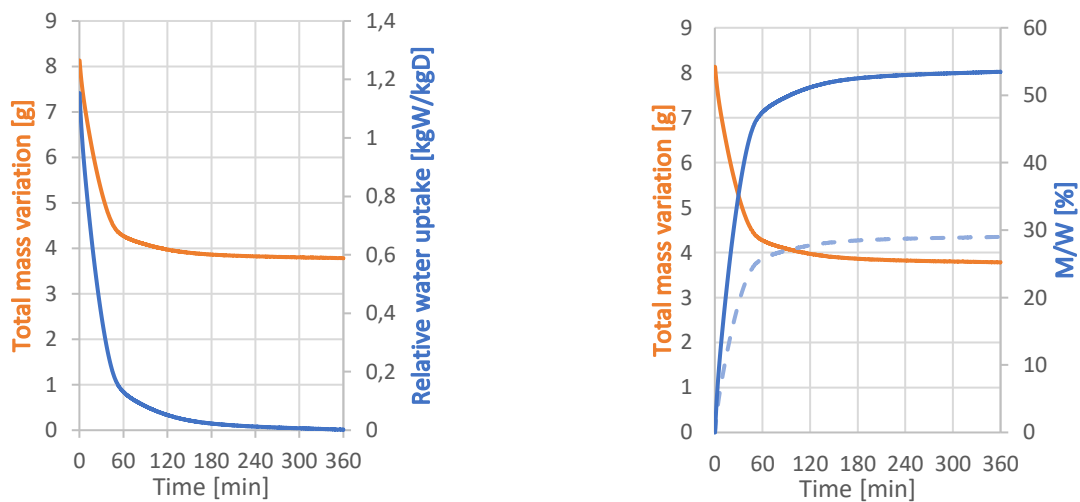


Figure 5.29--The graph on the right-hand side displays the ratio between the water extracted and the initial we mass in comparison to the total mass variation during the transient at 100°C, on the left-hand side it is shown the behavior of the water uptake during the adsorption process and the variation of the mass of the sample when the regeneration process was performed at 100°C

5.6.3 Testing Alginate at 40% of relative humidity

The sample under investigation was prepared in the box where the solution of water and calcium chloride is such as to reach a relative humidity of 40%.

From the monitored data, it was evident that the relative humidity obtained was around 37%. The following table displays the characteristics of the three tests and the related initial and final mass of the sample.

<i>Date</i>	<i>Hour</i>	<i>Operating Temperature</i>	<i>N. Hours</i>	<i>Starter Temperature</i>	<i>Relative humidity</i>	<i>Initial weight</i>	<i>Final weight</i>
07/11/2020	00:10	70°C	8	23°C	37%	6.08	3.978
08/11/2020	11:53	100°C	5	23°C	37%	6.033	3.68
11/11/2020	8:39	50°C	6	23°C	37%	6.058	4.446

Table 5.16- Alginate (40%) and moisture analyser properties

Results are shown in the figures below:

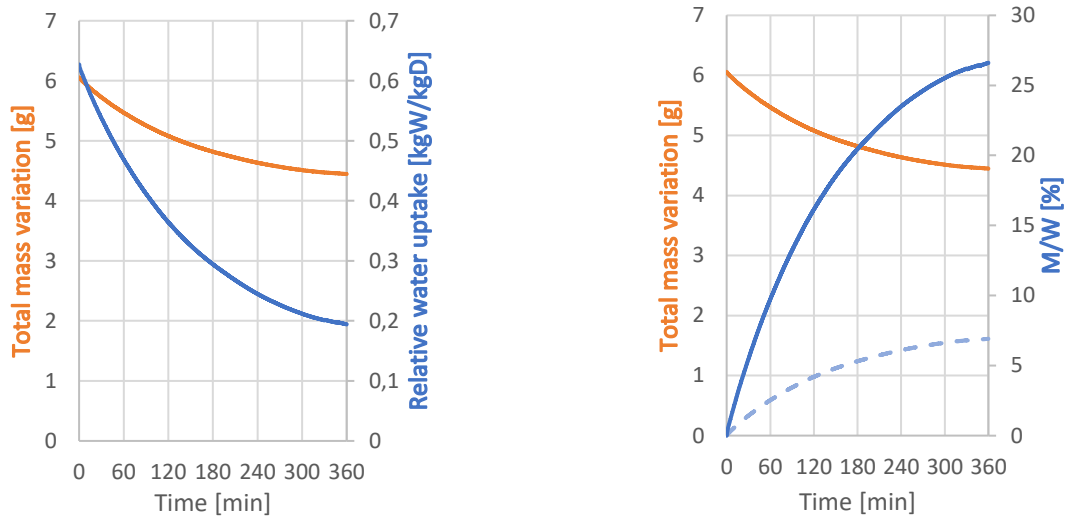


Figure 5.30-The graph on the right-hand side displays the ratio between the water extracted and the initial mass in comparison to the total mass variation during the transient at 50°C, on the left-hand side it is shown the behavior of the water uptake during the adsorption process and the variation of the mass of the sample when the regeneration process was performed at 50°C

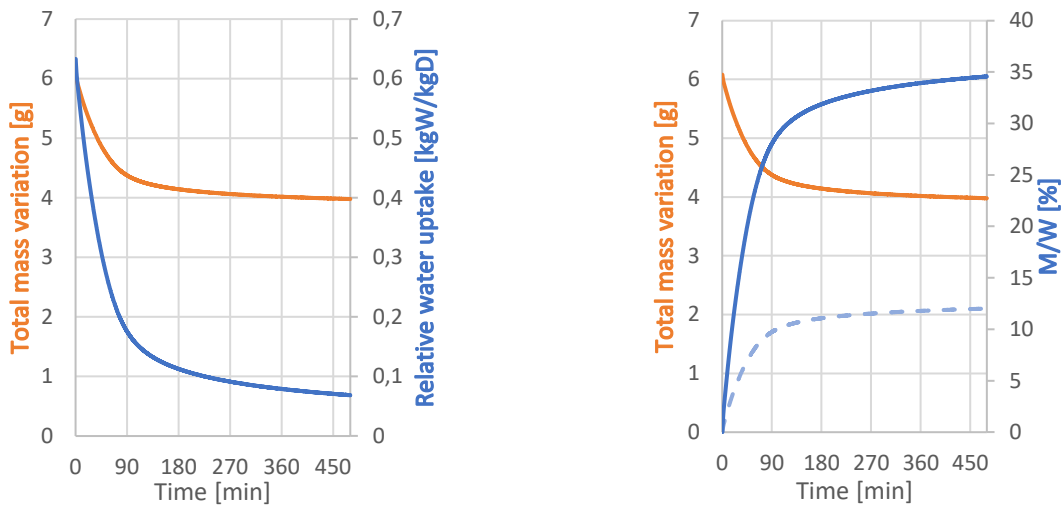


Figure 5.31- The graph on the right-hand side displays the ratio between the water extracted and the initial mass in comparison to the total mass variation during the transient at 70°C, on the left-hand side it is shown the behavior of the water uptake during the adsorption process and the variation of the mass of the sample when the regeneration process was performed at 70°C

The water uptake has been evaluated by putting as reference value the dry mass of the sample regenerated at 100°C. For this reason, the graph of the water uptake evaluated at 70°C and 50°C is not reaching the 0 value.

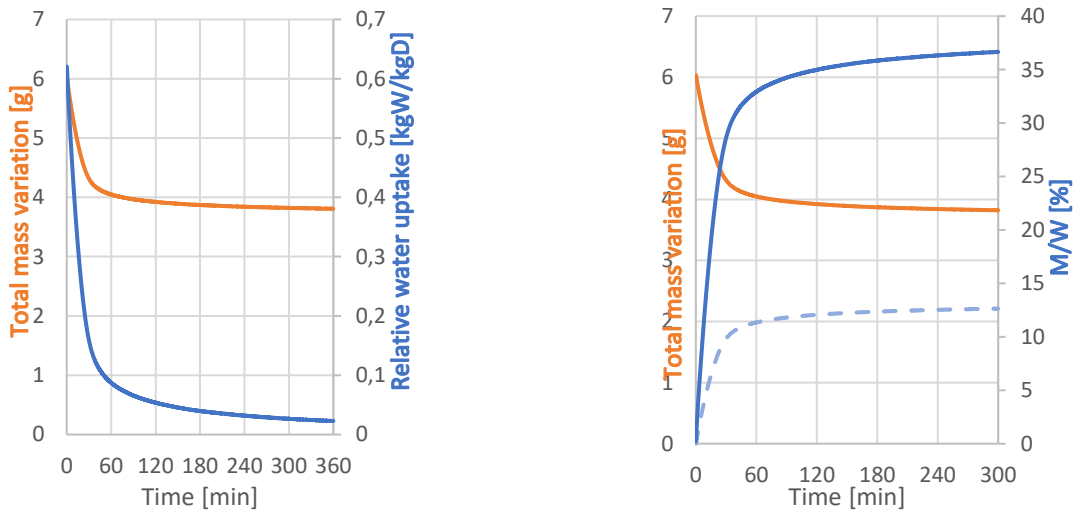


Figure 5.32-The graph on the right-hand side displays the ratio between the water extracted and the initial mass in comparison to the total mass variation during the transient at 100°C, on the left-hand side it is shown the behavior of the water uptake during the adsorption process and the variation of the mass of the sample when the regeneration process was performed at 100°C

6 Results and discussion

Results can be evaluated by making some comparisons between tests at the same operating temperature condition and different relative humidity of the same sample and vice versa or it is possible to compare the two materials tested at the same temperature and relative humidity condition. In this way, it is easy to highlight the different properties of the materials and to have a panoramic view of which are pros and cons of using one material rather than another.

6.1 Silica gel comparisons

As a general comment, it is evident that by performing the regeneration process at 100°C of samples with 80% relative humidity as a starting condition, it will reach the highest value of water content extracted from the sample and of water uptake. But even at lower temperature operating conditions, the amount of water extracted is significant. The relative humidity is defined as the ratio between the partial pressure of the water vapor and the equilibrium vapor pressure of the water at a given temperature. Relative humidity depends on the temperature and pressure of the system of interest. In particular, high relative humidity can be reached in cool air rather than warm air. High relative humidity means a high rate of water vapor in the air surrounding, so a great possibility for the material to adsorb the water vapor between its pores.

Results can be also expressed in terms of water uptake, which represents the amount of water adsorbed in the adsorbent solid or liquid phase. This value can be evaluated from the data collected with the moisture analyser.

The results obtained from the moisture analyser are expressed in terms of water extracted, so the ratio between the amount of water within the sample and the wet mass at the beginning of the test, according to the following equation:

$$\frac{M}{W} [\%] = \frac{W - D_i}{W} * 100 \quad \text{Eq. 6.1}$$

Where W is the initial wet mass of the material, and D_i is the weight, at each measurement, of the sample deprived of the water extracted.

By knowing the initial wet mass, through the inverse formula, it is possible to evaluate the mass of water extracted from the sample, which results equal to:

$$M_{H_2O} = W - D_i = \frac{M}{\overline{W}} * W \quad \text{Eq. 6.2}$$

Therefore, at each measurement the behavior of the mass of the adsorbent material can be expressed as:

$$M_{trans} = D_i = W - M_{H_2O} = W - \frac{M}{\overline{W}} * W \quad \text{Eq. 6.3}$$

The water uptake is defined as the amount of water adsorbed by the sample during the adsorption process, but starting from the regeneration, it will have a decreasing behavior. Indeed, by providing heat to the sample, it will release all or most of the water content inside. This parameter can be calculated as:

$$W_{upt} = \frac{(W - D) - M_{H_2O}}{D} * 100 \quad \text{Eq. 6.4}$$

Where W is the initial wet mass and D represents the final dry mass of the sample- To perform the calculation, for each sample, one value of the final dry mass has been taken as a reference value to evaluate the water uptake of the same sample at different operating temperature conditions.

In particular, for all the three samples, the final dry mass used was that resulted from the regeneration process at 100°C.

Results have been manipulated to compare the behaviors of the water uptake and the water extracted from the sample during the regeneration process at constant relative humidity and for the three different temperature operating conditions. The same procedure has been developed for all the relative humidity starting state.

The results of the above-mentioned analysis are displayed in the following:

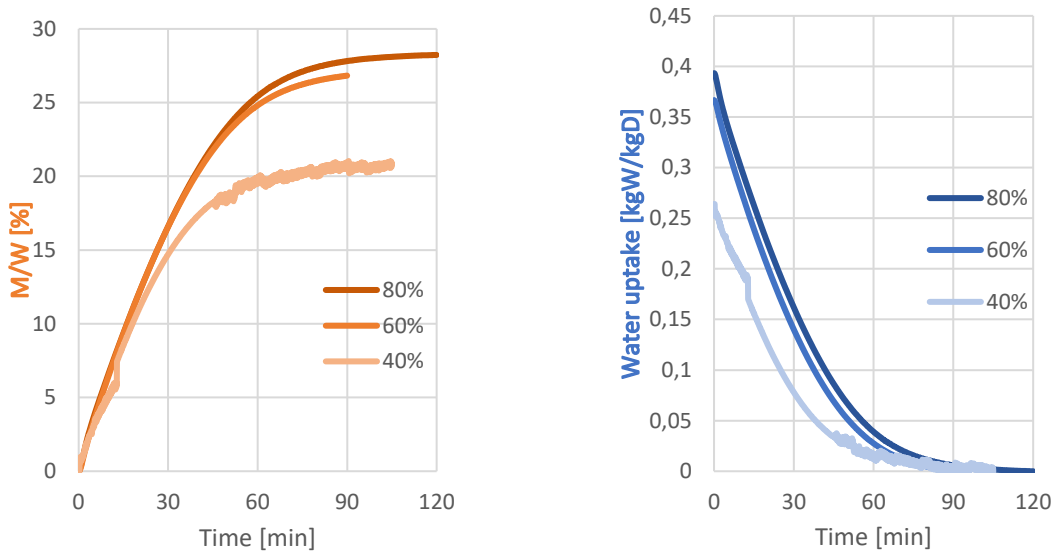


Figure 6.1- The graph on the left-hand side shows the comparison of water extracted from the silica gel sample concerning the initial wet mass for the three levels of RH when the regeneration process was performed at 100°C. On the right-hand side the behavior of the water uptake for the three levels of relative humidity

As it was expected, the sample prepared in the container where the relative humidity reaches the value of 80% has the highest water content rate equal to 28.23% and of course the highest amount of water uptake.

The sample that had as initial condition a relative humidity equal to 60% can reach nearly the same values of the sample at 80%. In particular, 26.83% of water content is extracted from the silica gel sample during the regeneration process.

Tests carried out with the sample at 40% of relative humidity, even at 100°C, have the lower water content. This phenomenon maybe happens because during the preparation process, due to the low relative humidity condition of the box, the water adsorbed within the sample is low. Indeed, by looking at the graph on the right-hand side the water uptake from the sample at 40% of relative humidity is only $0.26 \frac{kgW}{kgD}$, which is enough different from the others.

Figure 6.2 and Figure 6.3 shows the behaviors of the same quantities for the three samples at 80%, 60%, and 40% of relative humidity when the tests were carried out at a temperature of 70°C and 50°C.

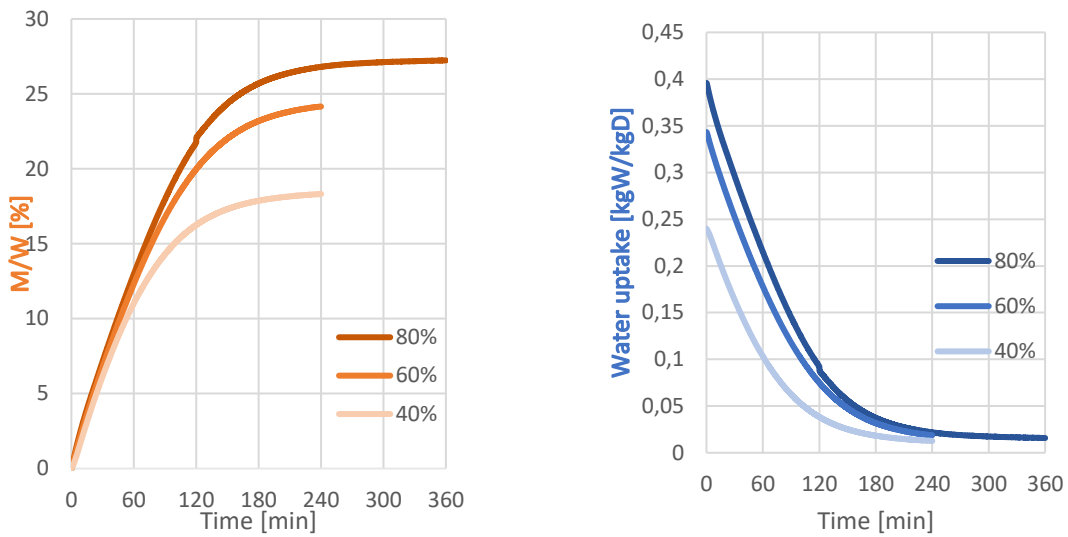


Figure 6.2- The graph on the left-hand side shows the comparison of water extracted from the silica gel sample concerning the initial wet mass for the three levels of RH when the regeneration process was performed at 70°C. On the right-hand side the behavior of the water uptake for the three levels of relative humidity

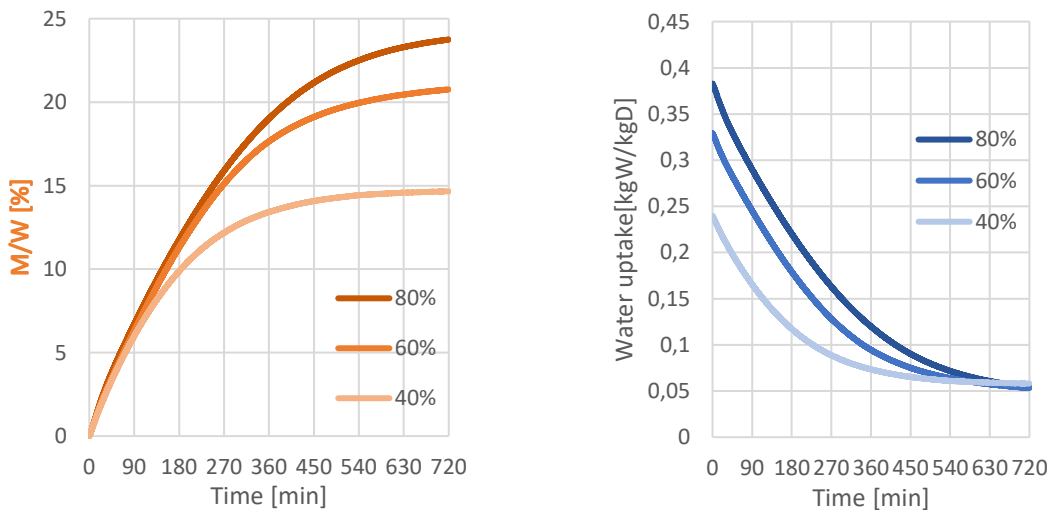


Figure 6.3- The graph on the left-hand side shows the comparison of water extracted from the silica gel sample concerning the initial wet mass for the three levels of RH when the regeneration process was performed at 50°C. On the right-hand side the behavior of the water uptake for the three levels of relative humidity

For the tests performed at 70°C, the sample with 80% of relative humidity displays a water content that is close to that of the test a 100°C, but the first one takes 6 hours to perform the regeneration process while the second has taken only 2 hours.

Even for the sample's conditions at 60% and 40%, the water content reached is a little bit lower concerning that of the samples regenerated at 100°C, but spending twice as much time.

As well displayed in the graph above, the behavior of the water uptake is almost the same for the three samples but what change is the starting point of the line. As it was expected, with the increasing of the relative humidity condition of the boxes containing the sample, it is shown also an increase in the water content within the sample, results of the adsorption process.

When the regeneration process is performed at 100°C the behavior of the water uptake goes to zero quickly, so it means that at that temperature, the regeneration process is ended and the samples are totally dried, ready for another cycle of tests.

After the first test, the samples were reinserted within the containers where the conditions of temperature and relative humidity were not changed, and the adsorption process starts again.

Of course, maybe due to the loss of material during the transportation of the sample or due to the low cycle stability of the material, the water adsorbed in the three cases of relative humidity will be a little bit lower with respect to the first cycle.

The final water uptake reached with tests performed at 70°C and 50°C is not equal to zero but reach the values of 1% and 5% respectively, and this phenomenon can be explained by the fact that, at each of these temperatures, the regeneration process is ended and this is evident from the constant trend of the curves, but the samples were no totally dried. At those temperatures, no more water can be extracted from the sample anymore.

Results have been also monitored to obtain the behaviors of total mass variation during the transient to make a comparison of this parameter concerning the three different operating conditions set within the moisture analyser and equal to 50°C, 70°C, and 100°C.

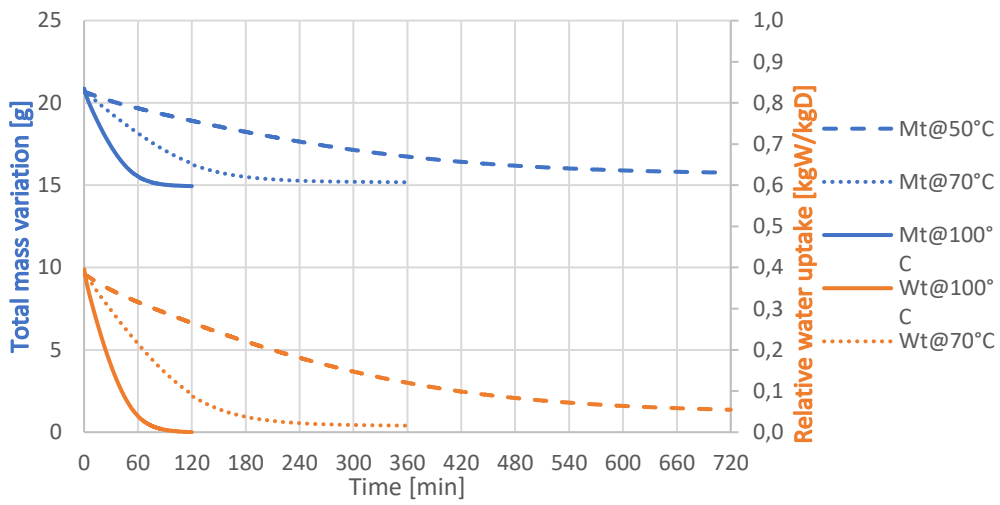


Figure 6.4- Comparison of the total mass variation and water uptake of the silica gel sample at constant relative humidity equal to 80% and varying the operating temperature conditions

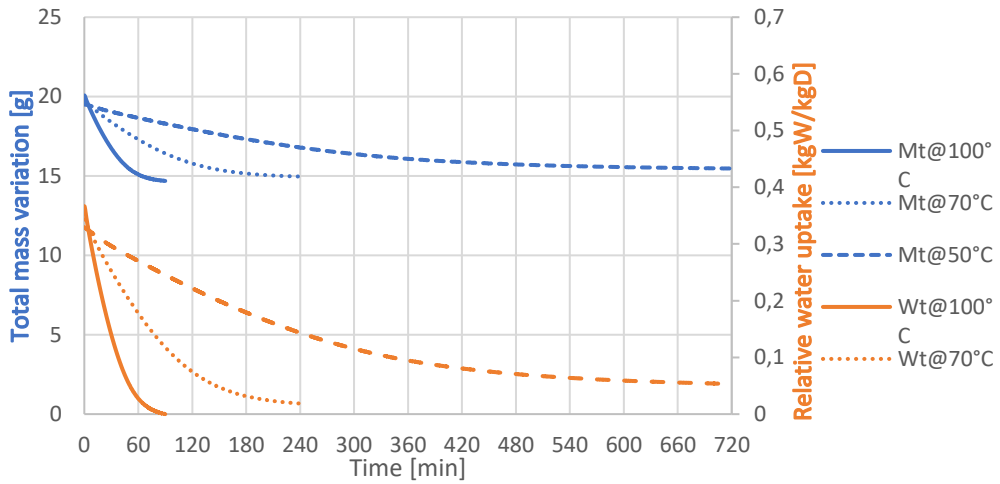


Figure 6.5- Comparison of the total mass variation and water uptake of the silica gel sample at constant relative humidity equal to 60% and varying the operating temperature conditions

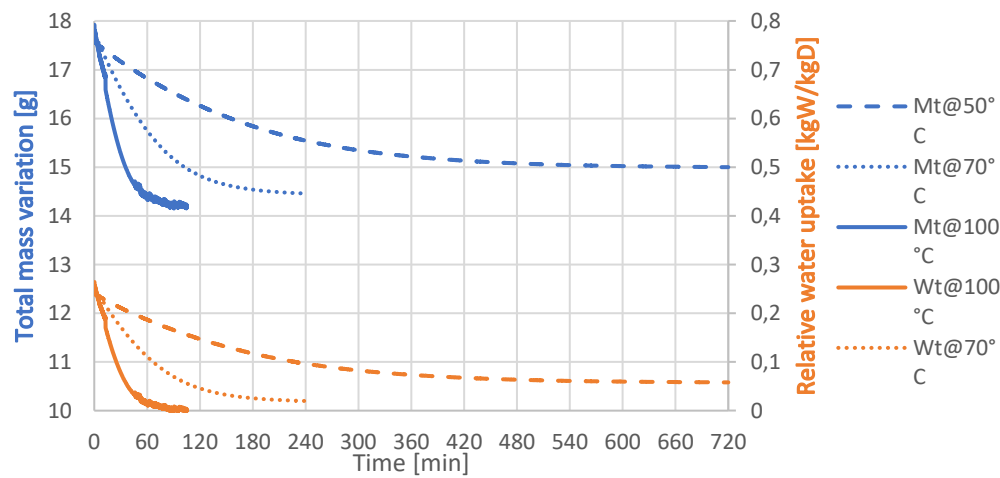


Figure 6.6- Comparison of the total mass variation and water uptake at constant relative humidity equal to 40% and varying the operating temperature conditions

6.2 Alginate comparisons

As in the case of silica gel samples, the amount of water that can be extracted from alginate has the highest value when the regeneration process is performed at 100°C and the relative humidity of the sample at the starting point is equal to 80%. But it is important to remember that at 80% of relative humidity liquid water showed up over the dish. During the regeneration process, all the water collected in the aluminum dish is removed, and after that, the extraction of water from the sample, so the true and proper regeneration process starts. Moreover, it is difficult to determine when the removal of liquid water ends and the true regeneration process starts.

However, this material shows high values of water extracted even at a lower temperature of 70°C or 50°C, which are one of the most important requests of an efficient water harvesting system.

All the variables needed to compare the material at different operating conditions have been evaluated with the same equation explained before used for the silica gel samples. Results are shown in the following figures:

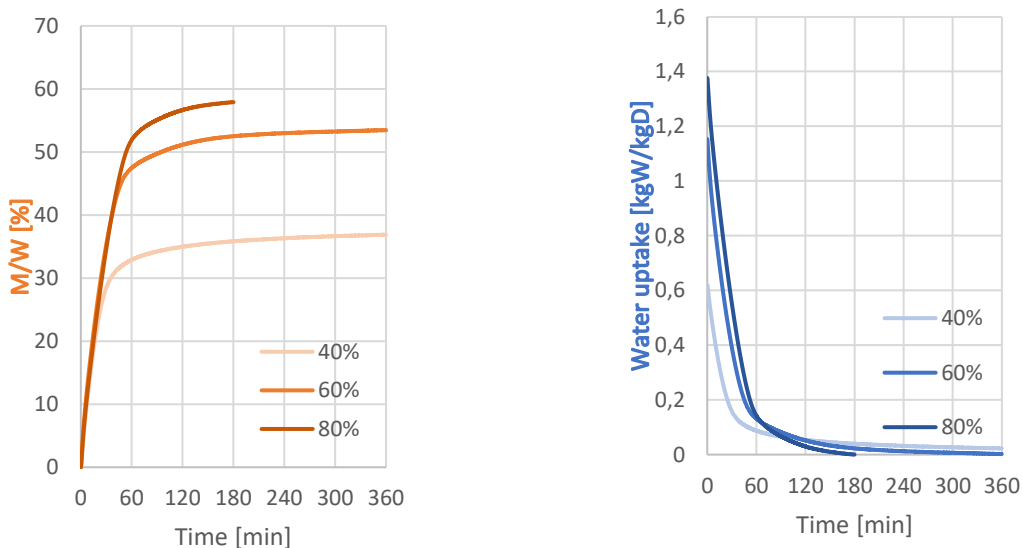


Figure 6.7- Graph on the left-hand side shows the comparison of water extracted from the alginate sample concerning the initial wet mass for the three levels of RH when the regeneration process was performed at 100°C. On the right-hand side the behavior of the water uptake for the three levels of relative humidity

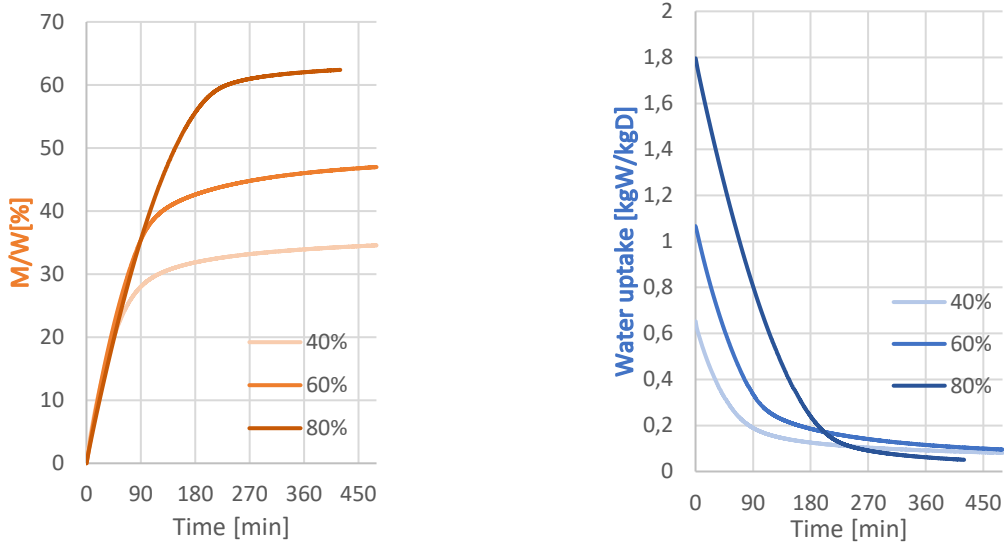


Figure 6.8- Graph on the left-hand side shows the comparison of water extracted from the alginate sample concerning the initial wet mass for the three levels of RH when the regeneration process was performed at 70°C. On the right-hand side the behavior of the water uptake for the three levels of relative humidity

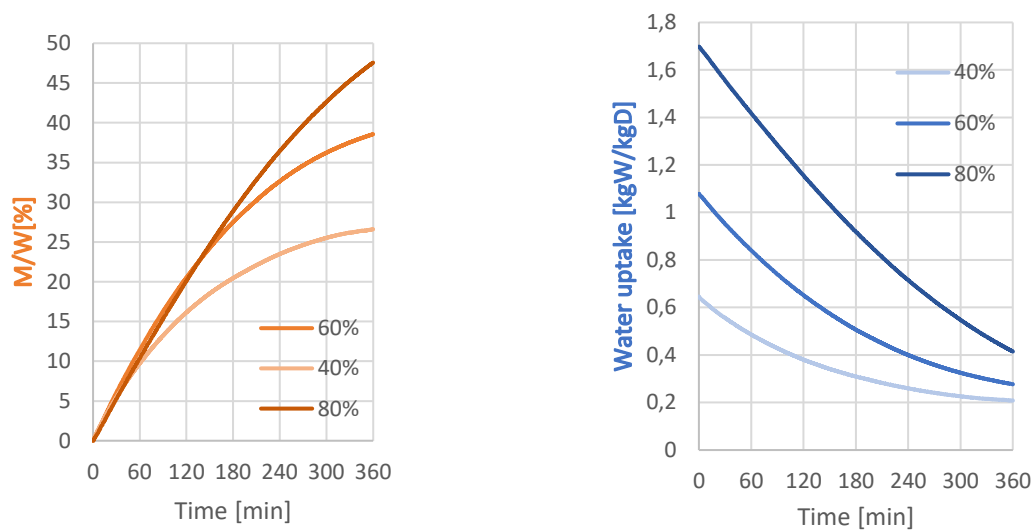


Figure 6.9- Graph on the left-hand side shows the comparison of water extracted from the alginate sample concerning the initial wet mass for the three levels of RH when the regeneration process was performed at 50°C. On the right-hand side the behavior of the water uptake for the three levels of relative humidity

From the picture displayed above, it is evident that the amount of water uptake from the alginate samples in the boxes where the relative humidity reaches the value of 60% and 80% is higher than 1 in relative terms. It seems to be a very good property of the material, even if in the sample at a relative humidity of 80% the formation of a little amount of liquid water in the aluminum dish has been observed. It means that the

alginate was not more able to hold the water vapor molecules, which is forced to condense. In any case, even at the lowest relative humidity conditions, the amount of water adsorbed within the alginate samples is higher with respect to that captured with the silica gel sorption material.

What could be also interesting is to compare the variation of the mass of the sample during the transient regeneration process.

To do that, some graphs have been carried out at the three different relative humidity conditions of the samples at the beginning of each test, comparing the three operating temperature conditions which of course influence the amount of water extracted.

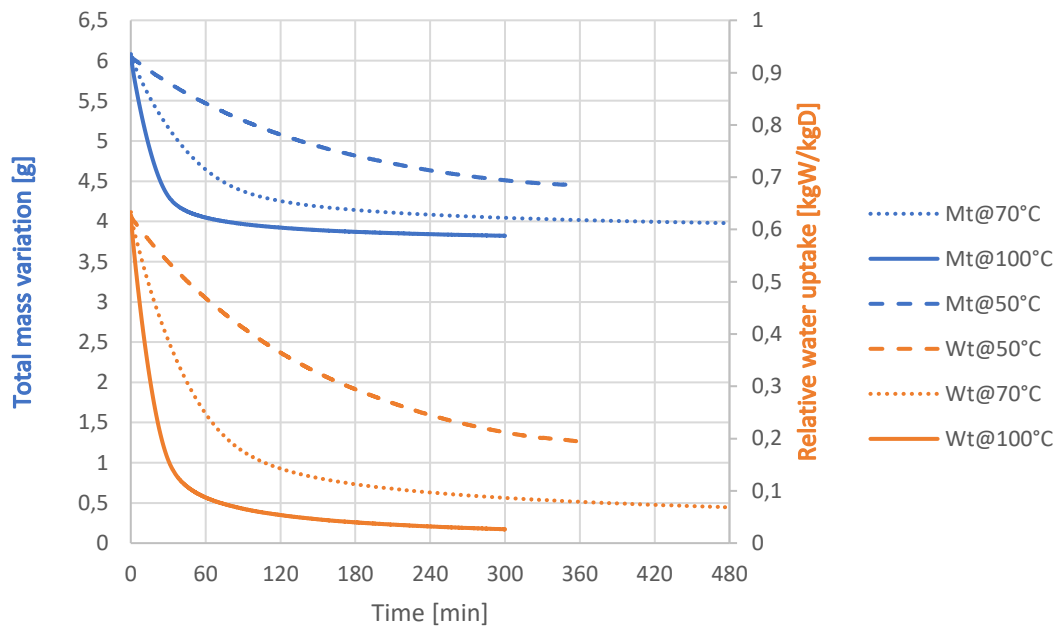


Figure 6.10- Comparison of the total mass variation and the water uptake of the alginate sample at 37% of relative humidity for three different levels of operating temperature conditions

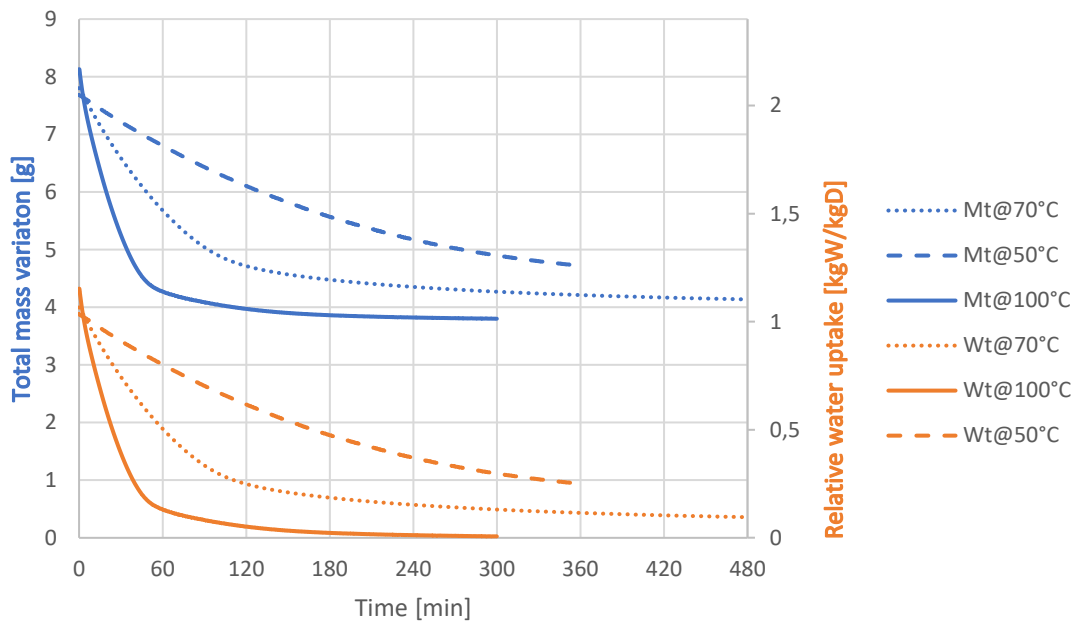


Figure 6.11- Comparison of the total mass variation and the water uptake of the sample at 60% of relative humidity for three different levels of operating temperature conditions

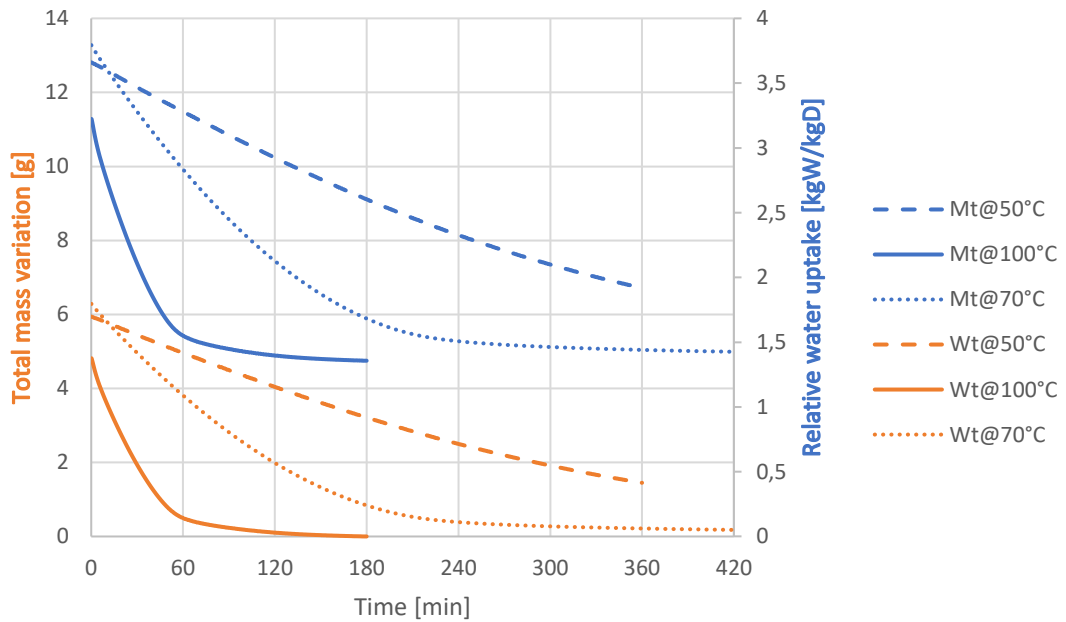


Figure 6.12- Comparison of the total mass variation and the water uptake of the sample at 80% of relative humidity for three different levels of operating temperature conditions

It is evident that at the maximum regeneration temperature, the variation of the mass during the transient has the highest gap.

At lower temperature conditions, the difference between the initial and the final dry mass is very close to the maximum achievable. It means that the regeneration process at low temperature, is able to remove almost entirely the water content within the samples, and it is also evident from the graphs representing the water uptake.

The water uptake for temperature lower than 100°C is not able to reach the completely dried state because they have been evaluated taking as reference value the dry mass of the sample at 100°C.

6.3 Silica gel and Alginate comparisons

Based on the data collected it was possible to compare the two materials. Since the samples used have different initial weights, the comparison between the mass variations during the transient of the regeneration process has been done in percentage terms: each sample was normalized with respect to its initial wet mass.

The second parameter analyzed was the relative water uptake from the two samples. Figure 6.13, shows the comparisons between silica gel and alginate samples, at 40% as relative humidity, of the two parameters mentioned above at three different levels of operating temperature conditions. The continuous line represents the silica gel sample, while the dashed one is the alginate.

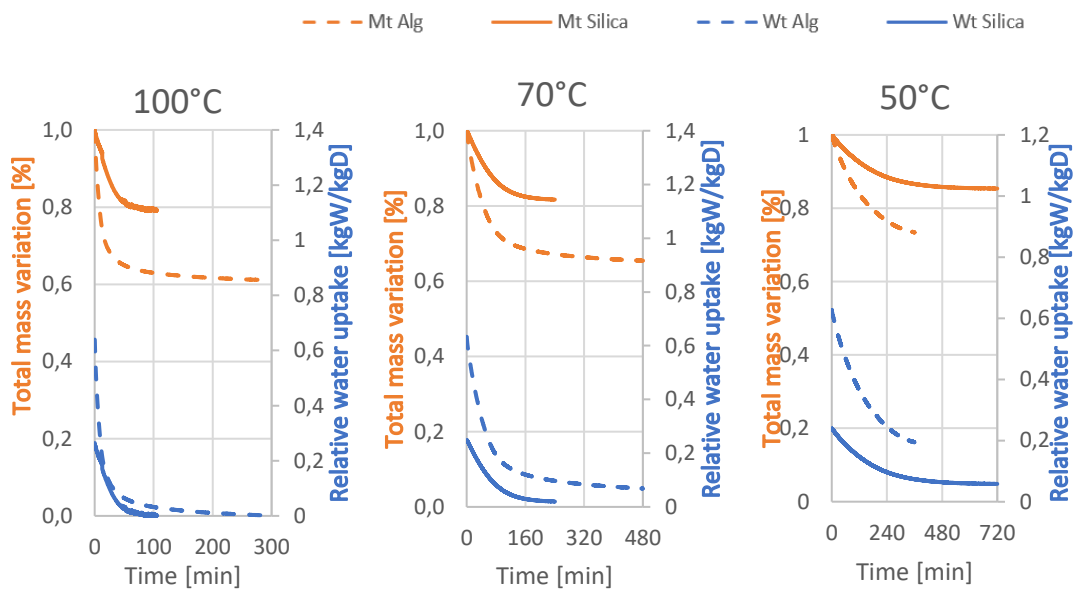


Figure 6.13- Comparison of the total mass variation and water uptake between silica gel and alginate at 40% of relative humidity and different temperatures: from left to right equal to 100°C, 70°C, 50°C

From these graphs, it is evident that the alginate material has a high adsorption capacity, so it can host a significant amount of water molecules within its pores, and also a very good inclination to release all the water content.

Looking at the last graph, where the regeneration process was carried out at 50°C, even if the test of the alginate sample lasts only six hours, the percentage of total mass variation during the process is higher with respect to that of the silica gel sample, whose regeneration step last 12 hours. The reductions mentioned above are equal to 26% and 16% respectively. It means that, at the same operating and starting conditions, the alginate is able to release more water in specific terms.

Another important consideration is that the alginate samples take more time to end the regeneration process, and this can be explained by the fact that being full of water molecules, it may find more resistance to overcome. But if we look within a closed interval of time the amount of water released from the alginate samples is very high, and after that, the sample can be ready for another adsorption cycle.

Of course, the release rate depends also on the amount of water adsorbed from the samples with a direct proportionality.

An interesting question for the posterity is to investigate the behaviors of the total mass variation during the regeneration process of the two materials at the same operating conditions when the amount of water uptake is the same.

As regards the relative water uptake, it is clear that the lines which represents the two material have different starting conditions, it means that the alginate, at the lowest relative humidity condition, has a high water uptake equal to $0.63 \frac{kgW}{kgD}$, while the silica gel samples can uptake only 20% of water with respect to its dry mass.

The major difference between the three graphs is the slope which is due to the different regeneration temperatures.

The same comments as before can be made by comparing the samples of alginate and silica gel arranged in the container where the relative humidity reaches the value of 60%.

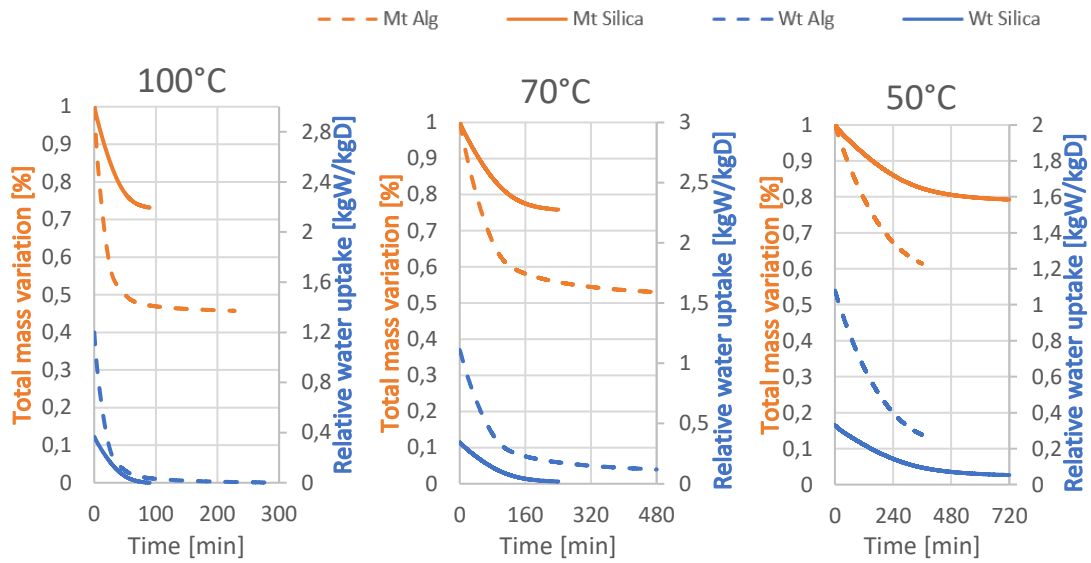


Figure 6.14- Comparison of total mass variation and water uptake between silica gel and alginate at 60% of relative humidity and different temperatures: from left to right equal to 100°C, 70°C, 50°C

Even so, the line representing the water uptake of alginate sorption material is higher concerning the silica gel ones, and it also exceeds the value of 100%.

The amount of water adsorbed from the alginate sample exceeds 50% of that captured from the silica gel.

The capability of the alginate to release all or most of the water content even at relatively low temperatures like 50°C or 70°C, can be considered as one of the most important properties of this material. The only point not in favor of the alginate material is the fact that it takes a very long time to perform the regeneration process.

The last comparison sees the samples of alginate and silica gel prepared in the box where the relative humidity reaches the highest value of 80%.

The comparison of the total mass variation and the relative water uptake between the two materials at the above-mentioned conditions are shown in Figure 6.15

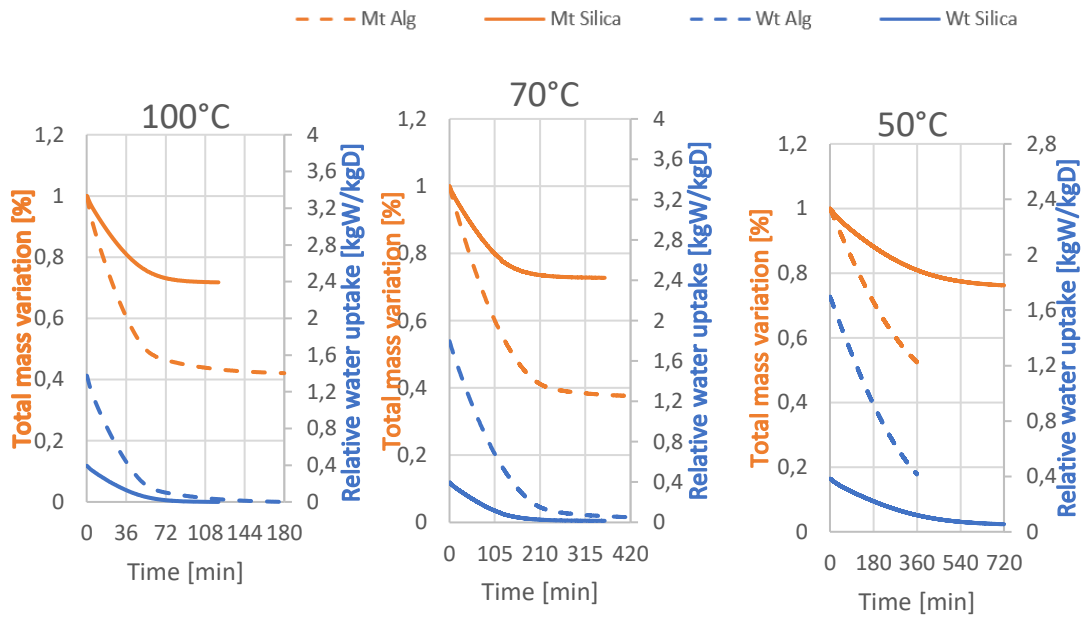


Figure 6.15- Comparison of water content and water uptake between silica gel and alginate at 80% of relative humidity and different temperatures: from left to right equal to 100°C, 70°C, 50°C

Conclusions

Water scarcity is a global challenge dealing with the life of humankind, especially for those people who live in arid regions and remote areas.

Current freshwater resources like lakes or groundwater, on which the modern and industrialized society rely, suffering continuous exploitation over the last decades. As a result, droughts events are becoming more frequent also in developed countries that, together with high pollution levels reached nowadays, are the main rationale behind this research: finding an alternative solution to the conventional use of water networks.

Recently, many alternative solutions have been developed such as filtration, reverse osmosis, or solar water purification which allow the exploitation of seawater or wastewater. Anyway, these alternatives, despite the high level of development reached, can be applied only in coastal areas, limiting their application to the rest of the inner areas. Atmospheric water, which is available regardless of the geographical condition, is emerging as an alternative water resource.

Atmospheric water harvesting systems have the advantage of being a decentralized water production system, overcoming the challenges of long-distance transport or the delivery of potable water in rural areas.

The conventional procedure used to produce freshwater from atmospheric air is to cool down the ambient air below the dew point and collecting the water condensed. The process requires a consistent amount of electrical power, resulting in a high cost for the produced water.

This research study explores the alternative offered by moisture harvesting materials, as an alternative method to the use of electricity. Appropriate materials used for moisture harvesting should have high water affinity. Indeed, they enable spontaneous vapor sorption to trap water molecules, extracting vapor from the air, and concentrating the moisture. Moreover, materials selected for the water harvesting system should be able to operate in both low and high relative humidity conditions.

The ideal moisture harvesters' materials are required to have high water uptake, low energy demand for the regeneration process, fast capture/release, high cycling

stability, and low cost. All these requirements can be simultaneously achieved by rational material and efficient structural design.

The alginate sorption material investigated in this study covers almost all the above-mentioned properties required to be disposed in an efficient water harvesting machine. From the graphs displayed before, it is evident that the produced polymer derived from sodium alginate can adsorb a very high amount of water even at low relative humidity conditions.

The most interesting result is that the alginate sample inserted in the ambient where the relative humidity did not exceed the value of 40%, reaches a value of water uptake of almost 60% and it was an incredible result.

As regards the property according to which an appropriate material for water harvesting should have low energy demand for the regeneration process (lower of 100°C), the sodium alginate perfectly matches this requirement. Indeed, the regeneration tests carried out at temperatures between 50°C and 70°C, showed a high variation of water uptakes, and the amount of water released from the samples is considerable. As an example, the mass variation of the alginate sample prepared in the container where the relative humidity reaches the value of 60% dropped by 47% and 39% for regeneration temperature equal to 70°C and 50°C respectively.

High cycling stability means that the material, after some cycle of adsorption and desorption, can recover all the weight and properties lost during the regeneration process. Even if the number of tests performed is not enough to determine in an accurate way the cycle stability property, by collecting the data of the weight of the samples at the beginning and at the end of the regeneration, it was evident that the alginate weight was not changed so much, so there is no residual weight lost during the process. The following table will show the weight of the alginate samples at the beginning and the end of each regeneration process:

<i>RH</i>	<i>Temperature [°C]</i>	<i>Initial weight [g]</i>	<i>Final weight [g]</i>
80%	70°C	13.277	4.99
	100°C	11.284	4.749
	50°C	12.812	6.718
60%	70°C	7.805	4.138
	100°C	8.133	3.698
	50°C	7.685	4.722
40%	70°C	6.08	3.978
	100°C	6.033	3.68

50°C	6.058	4.446
------	-------	-------

The only requirement that could be not the best one is the velocity at which the material can adsorb or release the water content.

This property can be evaluated by analyzing the values of the apparent diffusion coefficient obtained by manipulating the data collected. It is a measure of the kinetics of water adsorption and it is directly proportional to the average water uptake.

Looking at *Table 5.9*, it is evident that the apparent diffusion coefficient of the alginate material is in some cases lower than that of the silica gel. It means that the alginate will take more time to capture all the water vapor that it is able to adsorb, even if the water uptake is higher. As regards the releasing time, it may be analyzed from two different points of views: from one side the releasing process of the alginate is very long, also at the highest temperature, but from the other side, looking at the total mass variation during the transient of the regeneration process in a small period, the amount of water released from the alginate is higher concerning that extracted from the silica gel.

When the regeneration process was performed at 50°C, the test lasts only six hours but the amount of water released from the alginate was higher with respect to that of the silica gel.

Eventually, the low-cost requirement is also fulfilled by the alginate since it is cheap, easy to find, and the production process is not too complicated.

In the end, it is possible to conclude that sodium alginate could represent a great substitute to the silica gel sorption material since it matches all the property requested to be an efficient sorption material to be applicable in a water harvesting system.

Bibliography

- [1] United Nations, *The United Nations world water development report 2015: water for a sustainable world - UNESCO Digital Library*. 2015.
- [2] “access-water-and-sanitation_en @ ec.europa.eu.” .
- [3] “b5177cc7ebb47b6ad454a2989a206e324b246d4b @ www.un.org.” .
- [4] M. Shatat, M. Worall, and S. Riffat, “Opportunities for solar water desalination worldwide : Review,” *Sustain. Cities Soc.*, vol. 9, pp. 67–80, 2013.
- [5] A. Nannarone, C. Toro, and S. Enrico, “Multi-Stage Flash Desalination Process : Modeling and Simulation,” no. July, 2017.
- [6] A. Nannarone, C. Toro, and S. Enrico, “Multi-Effect Distillation Desalination Process : Modeling and Simulation,” no. July, 2017.
- [7] “School of Engineering - Classe di Ingegneria Energetica Course: Energy Economics Water, Energy & Food Nexus.”
- [8] N. A. Ahmad, P. S. Goh, L. T. Yogarathinam, A. K. Zulhairun, and A. F. Ismail, “Current advances in membrane technologies for produced water desalination,” *Desalination*, vol. 493, no. July, p. 114643, 2020.
- [9] S. Al-Amshawee, M. Y. B. M. Yunus, A. A. M. Azoddein, D. G. Hassell, I. H. Dakhil, and H. A. Hasan, “Electrodialysis desalination for water and wastewater: A review,” *Chem. Eng. J.*, vol. 380, no. March 2019, 2020.
- [10] F. E. Ahmed, B. S. Lalia, R. Hashaikeh, and N. Hilal, “Alternative heating techniques in membrane distillation : A review,” *Desalination*, vol. 496, no. June, p. 114713, 2020.
- [11] O. F. The, *RESOURCES OF THE WORLD AND THEIR USE.* .
- [12] “groundwater-resources @ scdhec.gov.” .
- [13] R. Tu and Y. Hwang, “Reviews of atmospheric water harvesting technologies,” *Energy*, vol. 201, p. 117630, 2020.
- [14] “solar-powered-super-sponge-can-harvest-water-thin-air-03272019

@ en.reset.org.” .

- [15] M. Eslami, F. Tajeddini, and N. Etaati, “Thermal analysis and optimization of a system for water harvesting from humid air using thermoelectric coolers,” *Energy Convers. Manag.*, vol. 174, no. April, pp. 417–429, 2018.
- [16] F. Bagheri, “Performance investigation of atmospheric water harvesting systems,” *Water Resour. Ind.*, vol. 20, no. May, pp. 23–28, 2018.
- [17] G. V Fracastoro and M. Perino, “Solar cooling.”
- [18] D. Bergmair, S. J. Metz, H. C. De Lange, and A. A. Van Steenhoven, “System analysis of membrane facilitated water generation from air humidity,” *DES*, vol. 339, pp. 26–33, 2014.
- [19] M. A. Al-Ghouti and D. A. Da’ana, “Guidelines for the use and interpretation of adsorption isotherm models: A review,” *J. Hazard. Mater.*, vol. 393, no. November 2019, 2020.
- [20] “a40d2d3b037216f631ba22b0d31fe65447f86d8d @ gasadsorptiontech.wordpress.com.” .
- [21] K. C. Ng *et al.*, “Experimental investigation of the silica gel-water adsorption isotherm characteristics,” *Appl. Therm. Eng.*, vol. 21, no. 16, pp. 1631–1642, 2001.
- [22] L. T. Zhuravlev, “The surface chemistry of amorphous silica. Zhuravlev model,” *Colloids Surfaces A Physicochem. Eng. Asp.*, vol. 173, no. 1–3, pp. 1–38, 2000.
- [23] R. H. Mohammed, O. Mesalhy, M. L. Elsayed, S. Hou, M. Su, and L. C. Chow, “Physical properties and adsorption kinetics of silica-gel / water for adsorption chillers,” *Appl. Therm. Eng.*, vol. 137, no. March, pp. 368–376, 2018.
- [24] A. Myat, N. Kim Choon, K. Thu, and Y. D. Kim, “Experimental investigation on the optimal performance of Zeolite-water adsorption chiller,” *Appl. Energy*, vol. 102, pp. 582–590, 2013.
- [25] “430 @ science.sciencemag.org.” .
- [26] M. Ejeian, A. Entezari, and R. Z. Wang, “Solar powered atmospheric water harvesting with enhanced LiCl /MgSO₄/ACF composite,” *Appl. Therm. Eng.*, vol. 176, no. May, p. 115396, 2020.
- [27] Y. I. Aristov, M. M. Tokarev, L. G. Gordeeva, V. N. Snytnikov, and

- V. N. Parmon, “New Composite Sorbents for Solar-Driven Technology of Fresh Water Production From the Atmosphere,” *Sol. Energy*, vol. 66, no. 2, pp. 165–168, 1999.
- [28] P. A. Kallenberger and M. Fröba, “Water harvesting from air with a hygroscopic salt in a hydrogel–derived matrix,” *Commun. Chem.*, vol. 1, no. 1, p. 28, Dec. 2018.
- [29] “4650594.pdf.” .
- [30] N. T. T. Uyen, Z. A. A. Hamid, N. X. T. Tram, and N. Ahmad, “Fabrication of alginate microspheres for drug delivery: A review,” *Int. J. Biol. Macromol.*, vol. 153, pp. 1035–1046, 2020.
- [31] “No Title,” no. 10.
- [32] P. Gurikov and I. Smirnova, “Non-Conventional Methods for Gelation of Alginate,” *Gels*, vol. 4, no. 1, p. 14, Feb. 2018.
- [33] M. R. Conde, “Properties of aqueous solutions of lithium and calcium chlorides: formulations for use in air conditioning equipment design,” *Int. J. Therm. Sci.*, vol. 43, no. 4, pp. 367–382, Apr. 2004.
- [34] Y. I. Aristov, M. M. Tokarev, A. Freni, I. S. Glaznev, and G. Restuccia, “Kinetics of water adsorption on silica Fuji Davison RD,” *Microporous Mesoporous Mater.*, vol. 96, no. 1–3, pp. 65–71, Nov. 2006.